1990

Depositional environments, ichnology and diagenesis of the upper Frobisher-Alida beds of the Elkhorn Ranch and Roughrider fields of western North Dakota

Jeffrey R. Valvik
University of North Dakota

DEPOSITIONAL ENVIRONMENTS, ICHNOLOGY AND DIAGENESIS OF THE UPPER FROBISHER-ALIDA BEDS OF THE ELKHORN RANCH AND ROUGHRIDER FIELDS OF WESTERN NORTH DAKOTA

Jeffrey R. Valvik, M.A.

University of North Dakota, 1990

Faculty Advisor: Professor Richard D. LeFever

The upper Frobisher-Alida interval of western North Dakota was studied in order to determine the depositional environments, bioturbation features, and the diagenetic history of these carbonate and evaporite rocks.

Detailed examination resulted in the identification of six distinct lithotypes: 1) crinoid, coral packstone-wackestone (LT-1); 2) brachiopod, skeletal wackestone (LT-2); 3) skeletal, burrowed mudstone-wackestone; 4) intraclast, peloid packstone-grainstone; 5) peloid, intraclast, ostracode packstone-wackestone; 6) nodular and bedded anhydrite (LT-6). Lithofacies generally follow a depositional sequence of thick units of sublittoral carbonates, followed by a thin sequence of littoral carbonates, and culminating in a thick unit of sublittoral evaporites. Sublittoral rocks dominate the basal lithologies throughout the study area.

Depositional environments illustrate a regressive sequence: normal marine wackestones and packstones; marginally restricted

wackestones; restricted wackestones and mudstones; littoral to sublittoral shoal complex with dominantly peloidal packstones; lagoonal mudstones; and littoral flats and ponds with anhydrite lithologies.

Early cementation of burrows inhibited compaction of burrowed carbonates. Rocks without evidence of early cementation of burrows would more readily compact and thus inhibit movement of pore fluids.

Diagenetic effects upon the rocks studied were varied and complex. Diagenetic effects which commenced prior to complete lithification included mechanical compaction, micritization and inversion of aragonite. Eogenetic diagenesis was the result of infiltration of hypersaline brines from overlying evaporite areas. Differential compaction, cementation and replacement were prevalent eogenetic diagenetic effects.

Mesogenetic diagenetic effects were due to periods of pore fluid movements. Mesogenetic diagenesis included dolomitization, silicification, replacement, chemical compaction, pressure solution and neomorphism. Multiple dolomitization episodes were due to the movements of magnesium-rich pore fluids released during pressure solution.

DEPOSITIONAL ENVIRONMENTS, ICHNOLOGY AND DIAGENESIS OF THE UPPER FROBISHER-ALIDA BEDS OF THE ELKHORN RANCH AND ROUGHRIDER FIELDS OF WESTERN NORTH DAKOTA

by

Jeffrey R. Valvik

Bachelor of Arts, City University of New York (Hunter College) 1980

A Thesis

Submitted to the Graduate Faculty

of the University of North Dakota

in partial fulfillment of the requirements for the degree of

Master of Arts

Grand Forks, North Dakota

August

1990

This thesis submitted by Jeffrey R. Valvik in partial fulfillment of the requirements for the Degree of Master of Arts from the University of North Dakota has been read by the Faculty Advisory Committee under whom the work has been done, and is hereby approved.

_____
(Chairperson)

_____

_____

This thesis meets the standards for appearance and conforms to the style and format requirements of the Graduate School of the University of North Dakota, and is hereby approved.

_____
Dean of the Graduate School

Permission

Title: DEPOSITIONAL ENVIRONMENTS, ICHNOLOGY AND DIAGENESIS OF THE UPPER FROBISHER-ALIDA BEDS OF THE ELKHORN RANCH AND ROUGHRIDER FIELDS OF WESTERN NORTH DAKOTA.
University of North Dakota Department of Geology

Degree: Master of Arts

In presenting this thesis in partial fulfillment of the requirements for a graduate degree from the University of North Dakota, I agree that the Library of this University shall make it freely available for inspection. I further agree that permission for extensive copying for scholarly purposes may be granted by the professor who supervised my thesis work or, in his absence, by the Chairperson of the Department or the Dean of the Graduate School. It is understood that any copying or publication or other use of this thesis or part thereof for financial gain shall not be allowed without my written permission. It is also understood that due recognition shall be given to me and to the University of North Dakota in any scholarly use which may be made of any material in my thesis.

Signature 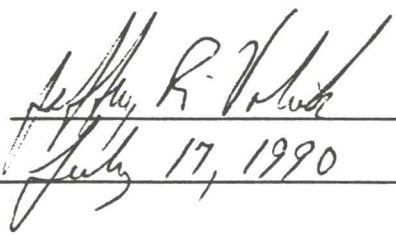

Date July 17, 1990

TABLE OF CONTENTS

DEPOSITIONAL ENVIRONMENTS, ICHNOLOGY AND DIAGENESIS OF THE UPPER FROBISHER-ALIDA BEDS OF THE ELKHORN RANCH AND ROUGHRIDER FIELDS OF WESTERN NORTH DAKOTA

LIST OF FIGURES

Figure

LIST OF TABLES

Table

ACKNOWLEDGMENTS

I would like to thank my advisory committee members, Drs. Richard D. LeFever, Patricia Videtich and Nels Forsman for reviewing the manuscripts and their helpful suggestions. I greatly appreciate the way they all agreed to serve as committee members at such a late stage in my program of study, and especially for Rich who took on the chairmanship.

The use of the electric logs, rock cores and thin sections made available by the North Dakota Geological Survey was invaluable to the completion of this project. Use of the library and research facilities of the Geology Department of the University of North Dakota is appreciated.

I would like to thank Mr. Don Mitchell and the Sun Exploration Company for funding for thin sections. Thanks is given to Mr. David Petty and the Tenneco Oil Company for loaning numerous thin sections for examination.

Special thanks is given to Dr. Howard J. Fischer for invaluable insight and encouragement.

Most importantly I thank my wife Janet for her encouragement, support and vision, without which, this all would not have been possible.

To Melissa, Jennifer and Gregory,

Daddy can play now.

ABSTRACT

The upper Frobisher-Alida interval of western North Dakota was studied in order to determine the depositional environments, bioturbation features, and the diagenetic history of these carbonate and evaporite rocks.

Detailed examination resulted in the identification of six distinct lithotypes: 1) crinoid, coral packstone-wackestone (LT-1); 2) brachiopod, skeletal wackestone (LT-2); 3) skeletal, burrowed mudstone-wackestone; 4) intraclast, peloid packstone-grainstone; 5) peloid, intraclast, ostracode packstone-wackestone; 6) nodular and bedded anhydrite (LT-6). Lithofacies generally follow a depositional sequence of thick units of sublittoral carbonates, followed by a thin sequence of littoral carbonates, and culminating in a thick unit of sublittoral evaporites. Sublittoral rocks dominate the basal lithologies throughout the study area.

Depositional environments illustrate a regressive sequence: normal marine wackestones and packstones; marginally restricted wackestones; restricted wackestones and mudstones; littoral to sublittoral shoal complex with dominantly peloidal packstones; lagoonal mudstones; and littoral flats and ponds with anhydrite lithologies.

Early cementation of burrows inhibited compaction of burrowed carbonates. Rocks without evidence of early cementation of burrows would more readily compact and thus inhibit movement of pore fluids.

Diagenetic effects upon the rocks studied were varied and complex. Diagenetic effects which commenced prior to complete lithification included mechanical compaction, micritization and inversion of aragonite. Eogenetic diagenesis was the result of infiltration of hypersaline brines from overlying evaporite areas. Differential compaction, cementation and replacement were prevalent eogenetic diagenetic effects.

Mesogenetic diagenetic effects were due to periods of pore fluid movements. Mesogenetic diagenesis included dolomitization, silicification, replacement, chemical compaction, pressure solution and neomorphism. Multiple dolomitization episodes were due to the movements of magnesium-rich pore fluids released during pressure solution.

INTRODUCTION

General Setting

The study area is located in McKenzie and Billings Counties of western North Dakota, and includes all or part of eight townships from T143N to T146N and from R100W to R102W (Fig. 1). The Elkhorn Ranch, Roughrider and adjoining fields of McKenzie and Billings Counties are situated on the western and northern flanks of the Billings Anticline (Fig. 2). These fields are prolific oil producers with cumulative production of over 21 million barrels of oil from the Madison pools (Halvorson, 1984). Significant production is also known in this area from the Devonian Duperow and Bakken Formations and from the Ordovician Red River Formation. The interval studied is part of the Mississippian Charles and Mission Canyon Formations of the Madison Group.

Purpose

The purpose of this study was threefold: 1) determine the depositional environments of the Upper Frobisher-Alida beds of western North Dakota, 2) determine the significance, if any, of the bioturbated rocks of these beds, and 3) demonstrate some of the relationships between the environments of deposition and the subsequent diagenetic history of the rocks in this study area.

Figure 1. Location of study area. Well symbols are those used on the North Dakota Geological Survey's field maps and are presented to show mapping control points. Circled well symbols denote a well with rock core.

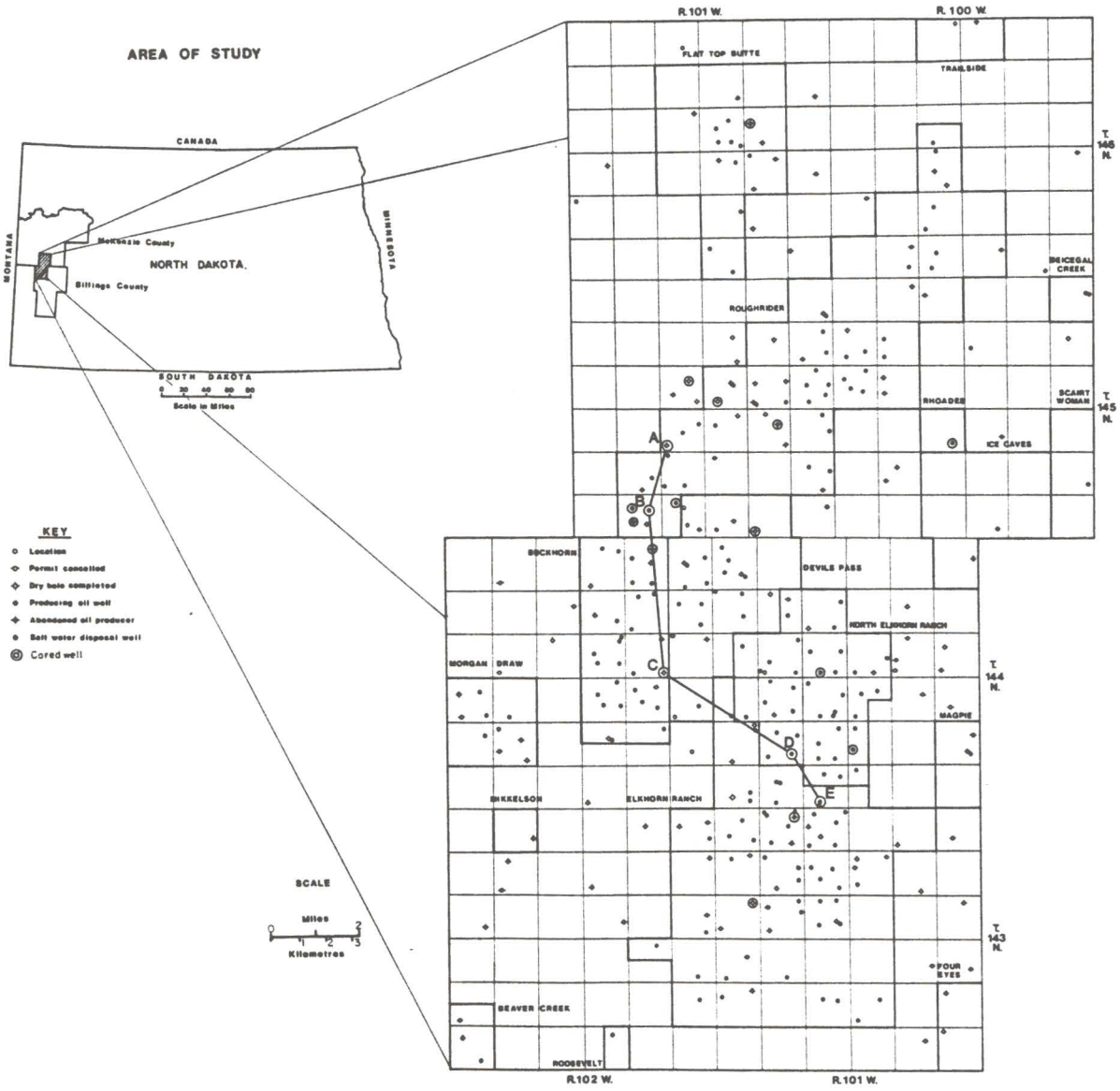
AREA OF STUDY
CANADA
MONTANA
MINNESOTA
McKenzie County
NORTH DAKOTA
Billings County
SOUTH DAKOTA
0 30 40 60 80
Scale in Miles
KEY
Location
Permit cancelled
Dry hole completed
Producing oil well
Abandoned oil producer
Salt water disposal well
Cored well
SCALE
Miles
Kilometres
R.101 W.
R.100 W.
R.102 W.
R.101 W.
FLAT TOP BUTTE
TRAILSIDE
T. 146 N.
BEICEGAL CREEK
ROUGHRIDER
RHOADES
SCAIRT WOMAN
T. 145 N.
ICE CAVES
A
B
C
D
E
BUCKHORN
DEVILS PASS
NORTH ELKHORN RANCH
MORGAN DRAW
T. 144 N.
MAGPIE
BIKKELSON
ELKHORN RANCH
T. 143 N.
FOUR EYES
BEAVER CREEK
ROOSEVELT

Figure 2. Location of structural features in the Williston Basin. After Horner (1986).

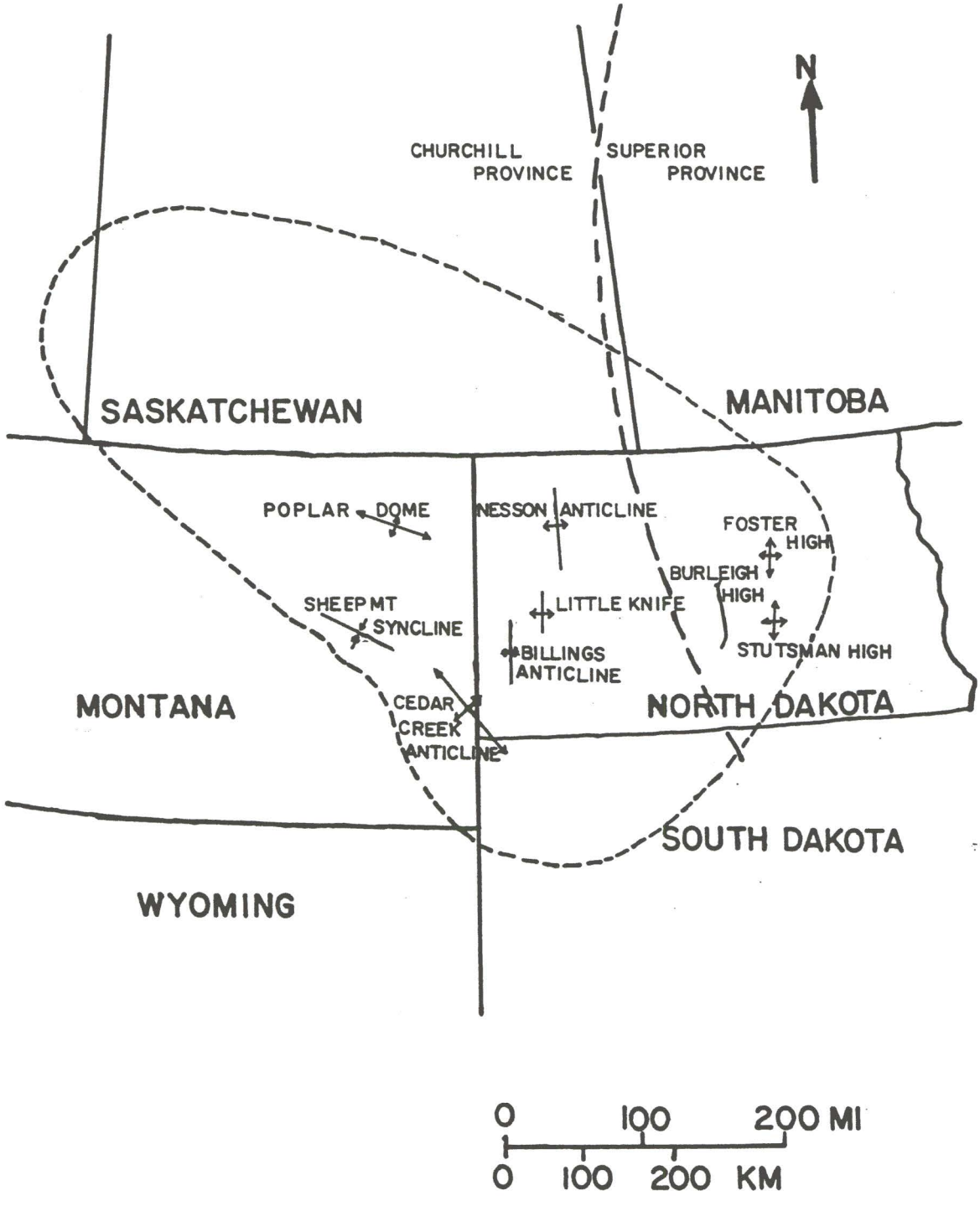
N
CHURCHILL PROVINCE
SUPERIOR PROVINCE
SASKATCHEWAN
MANITOBA
POPLAR DOME
NESSON ANTICLINE
FOSTER HIGH
BURLEIGH HIGH
SHEEP MT SYNCLINE
LITTLE KNIFE
BILLINGS ANTICLINE
STUTSMAN HIGH
MONTANA
CEDAR CREEK ANTICLINE
NORTH DAKOTA
SOUTH DAKOTA
WYOMING
0 100 200 MI
0 100 200 KM

Regional Geologic Setting

The Williston Basin is a large intracratonic basin covering approximately 200,000 square miles (Sheldon and Carter, 1979) of central North America, including western North Dakota, eastern Montana, and portions of South Dakota, southern Manitoba and southern Saskatchewan (Fig. 2). The basin is centered near Watford City, North Dakota, where approximately 16,000 feet of sedimentary rocks cover basement (Gerhard and others, 1982).

Major structural features of the Williston Basin include the Billings, Little Knife, Nesson, and Cedar Creek anticlines, the Sheep Mountain Syncline and the Poplar Dome. The area of this study lies on the western and northern flank of the Billings Anticline (Fig. 2).

The sedimentary history of the pre-Phanerozoic of the Williston Basin is not known due to deformation of these rocks. Peterman and Hedge (1964) dated the crystalline basement rocks of North Dakota at 1.7 to 2.4 Ga., and suggested that the border of the Superior and Churchill orogenic provinces lies within the Williston Basin (Fig. 2). The earliest known Paleozoic rocks were deposited during a Late Cambrian (about 520 Ma.) transgression (LeFever and others, 1987). Evidence presented by LeFever and others (1987) indicates that the initial subsidence and origin of the Williston Basin itself began no later than deposition of the Ordovician Deadwood Formation (about 490 Ma.).

Peterson (1981) noted that a structural connection existed between the Mississippian Williston Basin and the Central Montana Trough. Bickford and others (1986) postulated that basement faulting,

associated with the contact between the Superior and Churchill orogenic provinces, may have affected Paleozoic sedimentation within the Williston Basin.

By Mississippian time the Williston Basin was subsiding rapidly, and deposition of about 2500 feet of section occurred during the Paleozoic (Carlson and Anderson, 1965). Open marine conditions prevailed during deposition of the Lodgepole Formation as subsidence overtook sedimentation within the basin. The Mission Canyon Formation is late Osagean to early Meramacian, and was deposited in an increasingly restricted sea with alternating periods of carbonate and evaporite deposition. Eventually evaporite deposition dominated within the basin as evaporites prograded towards the basin center (Carlson and Anderson, 1966).

Madison Group Nomenclature

The stratigraphic nomenclature of the Mississippian of the Williston Basin has been in a state of transition and flux since attempts to extend surface nomenclature into the subsurface were first made. Peale (1893) first named the Madison Formation while working in the Three Forks region of Montana. Peale did not define a type section but divided the Madison into an upper massive "jaspery" limestone, a middle massive limestone, and a lower laminated limestone (Fig. 3). Weed (1896) considered the Madison Formation type section to be in the Madison Range south of Three Forks, Montana. Collier and Cathcart (1922) divided the Madison into two formations, the Lodgepole and the Mission Canyon, thus elevating the Madison to

Figure 3. Nomenclature of the Madison Group.

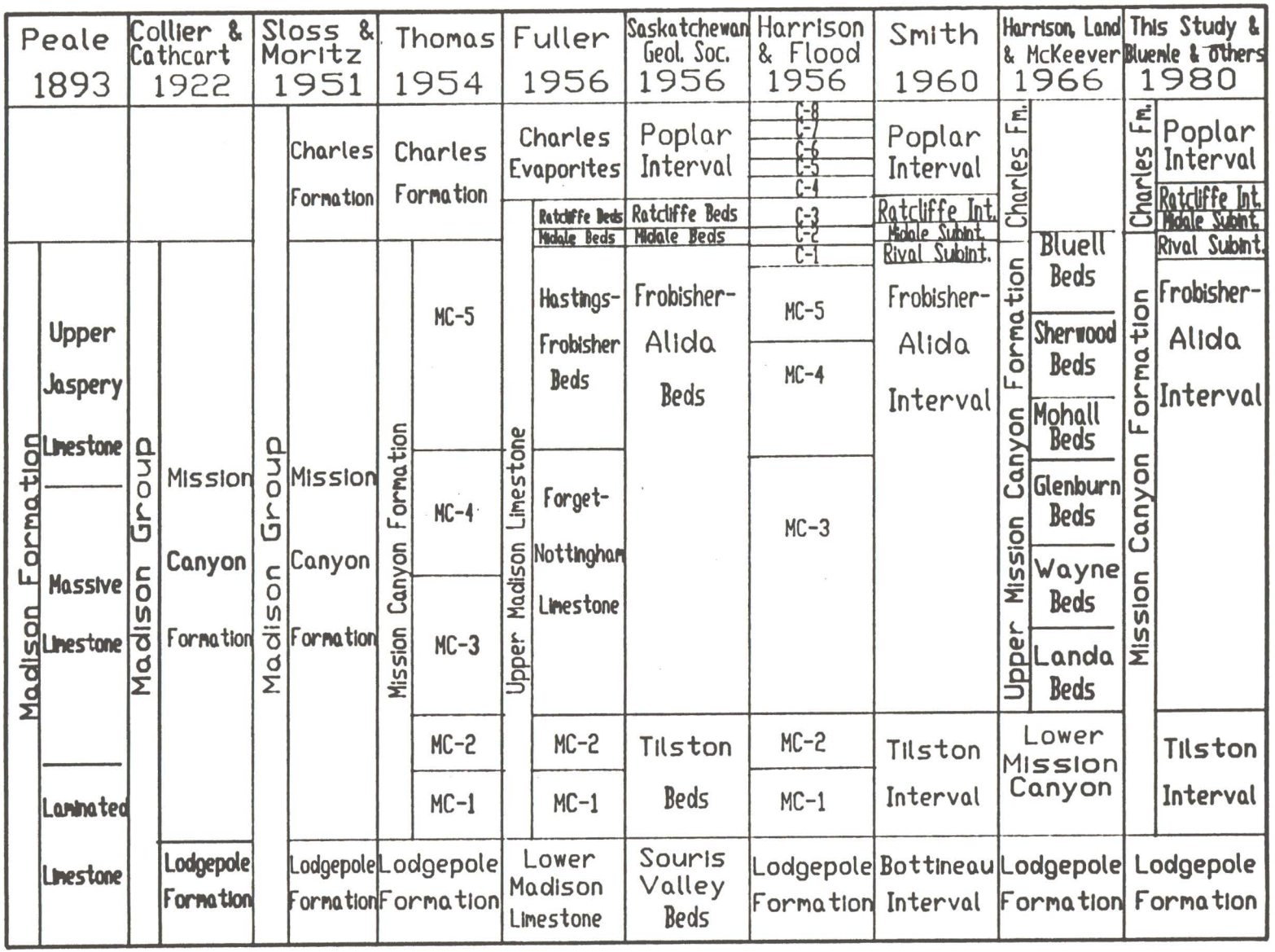
Peale 1893
Collier & Cathcart 1922
Sloss & Moritz 1951
Thomas 1954
Fuller 1956
Saskatchewan Geol. Soc. 1956
Harrison & Flood 1956
Smith 1960
Harrison, Land & McKeever 1966
This Study & Bluemle & Others 1980
Madison Formation
Upper Jaspery Limestone
Massive Limestone
Laminated Limestone
Madison Group
Mission Canyon Formation
Lodgepole Formation
Charles Formation
Charles Evaporites
Poplar Interval
Ratcliffe Beds
Middle Beds
Hastings-Frobisher Beds
Forget-Nottingham Limestone
Upper Madison Limestone
Frobisher-Alida Beds
Tilston Beds
Lower Madison Limestone
Souris Valley Beds
MC-5
MC-4
MC-3
MC-2
MC-1
C-8
C-7
C-6
C-5
C-4
C-3
C-2
C-1
Ratcliffe Int.
Middle Subint.
Rival Subint.
Frobisher-Alida Interval
Tilston Interval
Bottineau Interval
Charles Fm.
Upper Mission Canyon Formation
Lower Mission Canyon
Bluell Beds
Sherwood Beds
Mohall Beds
Glenburn Beds
Wayne Beds
Landa Beds
Mission Canyon Formation

group status (Fig. 3). Both of these formations were named for exposures along Lodgepole Canyon and Mission Canyon in northwest Montana.

Sloss and Hamblin (1942) noted the widespread extent of the Madison and suggested that the terms Lodgepole and Mission Canyon be used throughout Montana and Wyoming. They also subdivided the Lodgepole into the upper Woodhurst member and the lower Paine shale member. Holland (1952) was the first to locate a Madison Group type section precisely. He did detailed stratigraphic and paleontologic work on the Lodgepole Formation.

Seager (1942) first introduced the term Charles Formation into the subsurface to describe a series of interbedded limestone, dolomite, anhydrite, and shale beds located between the Madison Group and the overlying Big Snowy Group in a well on the Cedar Creek Anticline of eastern Montana. He placed the Charles Formation at the base of the Big Snowy Group. Sloss and Moritz (1951) placed the Charles Formation into the Madison Group after comparing the subsurface dolomites of the Williston Basin to Madison outcrops in southwestern Montana. Nordquist (1953) redefined the top of the Charles to be the top of the first massive salt bed.

As petroleum exploration and development expanded throughout the Williston Basin, workers attempted to use gamma-ray logs for correlation. Thomas (1954), working in the northeastern Williston Basin, subdivided the Mission Canyon Formation into five horizons, designated MC-1 through MC-5. He considered these persistent log-marker horizons to be silty beds of regressive depositional cycles.

Fuller (1956) also used log-marker horizons to redefine the Madison in the subsurface. He designated a "Lower Madison" limestone, an "Upper Madison" limestone, and changed the Charles Formation to the "Charles" evaporites. The Upper Madison Limestone was subdivided, in ascending order, into the MC-1 Limestone, MC-2 Anhydrite, Forget-Nottingham Limestone, Hastings-Frobisher Beds, Midale Beds, and Ratcliffe beds. The Saskatchewan Geological Society (1956) modified the work of Fuller and suggested that the Madison Group be subdivided in ascending order into the Souris Valley, Tilston, Frobisher-Alida, Midale, Ratcliffe, and Poplar beds as log-marker defined units (Fig. 3).

Increased subsurface data prompted Harrison and Flood (1956) to propose a subdivision of the Mission Canyon and Charles Formations based on log-marker horizons in northeastern North Dakota. In ascending order, they used the informal units MC-1 through MC-5 and C-1 through C-8. The top of the MC-5 or the equivalent Mission Canyon was at the base of the "State A" log-marker. Harrison and Flood (1956) recognized that their marker-defined units could not be carried towards the basin's center with any confidence. Edie (1958) lithologically recorded the Lodgepole, Mission Canyon, and Charles Formations at stratigraphically lower position towards the basin edge when compared to log-marker defined units.

Smith (1960) defined the Madison Group based on log-marker horizons while recognizing that these markers crossed facies boundaries. He modified the terminology of the Saskatchewan Geological Society (1956) by replacing the term "Souris Valley" with

"Bottineau" and adding the "Rival subinterval" to the top of the Frobisher-Alida interval and adding the "Midale subinterval" to the base of the Ratcliffe interval (Fig. 3).

Harris and others (1966) recognized six depositional "cycles" based on thin widespread silty marker beds found in cores and gamma-ray logs in north-central North Dakota. In ascending order these were the Landa, Glenburn, Mohall, Sherwood, and Bluell "beds". These cycles are separated by the Landa, K-3, K-2, K-1, Sherwood Argillaceous and the State A marker beds.

The nomenclature of Bluemle and others (1980), used in this study, is similar to Smith (1960) and is currently used by the North Dakota Geological Survey. The interval studied is within the upper Frobisher-Alida interval and extends from the Fryburg Gamma Ray marker up to the Rival subinterval (Fig. 4). The top of the Mission Canyon Formation is placed at the base of the lowest evaporite bed, so that the interval studied includes the uppermost Mission Canyon Formation and the lowermost Charles Formation.

For a more detailed and comprehensive review of the Madison Group stratigraphy and nomenclature refer to Anderson (1958), Sando and Dutro (1974), Obelenus (1985), and Carlson and LeFever (1987).

Previous Works

The numerous studies on the Mississippian Mission Canyon and Charles Formations can be broadly grouped into three (3) categories: 1) basin-wide or regional studies, 2) central and eastern Williston

Figure 4. Typical log response of the upper Mission Canyon and lower Charles Formations.

Tenneco
Amerada-State 1-16
T144N-R101W-16 SE SW
Billings County,North Dakota

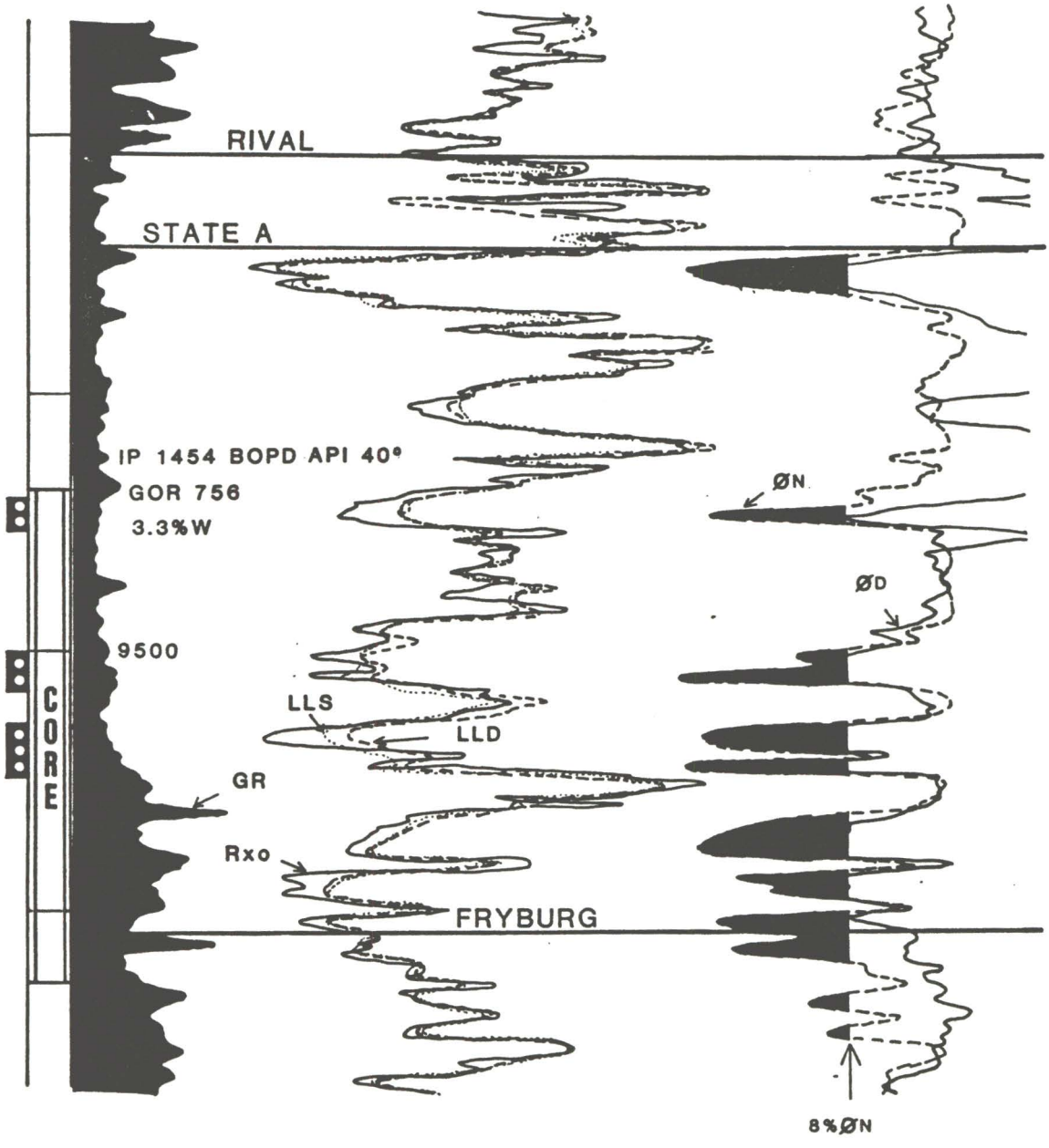

Basin studies and, 3) western Williston Basin studies. Regional studies within the Williston Basin were initiated in the late 1950's with the development of newly discovered oil fields. Edie (1958) characterized the rocks of the Mission Canyon and lower Charles Formations as having been deposited within four environmental settings: basinal, open marine, shoal, and lagoonal. Edie suggested that early compaction of the carbonates had resulted in reduced primary porosity. Harris and others (1966) recognized four similar rock types which were described as occurring in six shoaling-upward cycles.

Central and eastern Williston Basin studies were a result of the development of oil fields in which depositional environments and trapping mechanisms within the Frobisher-Alida interval were evaluated. Gerhard and others (1978) postulated that vadose dissolution of pisolites resulted in the development of porous intervals at the Glenburn Field. Elliott (1982) discussed lithofacies in a restricted circulation environment characterized by shoaling-upward cycles in the Haas Field. Elliott attributed porosity development in pisolith lithologies to mesogenetic diagenetic processes and not depositional processes. Beach and Schumacher (1982) attributed differential mechanical compaction as the petroleum trapping mechanism for the Stanley Field. Shanley (1983) suggested that the Frobisher-Alida interval represents deposition of peritidal sediments on a tidal flat which separated an evaporitic lagoon from

an open marine shelf. Shanley postulated that some prominent gamma-ray marker beds could be considered as time-stratigraphic because they represented eolian deposition during "eustatic sea level lowstands." Obelenus (1985) described the Frobisher-Alida interval as having been deposited in a complex mosaic of carbonate and evaporite facies. Obelenus, in contrast to Shanley (1983), concluded that lateral lithologic variations were not the result of sea level fluctuations but of lateral migration of facies.

Western Williston Basin studies have emphasized study of the dolomite reservoirs and stratigraphic trapping mechanisms of producing oil fields. Studies include: the Little Knife Field (Lindsay and Roth, 1982), Flaxton Field (Schwartz, 1987), and the Billings Anticline area (Mander, 1980; Altshuld and Kerr, 1982; Stephens, 1986; Horner, 1986; and Durall, 1987). A comprehensive analysis of hydrodynamic trapping and permeability development in the Billings Anticline area can be found in Petty (1989).

Methods

Preliminary work involved the examination of 265 sets of wireline logs of wells (on file with the North Dakota Geological Survey) drilled within the study area (see Appendix A). Formation tops, intervals, beds, and thicknesses of porosity were identified based upon log response (Appendix B). Cores described in this study are permanently stored at the Wilson M. Laird Core and Sample Library, operated by the North Dakota Geological Survey in Grand Forks, North Dakota.

All known cores that were available were examined. Approximately 1195 ft (365 m) of core from a total of 15 wells within the Elkhorn Ranch, Roughrider and adjoining fields were described (Appendix C). Stratigraphically, all cores examined were from the Rival and upper Frobisher-Alida intervals of the lower Charles and upper Mission Canyon Formations respectively (Fig. 4). A total of 874 ft (266 m) of the total core lengths lay between the State A and Fryburg gamma ray marker beds. Core lengths described varied between 15 ft (4.6 m) (NDGS 5258) and 101 ft (30.8 m) (NDGS 4455) and averaged about 65 ft (19 m) in length.

Continuous slabs were prepared from portions of all cores prior to description. Core surfaces were etched with dilute HCl (10%) to aid in the identification of dolostone, limestone and anhydrite gross mineralogies. Slabbed surfaces were polished with a mixture of water and #220 emery grit followed by #400 grit and then #600 grit. Polishing revealed rock textures and bioturbation structures to be more distinct. Cores were visually described using a reflected light binocular microscope and a hand lens (10X). Core samples were described using the textures of Dunham (1962) and Maiklem and others (1969) with modifiers. Coral genera were identified by comparison with photographs in Waters (1984). Burrows were identified using the figures and drawings of Chamberlain (1978) and Ekdale and others (1984). Descriptions of core were prepared and logged (see Appendix C). Selected representative polished slabs were coated with glycerin, obliquely illuminated and then photographed.

Small slabs were cut from representative portions of core for the preparation of 183 petrographic thin sections. An additional 102 thin sections were made available from the North Dakota Geological Survey and Tenneco Oil Company. Thin sections described from each cored well ranged in quantity from 1 (NDGS 4455) to 36 (NDGS 4088) and averaged 20 per well. All 285 thin sections were polished with 1 micron grit solution to aid in detailed examination. The surface of approximately one-third of each slide was stained using alizarin red-S (Friedman, 1959) to help differentiate between calcite and dolomite. A polarizing petrographic microscope was used to identify allochems and orthochems, and to identify rock textures, sedimentary features and porosity. A microfiche reader was used to describe textures and fabrics, particle packing relationships, to conduct grain size measurement, and to estimate relative porosity values. The JEOL 35C scanning electron microscope/electron probe microanalyzer was used to aid in mineral identifications.

Mechanical well logs made available by the North Dakota Geological Survey were used to pick stratigraphic intervals (see Appendix B). Structure contour maps, an isopach map of porosity, and a stratigraphic cross-section were also constructed.

RESULTS

Six distinct lithotypes have been differentiated in this study. Petrographic analysis of thin-sections and megascopic core observations were used to describe each lithotype. Lithotype distinctions were based upon common textural features, the relative abundances of allochems, and the associations between allochems. Significant sedimentary structures, bioturbation features, orthochems, and diagenetic features were also utilized in differentiating lithotypes.

Lithotype Descriptions

Crinoid Coral Packstone-Wackestone (LT-1)

Of the total core examined in this study, 249.4 feet (76 m) were of the crinoid coral packstone-wackestone lithotype with an average bed thickness of 6.4 feet (2.0 m). The crinoid coral lithotype (LT-1) is the stratigraphically lowest unit observed in this study (Fig. 5). This lithotype is often interbedded with and overlain by beds of the brachiopod skeletal wackestone (LT-2) or the skeletal burrowed mudstone-wackestone (LT-3) lithotypes. Colors of this lithotype are most commonly brownish gray or grayish black. The beds of LT-1 are massively bedded and visible sedimentary structures are absent (Table 1). Burrow mottling and bioturbation are present in much of the core.

A total of 44 thin sections of LT-1 were examined. Rock textures

Figure 5. Stratigraphic cross section A-B-C-D-E showing the relationship of lithotypes and marker defined intervals. Gamma-ray logs are to the left of each core log, and resistivity logs are to the right.

STRATIGRAPHIC CROSS-SECTION ABCDE

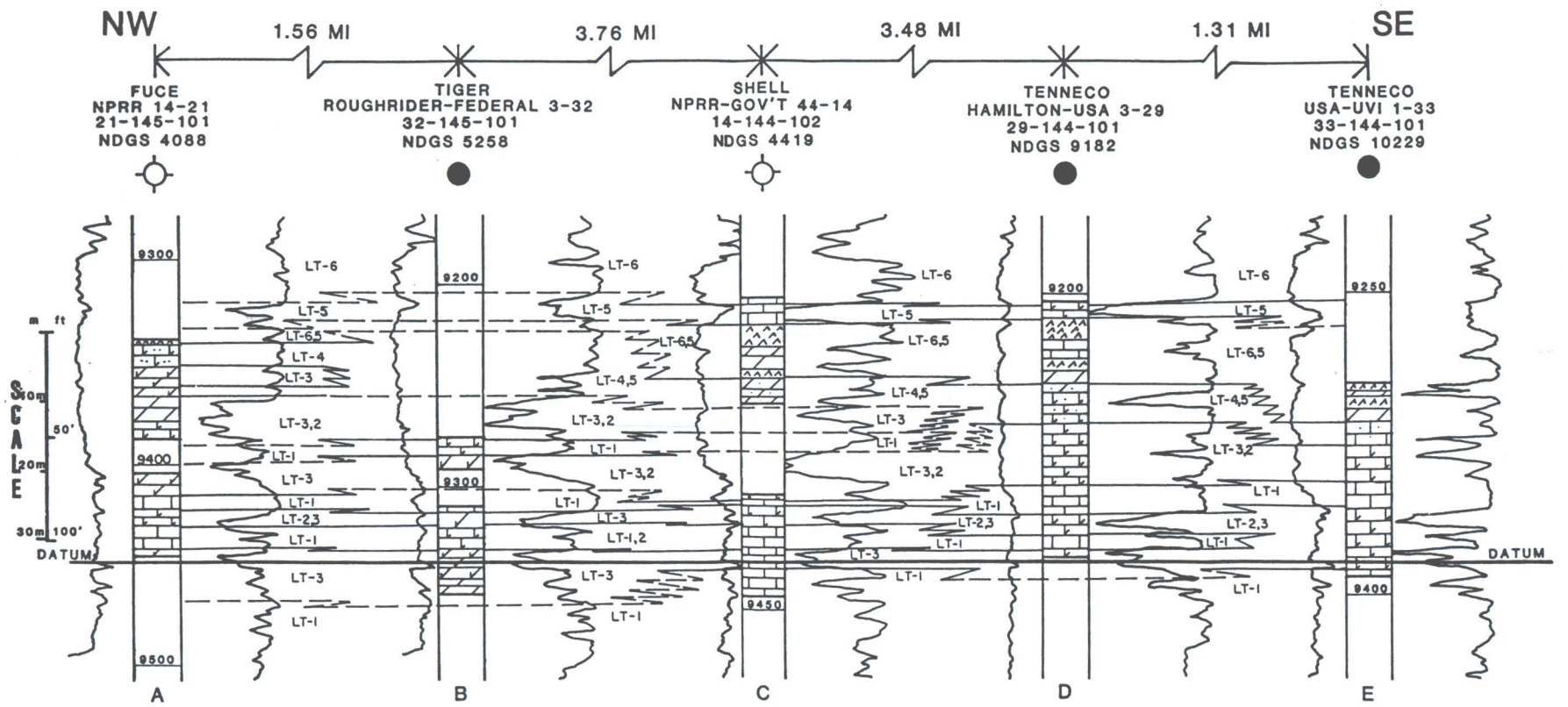

Table 1. Relative abundances of allochems and other features. Predominant= immediately obvious, dominates visually; abundant= major component; common= occurs throughout sample; some= scattered occurrences; rare= occurs with limited searching; trace= occurs with extensive searching; none= no occurrences, even with extensive searching.

TABLE 1

	LT–1	LT–2	LT–3	LT–4	LT–5	LT–6
ALLOCHEMS						
Echinoderms	Predominant	Abundant	Abundant	Some	Some	None
Brachiopods	Common	Common	Common	Trace	Trace	None
Corals	Abundant	Common	Common	Trace	None	None
Bioclasts	Common	Common	Abundant	Some	Some	None
Ostracodes	Trace	Rare	Rare	Rare	Common	Rare
Molluscs	Some	Rare	Trace	Trace	Rare	None
Forams	Rare	Trace	Rare	Rare	Rare	None
Bryozoans	Rare	Trace	Rare	None	None	None
Gastropods	Rare	Rare	Trace	Trace	Some	None
Trilobites	Rare	Trace	Rare	None	None	None
Calcispheres	Trace	Some	Rare	Some	Common	Rare
Algae	None	Trace	Rare	Trace	Some	Trace
Intraclasts	Some	Some	Common	Abundant	Common	None
Peloids	Some	Some	Common	Common	Abundant	None
Pellets	Trace	Rare	Rare	Trace	Common	None
Pisoids	None	None	None	Rare	Rare	None
Ooids	None	None	None	Some	Some	None
OTHER FEATURES						
Chondrites	None	Rare	Abundant	None	Common	None
Zoophycos	Trace	Trace	Common	None	None	None
Teichichnus	None	None	Some	None	None	None
Halo burrows	None	None	Some	None	None	None
Bioturbated	Some	Abundant	Predominant	Rare	Common	None
Thick Laminae	None	None	None	Common	Abundant	Some
Thin Laminae	None	None	None	Rare	Abundant	Some
X–Laminae	None	None	None	Abundant	Some	None

of LT-1 are wackestones and packstones (after Dunham, 1962) (Fig. 6). Skeletal and non-skeletal grains are more poorly sorted than the matrix and exhibit point and longitudinal grain contacts after Taylor (1950) and Kahle (1966). Concavo-convex and sutured grain contacts are also common (Fig. 7).

The rock type of LT-1 is limestone to dolomitic limestone. Micrite is the most common orthochem of LT-1 (Table 2). Microcrystalline dolomite (<40 um in crystal size) is common and coarser dolomite (average size of 60 to 80 um) is present in lesser amounts. Microspar is common and characterisitic of this lithotype, and pseudospar grades downward in size to microspar. Some calcspar occurs together with pervasive dolomite in the more porous sections. Bitumen occurs in intercrystalline pores adjacent to dolomite.

Pressure solution features which occur in LT-1 include the Type I and Type II stylolites of Wanless (1979). Type II stylolites, or microstylolites, are abundant in LT-1 (Fig. 8) and are associated with the less dolomitic sections and the low porosity limestones. Type I stylolites, or sutured seam stylolites, are commonly found in two ranges of amplitude; <0.5 to 4.0 cm for low stylolites, and 3.0 to 9.0 cm for high amplitude stylolites.

Porosity of LT-1 is generally poor to absent. Moldic porosity is common in LT-1 and visually ranges, where present, from 5 to 10%. Intercrystalline porosity is rare. Microfractures occur in isolated

Figure 6. Core photograph of LT-1 showing wackestone-packstone texture. Note the abundant crinoid columnals and scattered coralites. Bar scale is 1.0 in. (2.5 cm) long. NDGS 5258 at 9282 ft (2822 m).

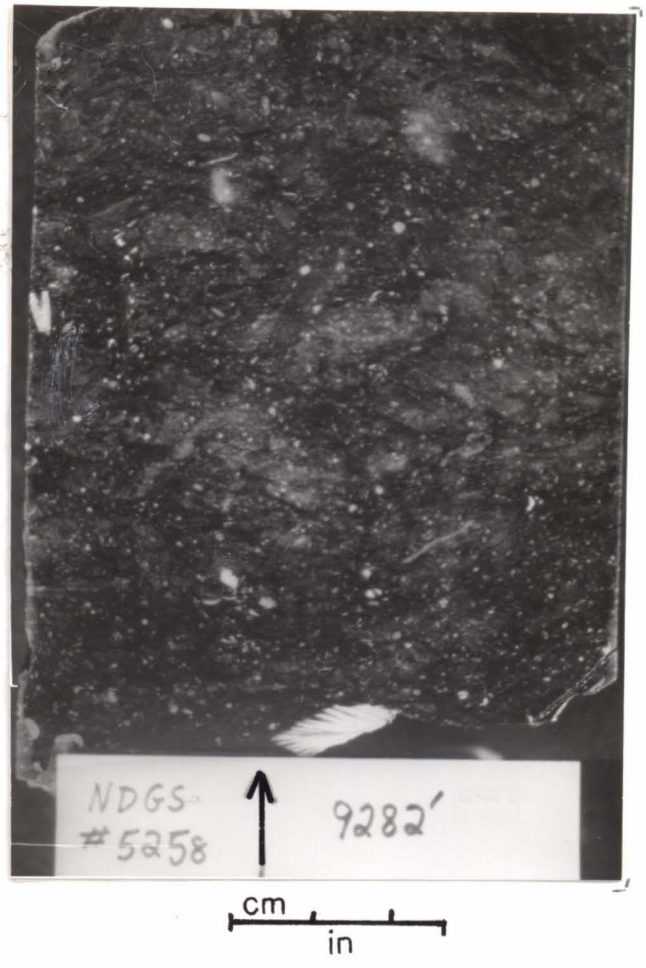
NDGS
#5258
9282'
cm
in

Figure 7. Photomicrograph of LT-1 showing grain contacts. Note sutured (S), concavo-convex (C), and longitudinal (L) grain contacts. Bar scale is 0.04 in. (1.0 mm). NDGS 5258 at 9340.5 ft (2840 m).

Figure 8. Photomicrograph of LT-1 showing microstylolitic laminae. Note crinoid columnals (C). Bar scale is 0.02 in. (0.5 mm). NDGS 5258 at 9347 ft (2841 m).

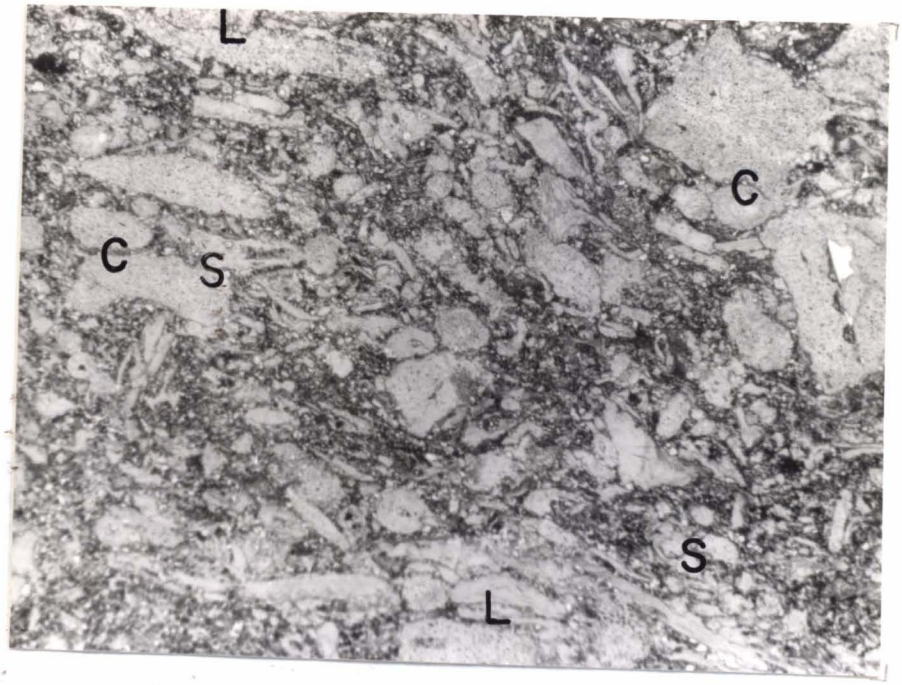
L
C
C
S
S
L

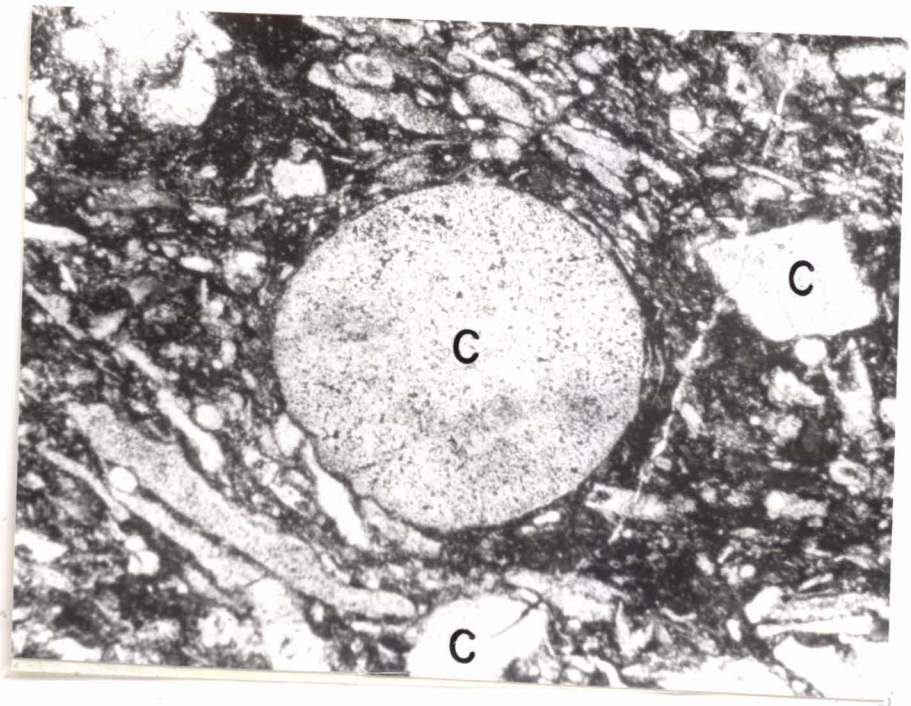
C
C
C

Table 2. Relative abundances of orthochems and diagenetic features. Predominant= immediately obvious, dominates visually; abundant= major component; common= occurs throughout sample; some= scattered occurrences; rare= occurs with limited searching; trace= occurs with extensive searching; none= no occurrences, even with extensive searching.

TABLE 2

	LT-1	LT-2	LT-3	LT-4	LT-5	LT-6
ORTHOCHEMS						
Micrite	Common	Abundant	Predominant	Common	Abundant	Rare
Microspar	Common	Some	Some	Rare	Some	None
Pseudospar	Rare	Trace	Trace	None	None	None
Micro-Dolomite	Common	Abundant	Predominant	Common	Common	Trace
Coarse Dolomite	Some	Common	Predominant	Trace	Rare	None
Saddle Dolomite	Trace	None	Common	Trace	Trace	None
Calcspar	Some	Trace	Common	Rare	Common	Trace
Dedolomite	Rare	Some	Common	Trace	Trace	None
Interxl Anhydrite	Some	Common	Common	Rare	Abundant	None
Crystallotopic Anhy	None	Trace	Rare	None	Trace	Common
Anhydrite Nodules	None	Rare	Some	Trace	Abundant	Predominant
Celestite	Trace	Rare	Some	Rare	Some	None
Detrital Quartz	Trace	Trace	Trace	Trace	Trace	Trace
Chert Cement	Rare	Trace	Some	Trace	Common	Trace
Cherty Nodules	Rare	None	Common	None	Some	None
Pyrite	Trace	Some	Some	None	Rare	Trace
Bitumen	Some	Some	Common	Trace	Rare	None
OTHER FEATURES						
Microstylolites	Abundant	Some	Common	Rare	Common	Trace
Stylolites	Common	Some	Common	Rare	Some	None
Seams	Rare	Rare	Common	Trace	Trace	None
Diagenetic Mottles	None	Rare	Some	None	Some	None
Chemical Packing	Abundant	Some	Some	Rare	Some	None
Dewatering Plumes	None	None	None	None	Rare	Rare
Microfractures	Rare	None	Trace	None	None	None

sections, and in all cases are filled with calcite or anhydrite.

The relative abundances of allochems of the various lithotypes is illustrated on Table 1. Echinoderms fragments are the predominant allochem of LT-1; unabraded crinoidal columnals are from 0.3 to 2.0 mm across. Locally, the abundance of crinoidal columnals is such that thinbedded packstones were formed (Fig. 9).

Corals and coral fragments are abundant in LT-1. Corals of the genera Vesiculophyllum, Syringopora, Sychnoelasma, and Stelechophyllum banffense are present in bioclast accumulations and are occasionally in growth position. Brachiopods range in size from 0.1 to 4.0 mm. Bioclasts are a common allochem in this lithotype, and are the debris of various skeletal allochems in a size range of 0.1 to 0.4 mm. Intraclasts are rounded and range from 0.2 to 2.0 mm in size. Other allochems present in LT-1, in decreasing abundance to trace amounts, are: peloids, molluscs, forams, bryozoans, gastropods, trilobites, ostracodes, calcispheres, and pellets.

Brachiopod Skeletal Wackestone (LT-2)

Of the total core examined in this study, 143 feet (43.6 m) was assigned to the brachiopod, skeletal wackestone lithotype (LT-2). This lithotype has an average bed thickness of 5.5 feet (1.7 m) in the cores examined. LT-2 is interbedded with LT-1 and LT-3. This lithotype is often a transitional lithotype between LT-1 and LT-3.

Figure 9. Photomicrograph of LT-1 showing packstone texture. Note the sutured grain contacts (S) and crinoid columnals (C). Bar scale is 0.04 in (1.0 mm). NDGS 5258 at 9347 ft (2841 m).

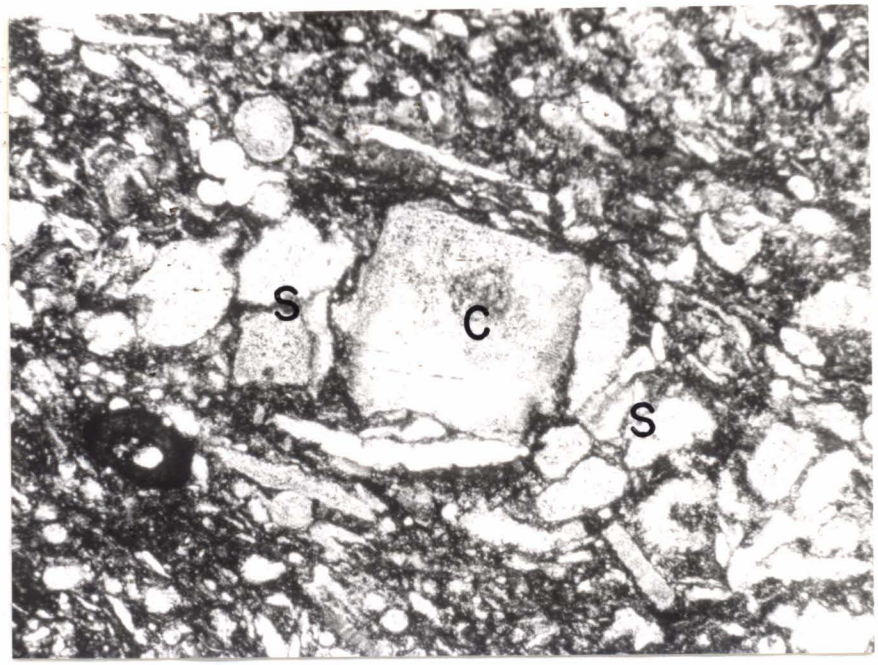
S
C
S

Dark yellow brown and dusky yellowish brown are the most dominant colors of the brachiopod, skeletal wackestone lithotype. This lithotype is massively bedded and bioturbated (Fig. 10). Ichnogenera Chondrites and Zoophycos have been rarely identified in this lithotype (Table 1).

A total of 34 thin sections were examined from this lithotype. Wackestone rock texture characterizes this lithotype with local beds of mudstone texture. Allochems are poorly sorted from the micritic matrix, and exhibit no packing.

Orthochems comprise the bulk of this lithotype; the mineralogy is calcitic dolostone to dolostone. Micrite is the most abundant orthochem, along with microcrystalline dolomite (<40 um). Coarse dolomite (30-120 um) and intercrystalline anhydrite are common. Dedolomite and traces of calcspar also occur. Bitumen, microcrystalline pyrite, metasomatic anhydrite nodules, and microspar are also present in LT-2 (Table 2).

Microstylolites and sutured seam stylolites are present in LT-2. Low amplitude stylolites range from 0.7 to 3.0 cm amplitude, and high amplitude stylolites range from 4.5 to 10.0 cm.

Intercrystalline porosity is common and ranges from 3 to 8% visually. Moldic porosity is also present and visually ranges from 1 to 9% in those sections where it is found. Microfractures are rare and are anhydrite-filled.

Crinoid columnals are relatively abundant (Table 1) and range

Figure 10. Core photograph of the brachiopod, skeletal wackestone lithotype (LT-2). Note burrows (B) and corallite (C). Bar scale is 1.0 in (2.5 cm). NDGS 4088 at 9443 ft (2861 m).

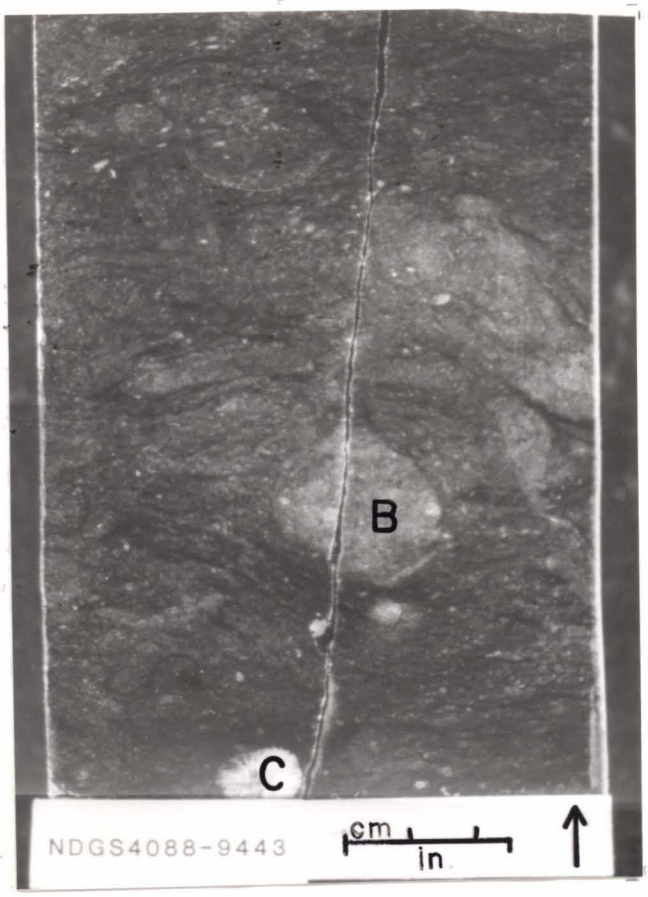
B
C
NDGS4088-9443
cm
in

from 0.3 to 2.0 mm diameter. Pseudopunctate brachiopod fragments are common with dimensions of 0.5-1.0 mm thickness and 1.0 to 6.0 cm width. Strophomenid brachiopods of the genus Schelwienella have been tentatively identified and are characteristic of this lithotype (LT-2). Corals are common and include Vesiculophyllum, Syringopora, and Sychnoelasma. Other allochems present in LT-2 are, in decreasing order of abundance: ostracodes, molluscs, gastropods, and peloids. Bioclastic debris and allochem fragments including those of foraminifera, trilobites, bryozoans and calcispheres occur in lesser amounts (Table 1).

Skeletal Burrowed Mudstone-Wackestone (LT-3)

The skeletal burrowed mudstone-wackestone lithotype (LT-3) is the most common lithotype examined in this study. Altogether, 357.5 feet (109.0 m) of this lithotype were described with an average bed thickness of 6.0 feet (1.8 m). Rocks of LT-3 are massively bedded and are interbedded with those of LT-1 and LT-2. Color is most commonly dusky yellowish brown and brownish gray.

Deposits of LT-3 were extensively burrowed by the ichnogenera Chondrites, Zoophycos, Tiechichnus, Planolites, and Corophiodes (Figs. 11, 12 and 13). Burrows are predominant and samples occasionally show complete bioturbation. Halo-type burrows (Chamberlain, 1978) are also present (Fig. 14). Anhydrite nodules and chert nodules also occur in the skeletal, burrowed mudstone-

Figure 11. Core photograph of the skeletal, burrowed mudstone-wackestone lithotype (LT-3) showing burrows Zoophycos and Chondrites. Bar scale is 1.0 in (2.5 cm). NDGS 5258 at 9282.5 ft (3004 m).


NDGS
#5258
9282'
cm
in

Figure 12. Core photograph of LT-3 showing burrow Teichichnus. Bar scale is 1.0 in (2.5 cm). NDGS 4088 at 9412 ft (2861 m).

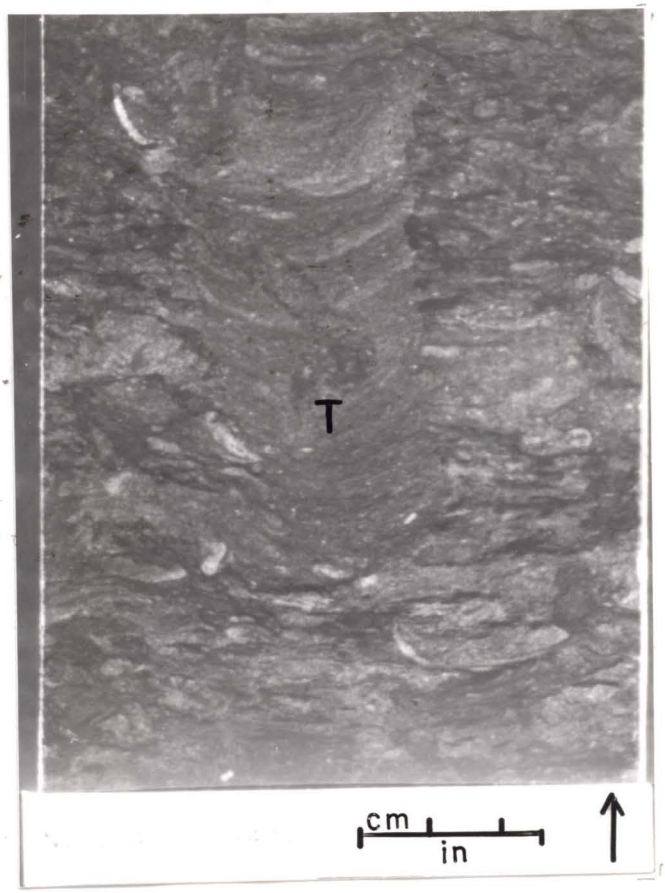
T
cm
in

Figure 13. Core photograph of LT-3 showing burrow Planolites. Bar scale is 1.0 in (2.5 cm). NDGS 5258 at 9336.5 ft (2838 m).


cm
in

Figure 14. Core photograph showing halo burrows (H). Note corallite (C). Bar scale is 1.0 in (2.5 cm). NDGS 5258 at 9331 ft (2837 m).

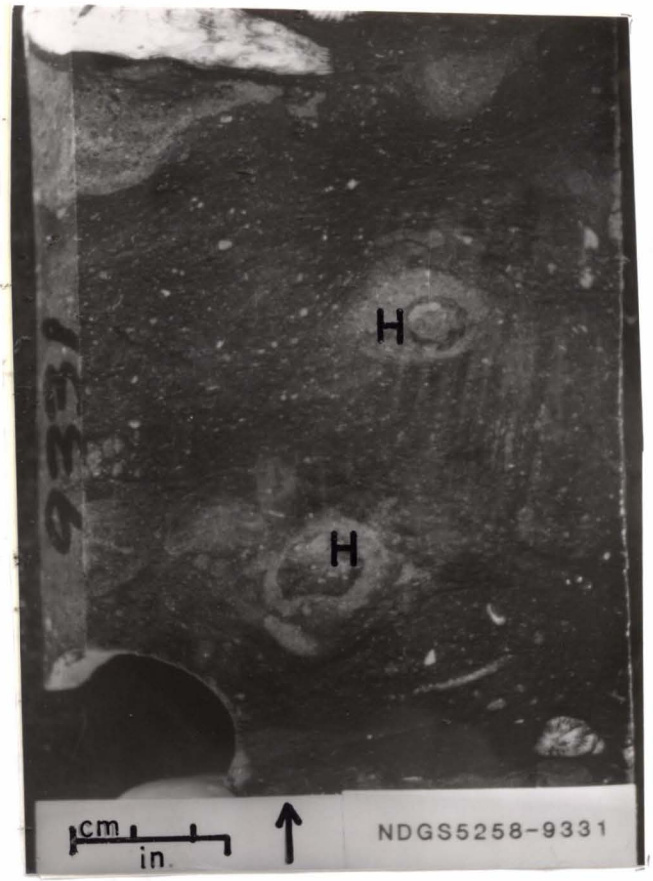
H
H
cm
in
NDGS5258-9331

wackestone lithotype (LT-3). The nodules are round to oblate and are often bounded by stylolites (Fig. 15). Sizes of nodules range from 1 to 3 cm, and occasionally reach 8 cm in diameter. The nodules are often composed of silicified skeletal packstones.

A total of 119 thin sections were examined from this lithotype. Rock textures of LT-3 are mudstones and wackestones and exhibit no particle packing. Rare cherty nodules show packstone textures, which is attributed to diagenetic processes (see diagenesis section).

The gross mineralogy of LT-3 is dolostone to calcitic dolostone. Orthochems found in LT-3 include micrite, microcrystalline dolomite (<40 um), and coarse dolomite (30-120 um), which comprise the bulk of LT-3, since this lithotype is matrix-supported. Micrite sometimes grades to microspar in thin section. Saddle dolomite is common and is characterisitic of this lithotype. Poikilitic calcite, as dedolomite and calcspar, and pore-filling microcrystalline anhydrite are common. Anhydrite nodules present range in size from 0.2 to 7.0 cm diameter and often occur along the margins of sutured seam stylolites. Chert nodules and chert cement occur in LT-3 and are associated with burrowed and bioturbated sections.

Pressure solution features commonly include microstylolites, and low and high amplitude stylolites (up to 10 cm). Thick (0.8 to 2.0 cm) seams of stylolites are characteristic of the skeletal, burrowed mudstone-wackestone lithotype (Table 2).

Abundant (5 to 12% visual) intercrystalline porosity is observed in LT-3 and is associated with the more dolomitic beds. Moldic porosity is also present but is minor in comparison.

Figure 15. Core photograph of LT-3 showing anhydrite nodules. Note the microstylolites (M) outlining the nodule (A). Bar scale is 1.0 in (2.5 cm). NDGS 2853 at 9593 ft (2916 m).

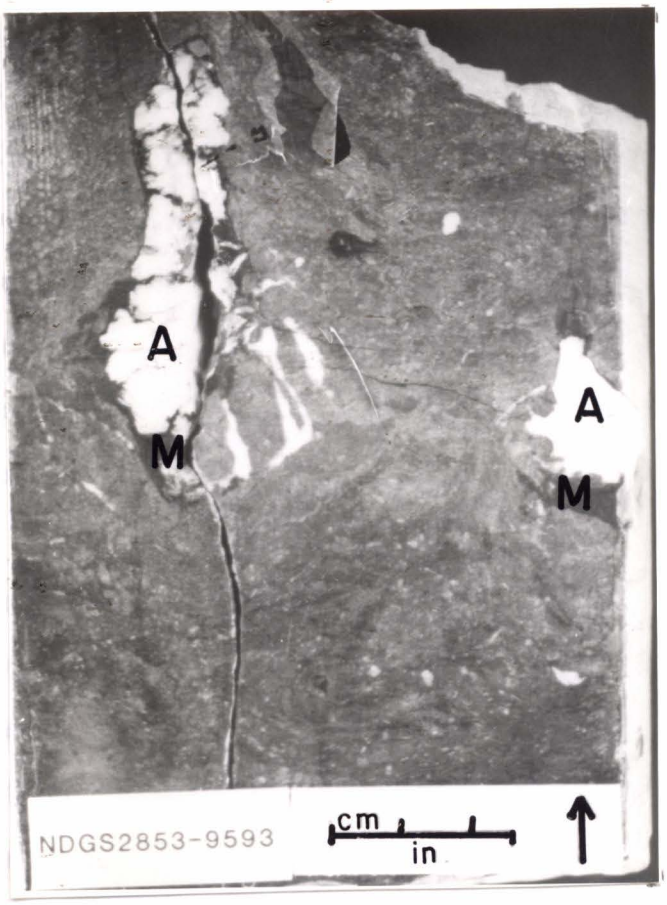
A
M
A
M
NDGS2853-9593
cm
in

Crinoid columnals and fragments from 0.3 to 2.0 mm diameter are relatively abundant (see Table 1). Bioclasts and skeletal fragments are also abundant. Thin shelled brachiopods (eg. Strophomenids such as Schelwienella) are common and range in width from 0.5 to 2.0 cm. Corals and coral fragments also occur, with the genera Syringopora and Sychnoelasma tentatively identified. Ostracodes, gastropods, and benthic forams are present in minor amount.

Non-skeletal allochems are common in the skeletal, burrowed mudstone-wackestone lithotype (LT-3). Discoidal and rounded intraclasts range in size from 0.2 to 2.0 mm diameter. Peloids are common as subrounded micritic allochems of less than 0.2 mm diameter. These particles often grade to sizes indistinguishable from the micrite or matrix material (Fig 16).

Intraclast Peloid Packstone-Grainstone (LT-4)

The intraclast, peloid packstone-grainstone lithotype (LT-4) is the most variable of the lithotypes examined in this study. A total of 125.5 feet (38.3 m) of core was examined. Rocks of this lithotype are interbedded with and most often underlain by beds of the skeletal, burrowed mudstone-wackestone lithotype (LT-3) (Fig. 17). This lithotype (LT-4) often grades into and is interbedded with packstones and wackestones of LT-5 and the anhydrites of LT-6. Rock color of this lithotype ranges from dark yellowish brown to dusky yellowish brown. Strata are commonly thickly laminated, and range in

Figure 16. Photomicrograph of LT-3 showing micritic/peloidal matrix. Bar scale is 0.04 in (1.0 mm). NDGS 4088 at 9356 ft (2844 m).

Figure 17. Core photograph of a contact between the skeletal burrowed mudstone-wackestone lithotype (LT-3) the intraclast peloid packstone-grainstone lithotype (LT-4). Note the burrow (B) which had moved peloids from LT-4 down into the sediments of LT-3. Bar scale is 1.0 in (2.5 cm). NDGS 2667 at 9612.5 ft (2922 m).

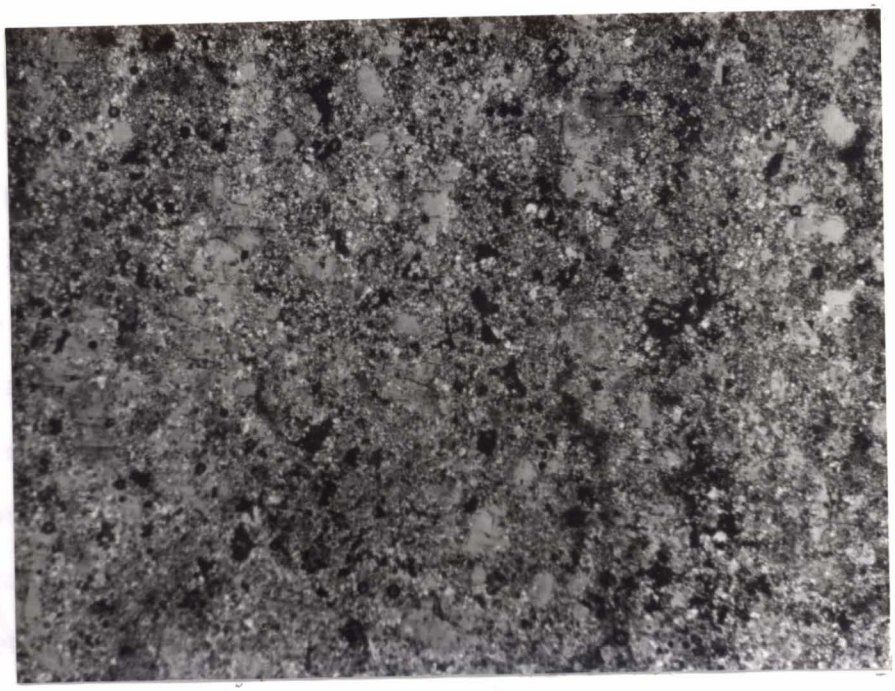

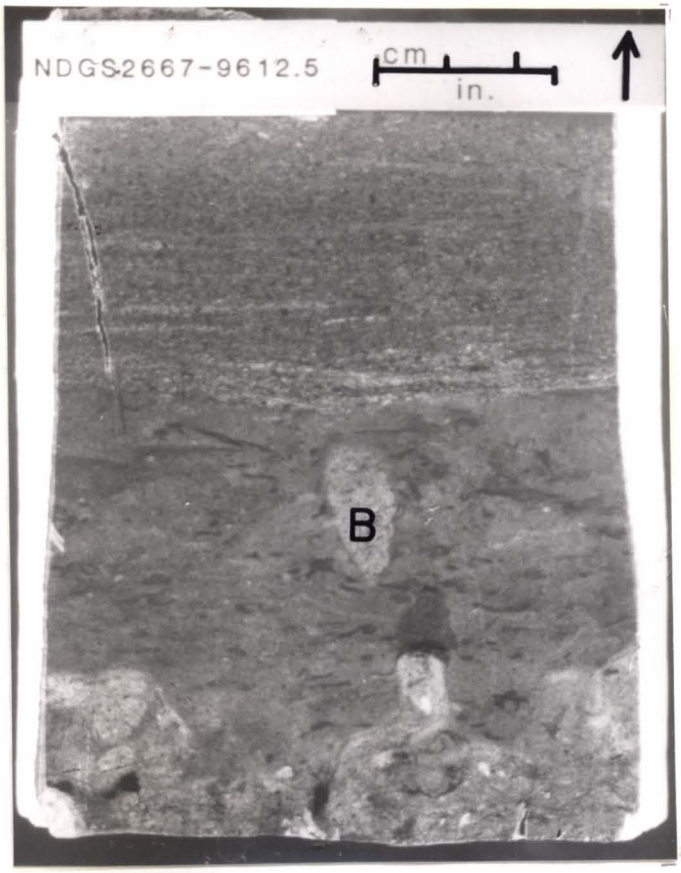
NDGS-2667-9612.5
cm
in.
B

thickness from thinly laminated to thinly bedded. Cross-laminated beds are relatively abundant in this lithotype.

Non-skeletal allochems are predominant over skeletal allochems in this lithotype. Intraclasts up to 4.0 mm diameter are abundant. These intraclasts are micritic and occasionally appear clotted in thin-section. Peloids are also common and characteristic of LT-4 (Table 1). Rounded intraclasts are variably sized and are often indistinguishable from peloids (Fig. 18). Ooliths are also present, although ooid sands are rare and/or minor in lateral extent. Minor skeletal allochems include, in decreasing order of abundance, crinoids, calcispheres, ostracodes and forams (Fig. 19). Larger skeletal allochems often have micritic envelopes.

A total of 31 thin sections were examined from this lithotype (LT-4). Packstone and grainstone textures are most common. Point packing contacts are predominant. Burrowing and bioturbation features are rare or absent. Rock type of LT-4 is limestone and dolomitic limestone. The matrix is commonly micritic, and microspar and calcspar are rare. Isopachous marine cement is common around allochems where micrite is absent. Isopachous chert cement and intercrystalline cherty cements are rare. Anhydrite intraparticle and crystallotopic cement are common in LT-4. Microcrystalline dolomite is a common cement, and is often isopachous around grains.

Pressure solution features are generally not evident in this lithotype, and stylolites and nodules are rare. These rocks

Figure 18. Photomicrograph of the intraclast, peloid packstone-grainstone lithotype (LT-4). Note peloids and clotted intraclasts. Bar scale is 0.02 in (0.5 mm). NDGS 5258 at 9347 ft (2841 m).

Figure 19. Photomicrograph of LT-4 showing ostracode. Note carapace (C) filled with pellets. Bar scale is 0.04 in (1.0 mm). NDGS 4088 at 9367 ft (2848 ft).

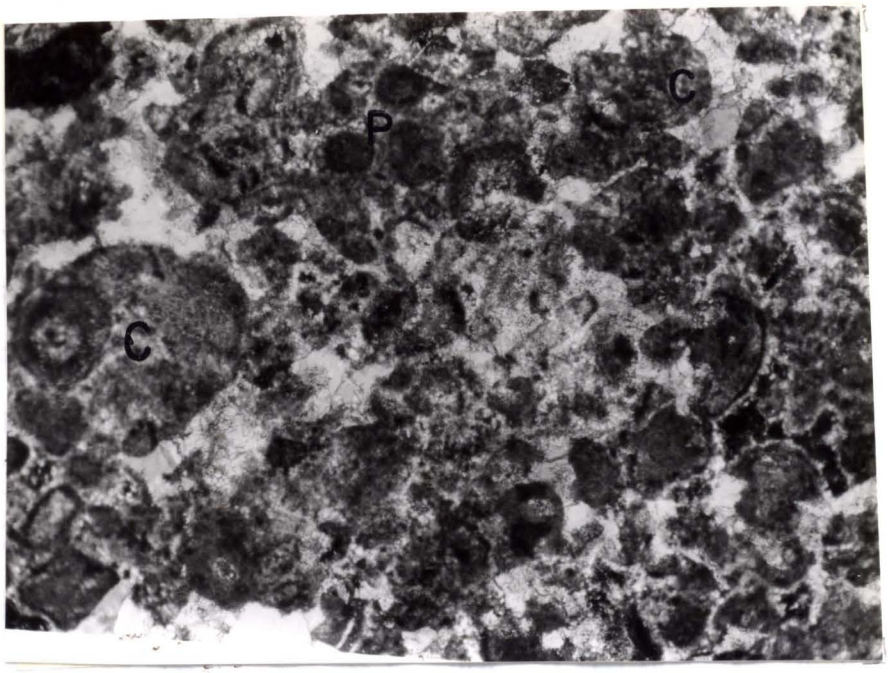
C
P
C

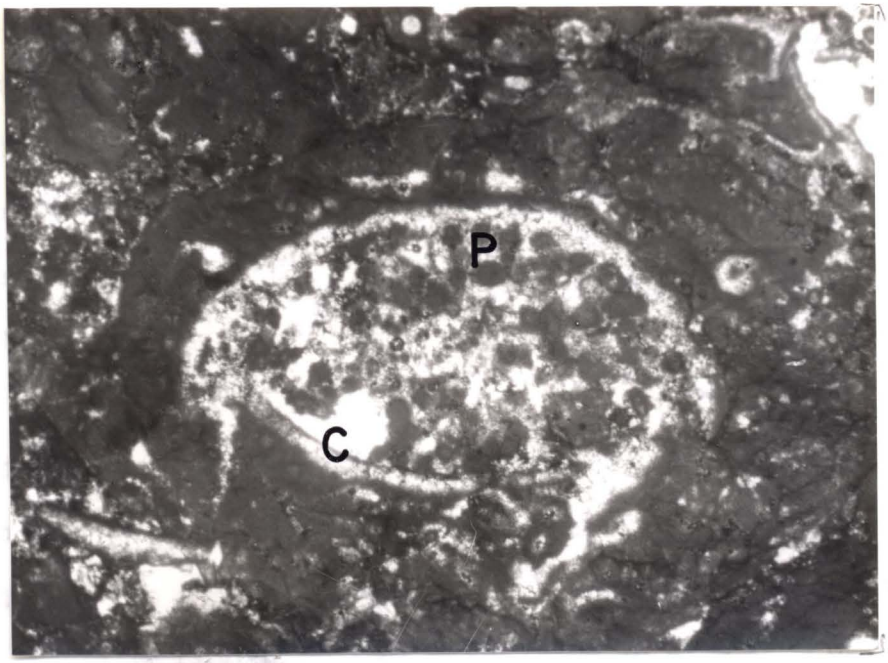
P
C

generally have insignificant amounts of porosity and only trace amounts of moldic and intercrystalline porosity are found.

Rocks of this intraclast, peloid packstone-grainstone lithotype are probably variable enough to be denoted as three separate lithotypes. However, the thinness and rarity of beds called for classification as a single lithotype based upon a commonality of texture and grain sizes. For descriptive purposes, three (3) sublithotypes are designated LT-4a, b, and c.

Cross-laminated sublithotype (LT-4a)

The cross-laminated sublithotype (LT-4a) is a distinct sublithotype based upon packstone texture and the presence of low angle current laminations (Figs. 20 and 21). Angular and rounded intraclasts and peloids are the predominant allochems in LT-4a.

Foram Algal Packstone sublithotype (LT-4b)

The foram, algal packstone sublithotype is distinguished by the presence of benthic foraminifera and algal clasts. Codiacean algal clasts are often large (>2.0 mm) and give a rudstone to packstone texture (Fig. 22).

Oolith Pisolith Packstone-Grainstone sublithotype (LT-4c)

The oolith, pisolith packstone-grainstone sublithotype is characterized by the presence of micritic, superficial ooliths and some rare, radially fibrous ooliths which range in size from 0.3 to 2.0 mm. Pisoliths occur in radially fibrous form, and as whole or

Figure 20. Core photograph of LT-4a. Note cross laminations (XL). Bar scale is 1.0 in (2.5 cm). NDGS 2667 at 9609 ft (2921 m).

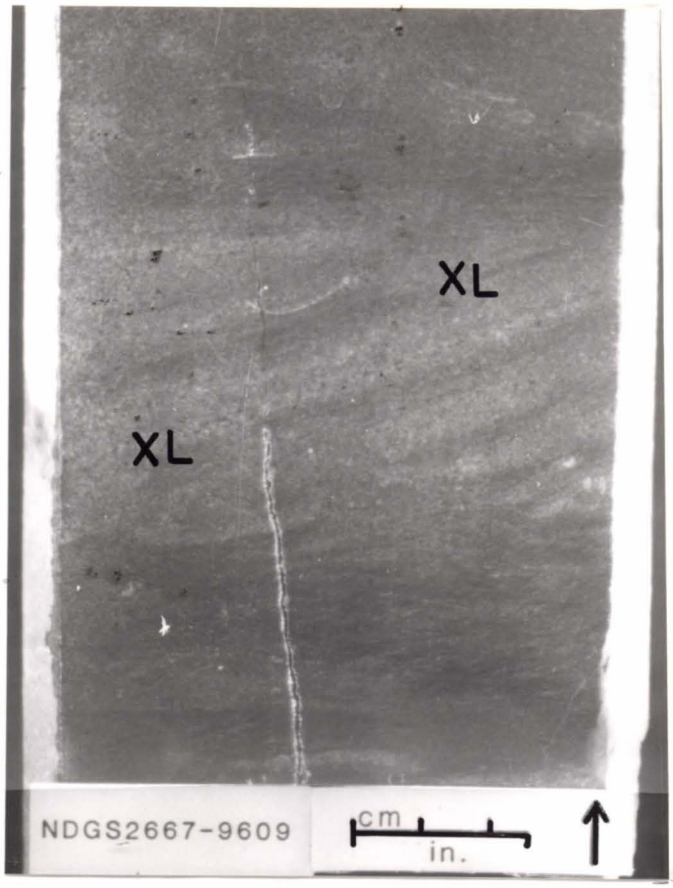
XL
XL
NDGS2667-9609
cm
in.

Figure 21. Core photograph of LT-4a. Note cross laminations (XL) and the chert nodule (CH) bounded by stylolites in the upper lithology (LT-3). Bar scale is 1.0 in (2.5 cm). NDGS 4088 at 9377 ft (2851 m).

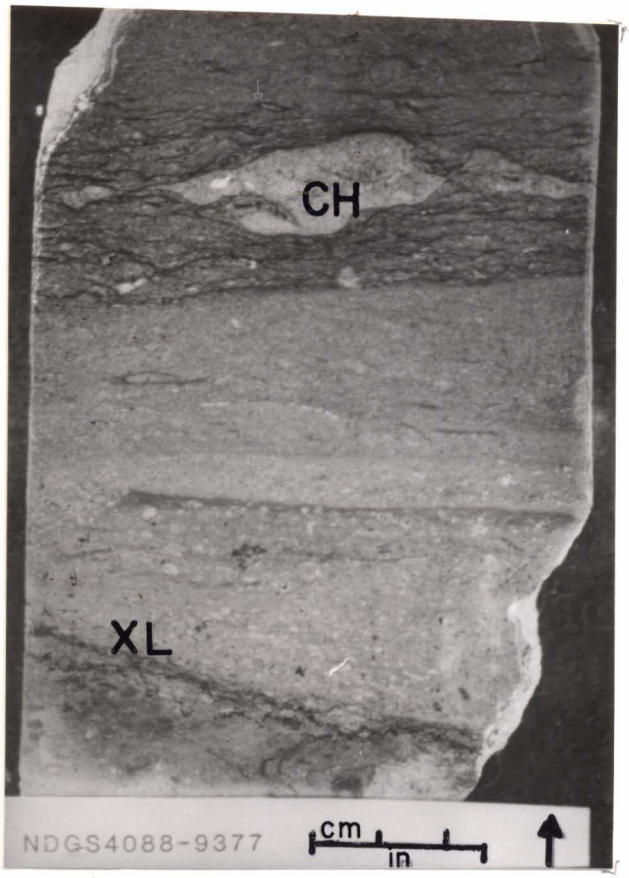
CH
XL
NDGS4088-9377
cm
in

Figure 22. Core photograph of the foram, algal packstone sublithotype (LT-4b) overlying the oolith, pisolith packstone-grainstone sublithotype (LT-4c). Note the foram/algal clasts (FA) and the thin crusts (CR). Bar scale is 1.0 in (2.5 cm). NDGS 4455 at 9373 ft (2849 m).

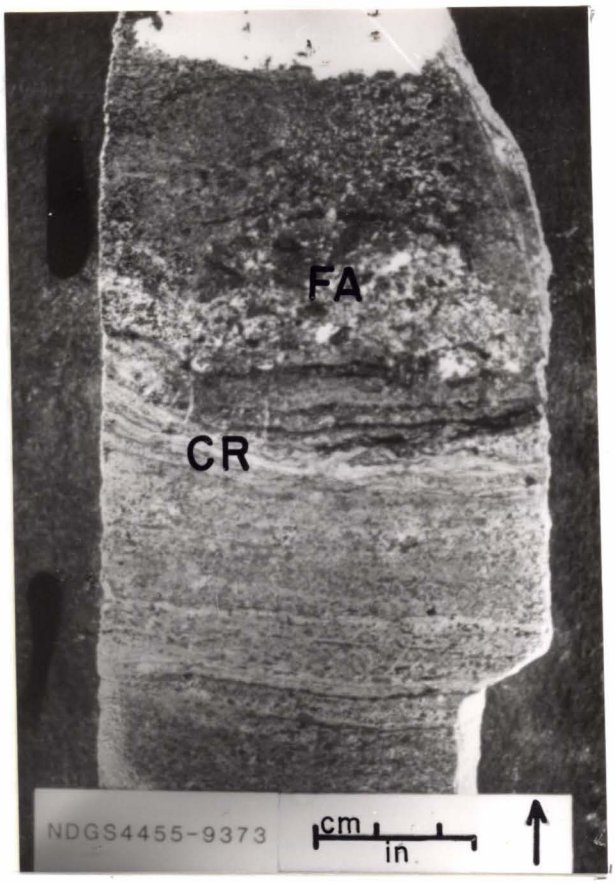
FA
CR
NDGS4455-9373
cm
in

broken grains. Pisoliths range in size from 2.0 to 4.0 mm diameter and often approach rudstone texture (Fig. 22).

Packstone and grainstone beds often exhibit graded bedding and current ripples. Allochems are isopachously cemented with calcite or are replaced by anhydrite.

Peloid Intraclast Ostracode Packstone-Wackestone (LT-5)

Of the total core examined in this study, 208.3 feet (63.5 m) were of LT-5. The average described bed thickness is 3.9 feet (1.2 m). LT-5 beds are often overlain or interbedded with the anhydrites of LT-6 and occasionally grade into the bedded anhydrites of LT-6. Color of LT-5 ranges from pale yellowish brown to dark yellow brown. Beds of this lithotype are thickly to thinly laminated (Fig. 23). Packstone and wackestone lamina are interspersed with thin laminae of mudstone texture. Many thick laminae resemble the subaerial crusts described by Elliott (1982). Mudcracks and mudchip accumulations are present (Fig. 24). Cross-laminations similar to those of LT-4a also occur. Anhydrite-filled fenestra are present in LT-5.

A total of 50 thin sections were examined from this peloid, intraclast, ostracode packstone-wackestone lithotype. Point, longitudinal and concavo-convex packing occur in this lithotype. Peloids, pellets and intraclasts are the dominant allochem types (Table 1). Packstone and wackestone textures predominate, with a tendency towards grain-supported fabric. The matrix is comprised

Figure 23. Core photograph of the peloid, intraclast, ostracode packstone-wackestone lithotype (LT-5). Note the inclined burrow (I) crossing laminations, and the burrow mottling (M). Bar scale is 1.0 in (2.5 cm). NDGS 2853 at 9470 ft (2879 m).

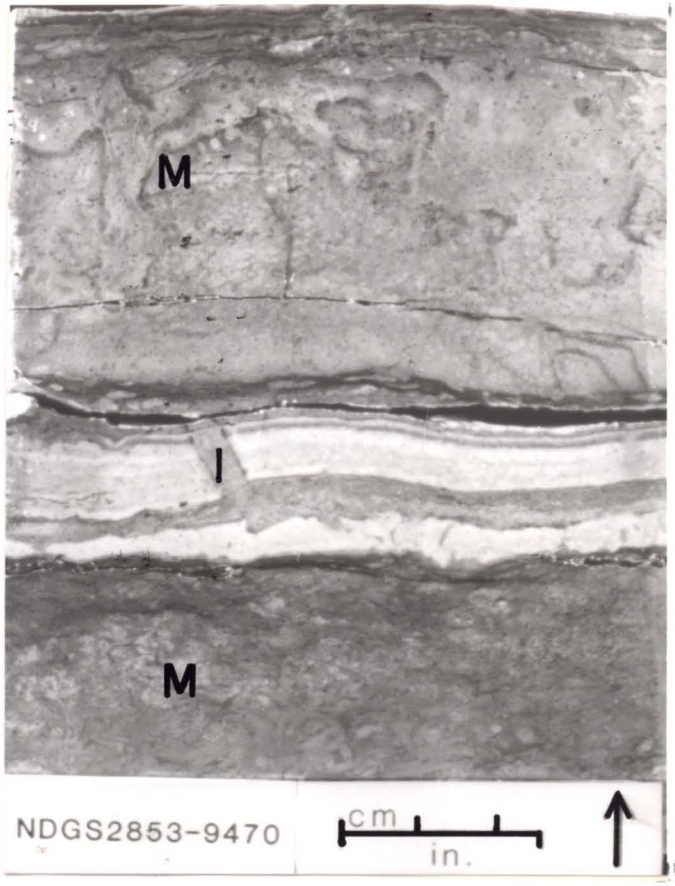
M
I
M
NDGS2853-9470
cm
in.

Figure 24. Core photograph of LT-5 showing laminated carbonate. Note the mudcracks (M), and possible teepee structure (TP). Bar scale is 1.0 in (2.5 cm). NDGS 4455 at 9307 ft (2829 m).

Figure 25. Photomicrogaph of LT-5 showing crystallotopic anhydrite. Note the felted anhydrite texture (F) and the pseudomorphs after gypsum (G). Bar scale is 0.02 in (0.5 mm). NDGS 5328 at 9291.5 ft (2825 m).

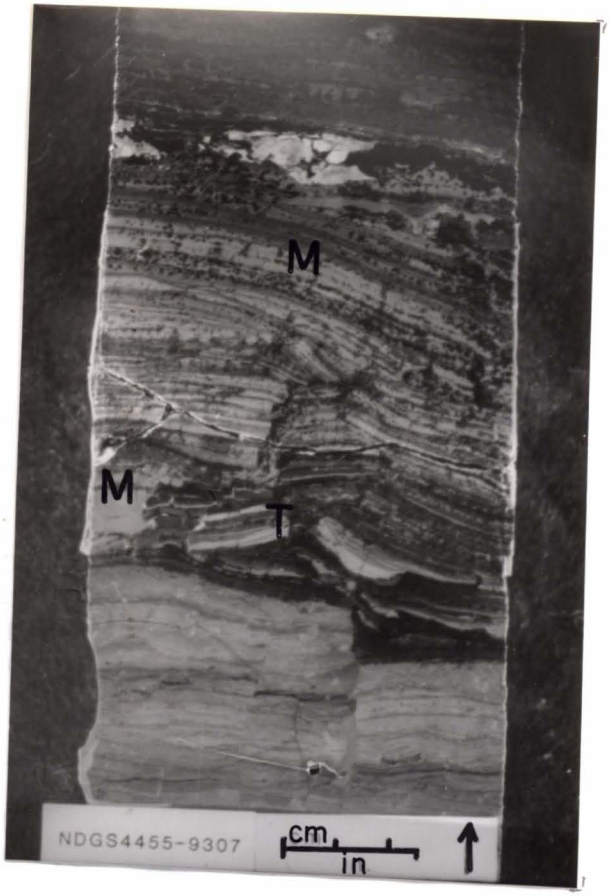
M
M
T
NDGS4455-9307
cm
in

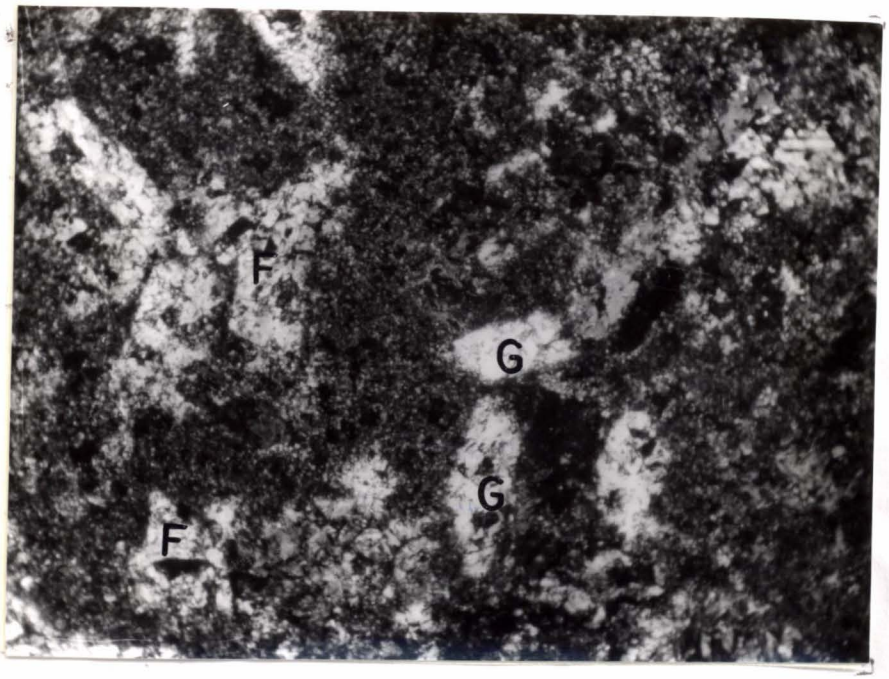
F
G
G
F

of micrite. Muddier, or more micritic, sections exhibit burrow structures including, the ichnogenera Planolites. Ostracodes are common and characteristic of LT-5. Carapaces range up to 1.0 mm in diameter and are both articulated and disarticulated. Other allochems in LT-5 are, in decreasing order of abundance, are calcispheres (50 to 100 um thick, double walled), ooliths, gastropods, codiacean algae, crinoids, forams, molluscs, and pisoliths.

The rock types range from dolostone to anhydritic dolomitic limestone. Micrite is the most abundant orthochem and is gradational to microspar. Microcrystalline dolomite is common and ranges in crystal size from 10 to 30 microns. Intercrystalline anhydrite is abundant and often replaces matrix and allochems. Anhydrite nodules are also abundant and range from 0.5 to 2.0 cm in diameter. Anhydrite nodules increase in size and number as proximity to the massive anhydrites increases. Crystallotopic anhydrite textures (Maiklem and others, 1969) are also present in this lithotype (Fig. 25).

Microstylolites are common and sutured seam stylolites also occur. Diagenetically mottled sections are characteristic of LT-5 and are discussed in the pressure solution subchapter to follow.

Porosity is poorly developed in this lithotype. Interparticle and fenestral porosity are the only pore types observed and are poorly developed to immeasurable.

Nodular and Bedded Anydrite (LT-6)

Of the total core examined for this study, 111 feet (33.8 m)

were assigned to the nodular and bedded anhydrite lithotype (LT-6). The anhydrite lithotype comprises the upper portion of the studied section. LT-6 is underlain by, and occasionally interbedded with, the laminated rocks of LT-5. Cryptalgally laminated carbonates often underlie and are intercalated with bedded massive anhydrites of LT-6. Anhydrite structural types and textures (after Maiklem and others, 1969) include, in decreasing order of abundance, massive, bedded massive, nodular mosaic, distorted bedded, and variations of those textures. Thick and thin laminae of dolomite and clay are scattered throughout the bedded and nodular anhydrites (Fig. 26).

A total of 7 thin sections were examined from LT-6. Allochems are rare in this lithotype. Rare amounts of double-walled calcispheres (80-150 um diameters), ostracodes, and codiacean algae are present within the beds of nodular anhydrite.

Dewatering plumes are present in the massively bedded anhydrites. Microstylolites are interspersed with organic laminae among nodules. Anhydrite pseudomorphs of gypsum crystals occur as laths. Clastic anhydrite is rare and is in the form of lithified, recrystallized gypsum sand (Fig. 27).

Interspersed with anhydrite nodules are pale yellow brown to brownish gray dolomudstone laminae (Fig. 26). Anhydrite color is very light to medium gray and occasionally light blue gray. Petrographic examination of the anhydrite reveals subfelted and felted crystal textures in the nodular lithologies and cryptocrystalline to subfelted textures in the massive anhydrite lithologies.

Figure 26. Core photograph of the nodular and bedded anhydrite lithotype (LT-6). Note the clay laminae (C), and laminated carbonate (L) between the nodular beds (N). Bar scale is 1.0 in (2.5 cm). NDGS 2667 at 9537.5 ft (2899 m).

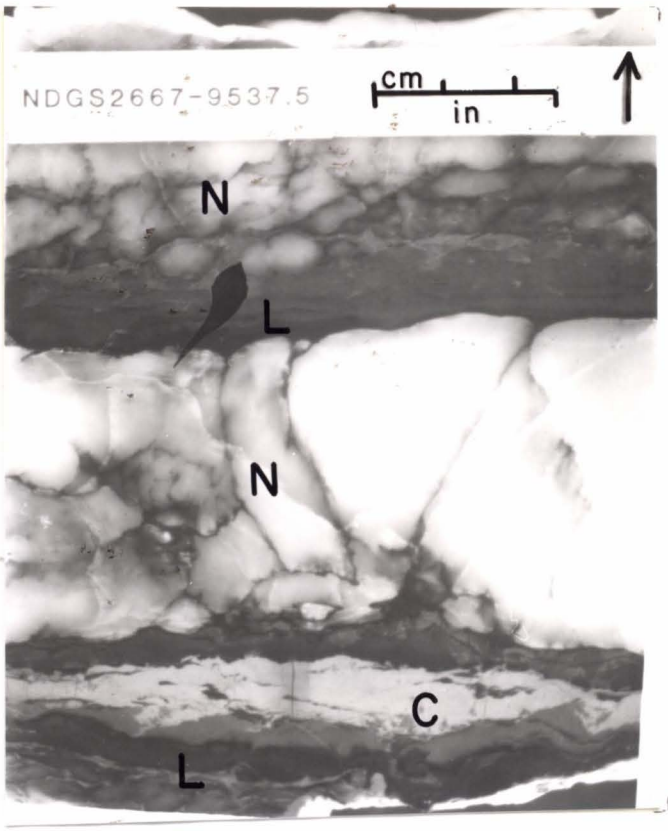
NDGS2667-9537.5
cm
in
N
L
N
C
L

Figure 27. Core photograph of the bedded anhydrite lithotype (LT-6). Note relict gypsum clasts (G) resembling a gypsum sand. Bar scale is 1.0 in (2.5 cm). NDGS 2853 at 9508 ft (2890 m).

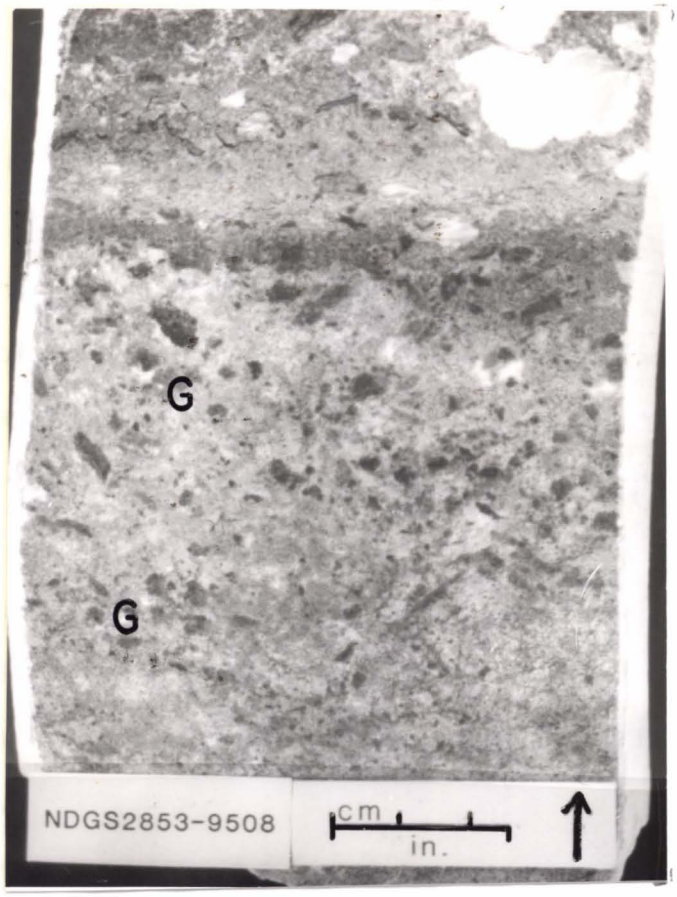
G
G
NDGS2853-9508
cm
in.

INTERPRETATIONS

The interpretation of the environment of deposition for each of the previously described lithotypes is based upon comparison with lithologies from ancient and modern environments as described in the literature. Textures, sedimentary structures, mineralogy, stratigraphic relationships, bioturbation features and other characteristics were used to establish that the carbonates and evaporites in this part of the Williston Basin were deposited in environments ranging from open marine to sabkha. Biotic associations from modern environments are used (Heckel, 1972) to interpret fossil assemblages observed in this study.

In an intracratonic basin, such as the Mississippian Williston Basin, the influence of diurnal tides may have been minimized or absent. Irwin (1965) postulated that the depositional setting of the Williston Basin was an epeiric sea. Shaw (1964) postulated that an epeiric sea would have gentle bottom slopes ranging from 0.1 to 0.5 ft/mile (0.02 to 0.1 m/km). Shaw suggested that paleogeography limited the range of tidal motions and that wind-generated wave actions were responsible for features found in marginal marine environments. Obelenus (1985) however, proposed that tides did have a significant impact upon deposition in the Frobisher-Alida, and produced common intertidal or tidal flat features in the basin margins.

The depositional center during Mississippian time has been

reconstructed to lie between 5 and 15 degrees north of the equator (Habicht, 1979; Scotese and others, 1979). Quinn (1986) found that a reconstruction of trade wind directions would have brought warm, dry air from continental areas westward over the epeiric sea. Generally evaporitic conditions would then have been a dominant factor influencing deposition. Luther (1987) theorized that dense evaporitic brines, together with an influx of marine waters entering through the Central Montana Trough, would have set up salinity gradients within the sublittoral waters of the basin.

Since there is no modern example of an epeiric sea, and the influence of diurnal tides may be in question, this study will use the terms sublittoral, littoral, and supralittoral as suggested by Hedgpeth (1957) in place of the terms subtidal, intertidal, and supratidal.

Lithotype Interpretations

Crinoid Coral Packstone-Wackestone (LT-1)

LT-1 was deposited in a sublittoral setting, on a surface of gentle slope, in moderate to low energy, and in normal marine waters with good circulation. The presence of stenohaline organisms (Fig. 28) indicate normal marine salinity of 30-40 ppt (Heckel, 1972, p. 234). The relatively unabraded crinoidal columnals, the presence of unbroken brachiopod shells, and the preservation of whole corals suggest low-energy conditions with little skeletal transport.

Figure 28. Photomicrograph of LT-1 showing crinoids (C), brachiopods (B), and molluscs (M). Note the concentration of organic microlaminations, and the overpacked texture. Bar scale is 0.04 in (1.0 mm). NDGS 5258 at 9310 ft (2830 m).

Figure 29. Core photograph of LT-1 showing bioturbate texture. Note burrows Chondrites (C) cutting through dark organic areas. Bar scale is 1.0 in (2.5 cm). NDGS 4088 at 9419 ft (2863 m).

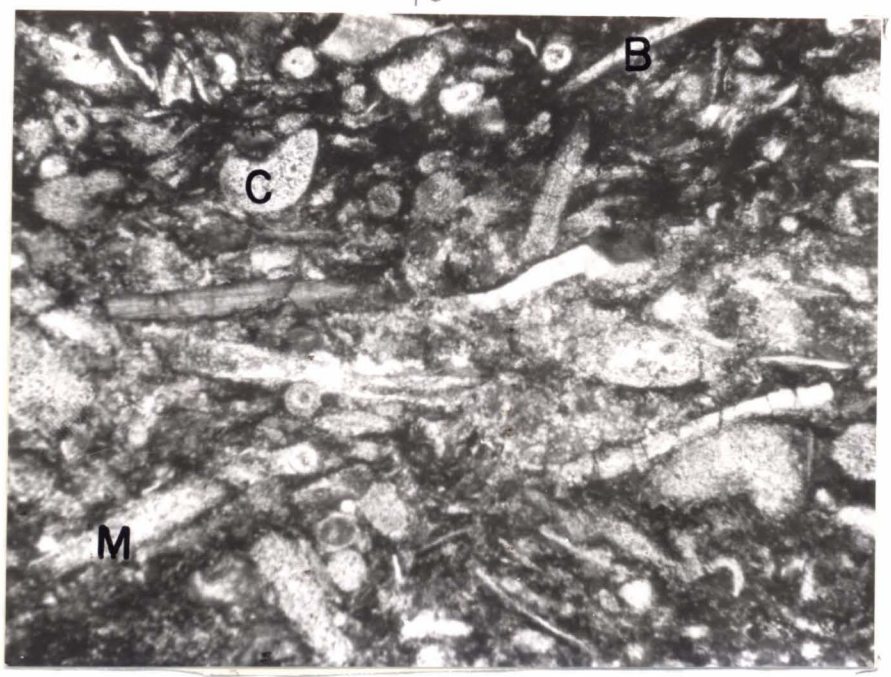
B
C
M

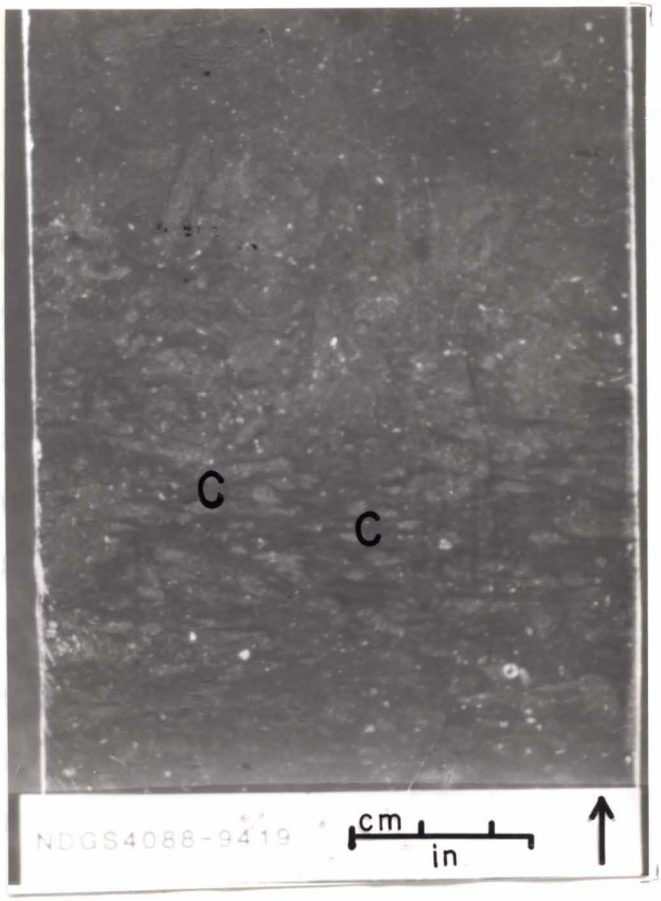
C
C
NDGS4088-9419
cm
in

Packstone or overpacked textures may indicate periods of higher energy variations within this environment, but this texture is more likely a result of chemical packing of grains (see compaction section). Localized packstone textures may also be a result of periodic storms or reflect an increased energy regimen due to the movement of oceanic density currents within the basin (Luther, 1987).

The significant mud fraction of this lithotype indicates that little winnowing occurred. The micrite or lime mud may have resulted from winnowing of adjacent higher energy environments, in-situ degradation (Stockman and others, 1967) of less resistant carbonate skeletons, or the biogenic activities of burrowing and boring organisms.

The relatively dark color of this lithotype often seems to be related to the presence of black organic micro-laminations (Figs. 8 and 28). Petrographic examination reveals that diagenetic pressure solution (see pressure solution subchapter) has resulted in the concentration of insoluble clay minerals, so that pseudolaminations occur in this lithotype. The lack of stratification would ordinarily indicate low energy to stagnant conditions, but the normal marine biota and the wackestone-packstone textures seem to preclude this. The lack of stratification is primarily due to the actions of burrowing organisms. Burrowers would churn or bioturbate the soft sediment in order to feed, move and dwell. Burrowers would seek out organic-rich laminae for feeding and in the process would destroy any

sedimentary structures. This results in a homogenized texture such as in Figure 29, which resembles a massively bedded sediment.

The presence of stenohaline organisms and a preponderance of organisms moving on and through the substrate indicate well-oxygenated and organic-rich conditions. The bioturbated textures indicate a soft, readily burrowed substrate.

Brachiopod Skeletal Wackestone (LT-2)

LT-2 was deposited in a shallow sublittoral setting, on a hummocky bottom surface, under low-energy conditions and in transitionally restricted waters. The presence of stenohaline crinoids, rugose corals, and brachiopods indicate that salinity was within the normal marine range (30-40 ppt). The appearance of euryhaline ostracodes, bivalve molluscs, algae, and gastropods indicate that the environment of LT-2 was periodically hypersaline (Heckel, 1972, p.234) relative to the environment of LT-1. The thin (0.5-1.0mm) shells of the brachiopod Schelwienella also indicate a stressed, perhaps restricted, environment with elevated salinity.

Water depth was in the sublittoral range, with occasional storm-generated currents depositing thin, localized packstone zones. The winnowing of muds was minor as evidenced by the abundance of micrite.

Bioturbation is a dominant influence upon the texture of this lithotype. Primary sedimentary structures were destroyed by the intense action of burrowing organisms. Cross-cutting burrows observed (see Figs. 11 and 13) suggest either intensive or multiple periods of burrowing, indicative of a soft substrate. The presence of the fixed

feeding trace Zoophycos (among others), supports this interpretation of a soft substrate and near-normal oxygenation and salinity at the sediment-water interface. A fixed feeding trace would require abundant organic material for feeding and sufficient water oxygenation to permeate the substrate.

Lithotype 2 offers somewhat conflicting evidence of normal and restricted salinity. This lithotype appears to be moderately restricted, with recurrent replenishment from adjacent open marine waters. This lithotype is often transitional with LT-1 and LT-3. A hummocky sediment surface of very low relief is suggested by the lack of current generated structures, and the massive bedding. Steady biologic generation of carbonate is indicated by the pervasiveness of bioturbation.

Skeletal Burrowed Mudstone-Wackestone (LT-3)

LT-3 was deposited in a sublittoral setting, on a undulating bottom surface, with low energy conditions and in waters of restricted circulation. The mudstone and wackestone textures indicate low energy conditions with little winnowing of muds. Undulating bottom surfaces are suggested by the lack of current generated sedimentary structures. Contrasting textures suggest varying interstitial oxygenation levels. Thin beds of organically-laminated mudstones accumulated under locally anoxic conditions within low areas of the sediment surface. Thin beds of skeletal wackestone accumulated on elevated areas, which were less anoxic. These beds were not observed to be continuous from one core to other cores as close as one-half mile away. Massive bedding of this lithotype

suggests steady generation of micritic carbonate. The brown colors of this lithotype are suggestive of reducing conditions.

Faunal forms suggest a wide range of salinity. Abundant crinoid columnals, corals and other stenohaline bioclasts were present. These suggest that salinities were in the normal marine (30-40 ppt) range. However, stressed conditions are indicated by the relative thinness (0.5 to 1.0 mm) of the brachiopod shells and the lack of corals in growth position. Other faunal forms, including ostracodes, benthic forams and gastropods are relatively minor, but suggest hypersalinity (Heckel, 1972). Bioclasts and skeletal debris are pervasive in this lithotype. These allochems include many stenohaline forms which probably were derived from the adjacent nearshore shoals or were carried from open marine waters. The very small sizes of these allochems and their fragmental condition suggest that they were buoyed by currents or upwellings into this quieter, more restricted environment.

Bioturbation and burrowing processes are important to the interpretion of the depositional environment of this lithotype. The bioturbation structures preserve a record of substrate and interstitial oxygenation conditions (Fig. 30). Feeding burrows such as Zoophycos indicate that interstitial oxygenation was good. This is because the burrower remains in one area for a period of time (Fig. 11). Vertically oriented burrows (Figs. 12 and 31) not only indicate a soft substrate that can readily be penetrated, but also suggest well-oxygenated waters. This is because oxygen must be able to reach

Figure 30. Schematic bioturbation profile for the skeletal, burrowed mudstone-wackestone lithotype.

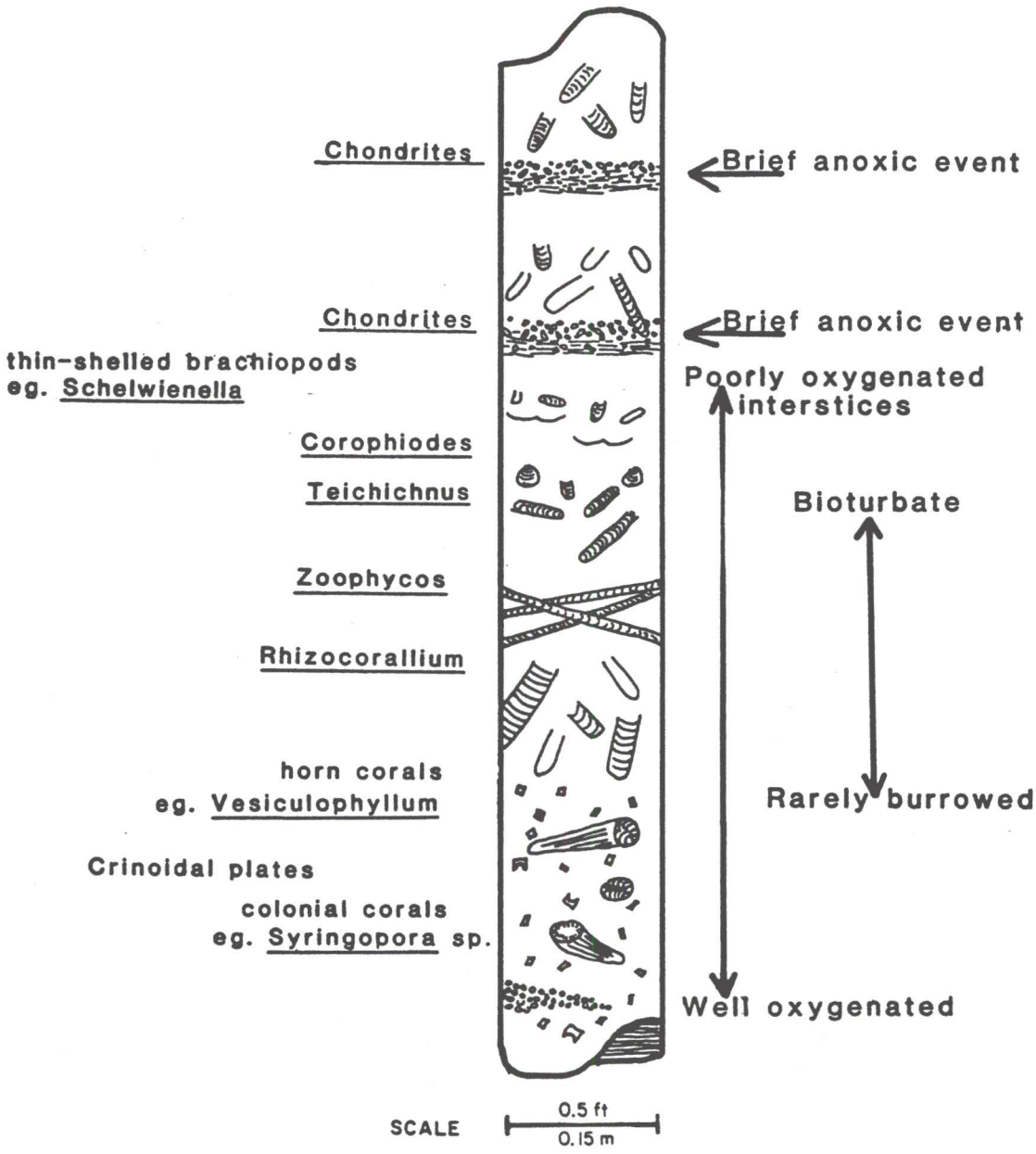
Chondrites
Brief anoxic event
Chondrites
Brief anoxic event
thin-shelled brachiopods
eg. Schelwienella
Poorly oxygenated interstices
Corophiodes
Teichichnus
Bioturbate
Zoophycos
Rhizocorallium
horn corals
eg. Vesiculophyllum
Rarely burrowed
Crinoidal plates
colonial corals
eg. Syringopora sp.
Well oxygenated
SCALE
0.5 ft
0.15 m

Figure 31. Core photograph of LT-3 showing vertical burrow. Note how the burrow changes direction at a brachiopod shell (S). Bar scale is 1.0 in (2.5 cm). NDGS 2667 at 9596 ft (2917 m).

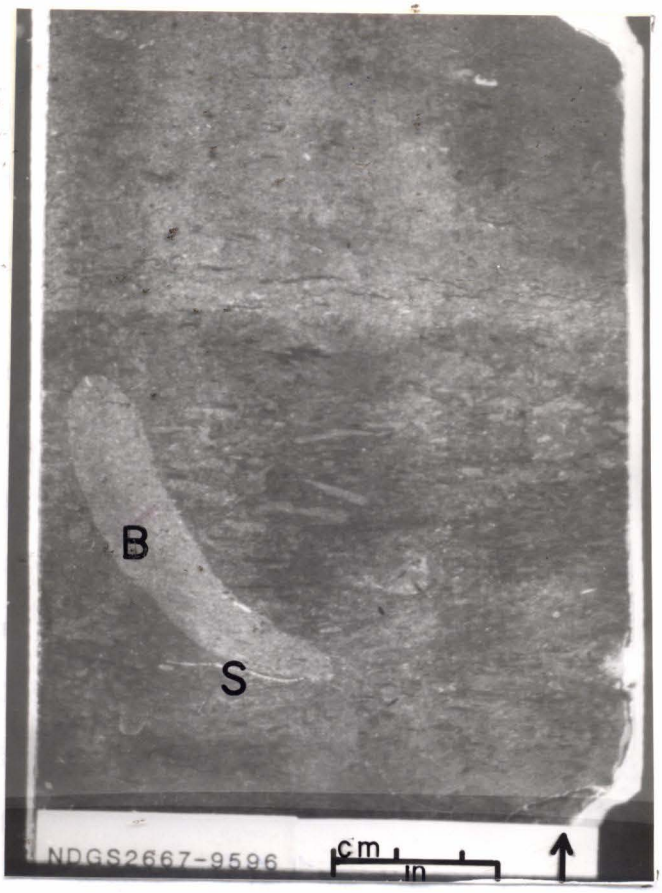
B
S
NDGS2667-9596
cm
in

the burrower at the bottom of the burrow for nourishment. Narrow, horizontally oriented burrows such as Chondrites suggest less oxygenated (dysaerobic) waters (Valvik, 1988). This is because they often occur where other burrow traces are absent, and within organic-rich laminated beds. Bromley and Ekdale (1984) suggested that the creators of Chondrites could tolerate lower oxygenation levels than any other trace fossil progenitor because they are often the last to disappear in a sequence changing from aerobic to anaerobic. The trace fossil Chondrites commonly occurs in the absence of other trace fossils in euxinic and disaerobic environments such as the Lower Cretaceous black micrites of northern Europe (Ekdale and others, 1984).

Chert nodules in this lithotype (Fig. 32) have replaced carbonate in burrow structures. The nodules are often composed of silicified skeletal debris with packstone textures (Fig. 33) within beds of mudstones or wackestones. Diagenetic processes have altered these beds but the burrows themselves have provided foci for later enrichment of silica.

Non-skeletal allochems are predominantly intraclasts and peloids. Intraclasts are rounded, which suggests transport from deeper littoral areas. Many peloids within this lithotype are also derived from winnowed littoral environments but the agglomeration of carbonate mud by burrowing activities or fecal means is considered to be significant.

A shallow sublittoral setting with regular influxes of winnowed

Figure 32. Core photograph of LT-3 showing silicified nodule. Note cherty packstone nodule (C). Bar scale is 1.0 in (2.5 cm). NDGS 2667 at 9601.5 ft (2919 m).

Figure 33. Photomicrograph of LT-3 showing chert cemented (C) peloidal (P) packstone. Bar scale is 0.008 in (0.2 mm). NDGS 5380 at 9237 ft (2808 m).


C
NDGS2667-9601.5
cm
in.

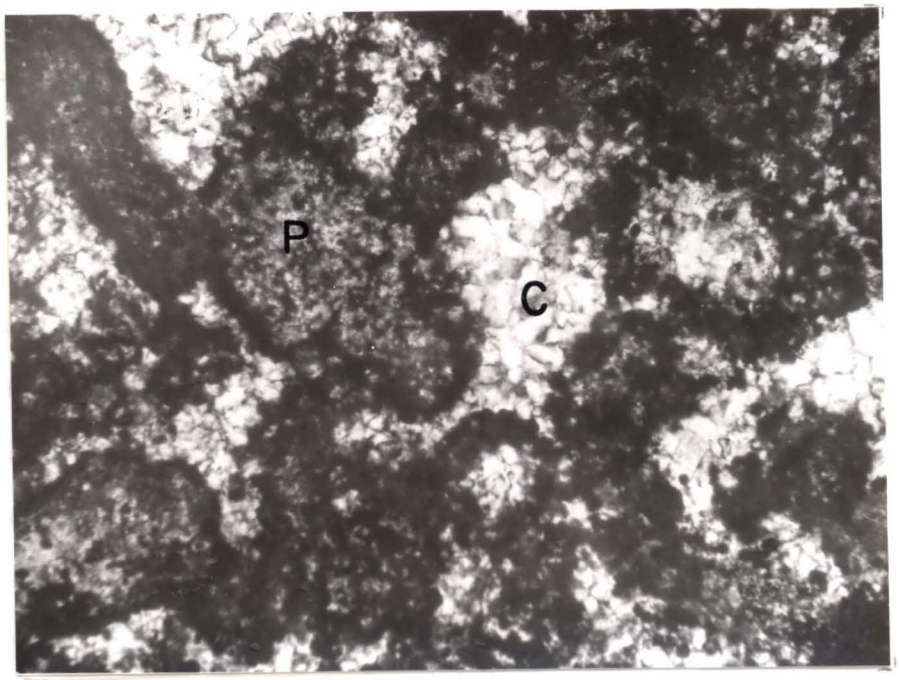
P
C

allochems from adjacent sublittoral shoals is postulated for LT-3. The substrate is considered to have been soft and variably oxygenated. A marginally euryhaline fauna and an abundant ichnofauna are considered to have been indigenous to this environment.

Intraclast Peloid Packstone-Grainstone (LT-4)

LT-4 was deposited in a shallow sublittoral setting, on a platform edge complex of low shoals and channels, in moderate to well circulated waters. Topographically positive areas persisted where wave agitation and the influence of currents had produced grainstone lithologies. Deposition took place around these broad shoals where currents winnowed muds, fragmented fossils, and introduced lithoclasts. Packstone deposition occurred in areas not directly subjected to winnowing currents. Skeletal allochems are often have coatings of micrite, and suggest considerable movement of grains prior to deposition.

The presence of grainstone and packstone fabrics and of stenohaline fauna suggests a well oxygenated environment with good circulation. The abundance of non-skeletal allochems such as angular intraclasts and peloids suggests that these grains were carried into the shoal complex from adjacent sublittoral flats during storms or periods of increased oceanic circulation.

The shifting substrate may have been unsuitable for an infaunal community; however, evidence of soft-bodied infaunal dwellers would have been obliterated by the nearly constant movement of grains.

These shallow shoals may have acted as a physical barrier to the

adjacent restricted sublittoral flats. The shoals may have dampened circulation enough to cause restricted conditions to persist shoreward of these shoals. Periodic storms and oceanic currents would have constantly shifted the shoals laterally, often resulting in irregular breaches of the shoal complex.

Due to the paucity of deposition within this environment, beds of this lithotype are relatively thin. The thinness of these beds may be a result of the current-energy which held the sediment in suspension while in the shoal area. Deposition occurred when the current-energy lessened, often in the adjacent depositional environment.

Cross-laminated sublithotype (LT-4a)

LT-4a was deposited in a shallow littoral setting of winnowing currents and shifting shoals. The mixture of angular and well rounded allochems suggests variable influxes of grains from proximate sublittoral sand bodies. The more rounded grains would have been subjected to more intensive abrasion within the shoal; the more angular grains spent less time within the shoal to be abraded. The presence of fragmented fossils along with occasional graded beds also support the shifting shoal interpretation. Low-angle cross-laminations, characteristic of this lithotype, suggest the lateral shifting of sublittoral shoals. These sediments are not likely to have been tidal channel deposits because of the absence of channel lag pebble conglomerates and large lithoclasts.

Foram Algal Packstone sublithotype (LT-4b)

LT-4b was deposited in a littoral setting of low shoals with slightly restricted water circulation. The relatively poor sorting of grains suggests that this environment was not subjected to the movement of strong currents.

Slightly abraded angular grains and the lime mud matrix suggest rapid deposition and little winnowing of the muds. Variable sorting and the presence of algal rip-up clasts, suggests that these sediments were laid down rapidly by strong currents or storm surges. This probably occurred during periodic storms which would carry algal lithoclasts from nearby littoral mud flats and drop them onto the shoreward edges of the shoal complex.

Abundant benthic forams occurring with algal lithoclasts suggest that the forams may have originated in the sublittoral areas of the shoreward mud flats. The presence of euryhaline forams suggest that LT-4b had waters of slightly elevated salinity, which would also indicate that restrictive circulation patterns existed. Deposition occurred on the shoreward margin of the sublittoral shoal complex, under conditions of elevated salinity, subject to periodic influxes of storm carried lithoclasts.

Oolith Pisolith Packstone-Grainstone sublithotype (LT-4c)

LT-4c was deposited in a shallow sublittoral to littoral setting of good water circulation on, and adjacent to shoals. Agitated water conditions allowed for the winnowing of muds from this environment.

Grainstones of ooids and pisoids indicate steady agitation of sublittoral waters. Ooliths observed are micritic in origen. Radially

fibrous ooids are minor in this study area. Swirydczuk (1988, p.342) considered radially fibrous ooids to be primary with "..radial fabrics recording originally calcitic cortices". Modern radially fibrous ooids and pisoids are found in quiet water environments (Loreau and Purser, 1973; Land and others, 1979). Friedman and others (1973) and Halley (1977) considered radial ooids to be characteristic of hypersaline environments. Kahle (1974), Davies (1976), and Loreau and Purser (1973) each disputed the need for hypersalinity in the formation of ooids. The ooids in this study area are often gradational to micrite coated intraclasts or peloids. Micritization of grains is indicative of the activities of boring algae in shallow, warm marine environments (Bathurst, 1966).

Elliott (1982), Obelenus (1985), and Schwartz (1987) have each interpreted the radially fibrous ooids of the Frobisher-Alida to be subaqueous. Estaban (1976) proposed that pisoids formed subaqueously, in contrast to Dunham (1969), who postulated a vadose origin.

The paucity of a stenohaline fauna is suggestive of hypersaline conditions (Elliott, 1982; Heckel, 1972). Euryhaline organisms are also uncommon in LT-4. Lack of faunal evidence suggests a shifting substrate. The presence of graded bedding and current laminations supports an interpretation of an active sublittoral shoal. The presence of broken ooids and pisoids as the nuclei for newer ooids and pisoids suggests movement of grains by waves and currents and thus discounts a subaerial (Dunham, 1969) origin. Common isopachous cement also supports a marine interpretation for this sublithotype.

Peloid Intraclast Ostracode Packstone-Wackestone (LT-5)

LT-5 was formed in a restricted lagoonal environment of high salinity, low energy, and low oxygen availability. These rocks were deposited in an area shoreward of the sublittoral shoals and seaward of the strandline. The sublittoral shoals acted as a barrier to circulation and dampened wave energy to form a restricted lagoon in the landward direction. The barrier was described above (see LT-4) as more or less discontinuous with periodic to infrequent breaches of the barrier which allowed influxes of normal saline, oxygenated waters into the lagoon.

The rock colors range from light to dark. The darker colors indicate reducing conditions in the substrate. Conversely, lighter colors represent influxes of well oxygenated seawater. Kendall and Skipwith (1969) associated darker colored lagoonal sediments in the Persian Gulf with restricted lagoons and light colored sediments with more open lagoons.

Mechanical abrasion, rounding, and sorting of allochems are minimal in LT-5, and reflect a low energy depositional environment. Peloids, intraclasts and pellets are the most abundant allochems of this lithotype. Luther (1987) reviewed the various modes of formation of these grains. Pellets by definition are considered to be fecal in origin (Bathurst, 1975). Peloids and intraclasts in this study are considered to have been formed by the brecciation of lagoonal muds (Luther, 1987, p.38) upon dissolution of evaporitic minerals within the partially lithified mud. Intraclasts may also have formed during periodic storm events which rip up lithified mud from the lagoon

bottom, or may have been derived from nearby exposed littoral muds which form mud chips upon desiccation or dewatering.

The abundance of euryhaline organisms such as ostracodes, gastropods and algae, indicates that elevated salinity (40-60 ppt) prevailed (Heckel, 1972). Abundant codiacean algae and calcispheres also indicate restricted conditions as well as depths shallow enough for photosynthetic algae to flourish. Mudstone laminations interspersed with discontinuous packstone laminae indicate that current energy within the lagoon was variable. Restriction of circulation (Fischer and others, 1987) allowed for evaporation to elevate salinity to the point where most biogenic activity ceased. Only organisms highly tolerant of salinity and low oxygenation could survive to feed on the organic-rich sediment. Evaporitic conditions would eventually allow for the precipitation of anhydrite in the form of nodules or as laths interspersed in the laminated carbonates of LT-5. Upon increased current activity, salinity would decrease and oxygen levels increase, thus allowing organisms to re-establish themselves.

Nodular and Bedded Anhydrite (LT-6)

LT-6 was deposited in a shallow sublittoral to supralittoral setting, under evaporitic conditions shoreward of protected restrictive lagoons. Nodular anhydrites are well documented in the modern sabkha setting of the Trucial Coast (e.g. Butler, 1969; Wood and Wolfe, 1969; Shearman, 1978). Nodular anhydrite is often interspersed with dolomitic mudstones and cryptalalgal carbonates.

These features are interpreted to indicate deposition in littoral flats where precipitation of anhydrite occurs in heated, briny pore waters, or through the replacement of gypsum crystals (Schreiber and Hsu, 1980). Cryptalgal carbonates of LT-6 formed in areas of lowered salinity, where algal activity can flourish in marine waters introduced during storm surges. Ostracodes, calcispheres, and codiacean algae also occur in these deposits, which would indicate a coastal rather than continental origin for these evaporitic lithologies. Red beds, caliche and fluvial deposits are all absent from this lithotype, which also supports a coastal origin (Schreiber and others, 1982).

The interspersed anhydrite crystals and lenticular gypsum crystals grow and displace the carbonates to form nodules (Schreiber, 1981), and result in bedded nodular anhydrites. Nodular mosaic anhydrites develop as the nodules increase in size. The nodules eventually push aside the surrounding sediment, resulting in thin dark laminations which wrap around the nodules (Fig. 26). The growth of anhydrite nodules is penecontemporaneous with sediment deposition and is considered a primary depositional feature (Shearman, 1978). The displacive growth of the anhydrite nodules often results in rupture of overlying algal-laminated structures (Kendall, 1984), which may give rise to an occasional teepee structure (Fig. 24).

Bedded and massive anhydrites often grade laterally into the nodular anhydrites of this lithotype. Massive anhydrite was deposited subaqueously in sublittoral ponds and lagoons (Kendall, 1984). Sulfate precipitation would occur due to the elevated salinity

and temperature of these areas isolated from marine waters. Thick accumulations of massive anhydrite would occur as subsidence kept pace with deposition. Lateral shifting of lithofacies would cause the interbedding of massive and nodular lithologies.

Depositional Model

Deposition of sediments from the upper Frobisher-Alida beds of this study area was in a broad epeiric sea. Deposition during Mississippian time occurred in environments which ranged from open marine with normal marine conditions to sabkha with evaporitic conditions.

The Madison Group (Mississippian) can be described as an overall regressive sequence of sediments beginning with transgressive open marine carbonate units, and terminating with a regressive evaporitic unit. Examination of structural maps (Figures 34 and 35) shows a close conformity of the distinctive Fryburg and Rival marker beds (Fig. 4). Harris and others (1966), Shanley (1983), and Quinn (1986) suggested that these marker beds were isochronous units. Quinn (1986, p.98) postulated a nearly flat Williston Basin depositional surface with a maximum slope of 1 foot per mile (0.2 m per km). The nearly flat Frobisher-Alida depositional surface is consistent with the gentle bottom slopes of epeiric seas (Irwin, 1965; Shaw, 1964).

The Frobisher-Alida interval was considered by Obelenus (1985, p.130) as one large carbonate to evaporite cycle. Studiers of the Billings Anticline (Altshuld and Kerr, 1982; Stephens, 1986; Petty, 1989) interpreted these rocks as a shallowing-upward succession produced by basinward progradation. The lower Frobisher-Alida beds are dominantly open-marine carbonates beginning with a transgressive event following the Tilston evaporitic unit (Himebaugh, 1979). Open

Figure 34. Structure contour map/ Top of Rival. Well symbols are those of the North Dakota Geological Survey's field maps and are presented to show mapping control points.

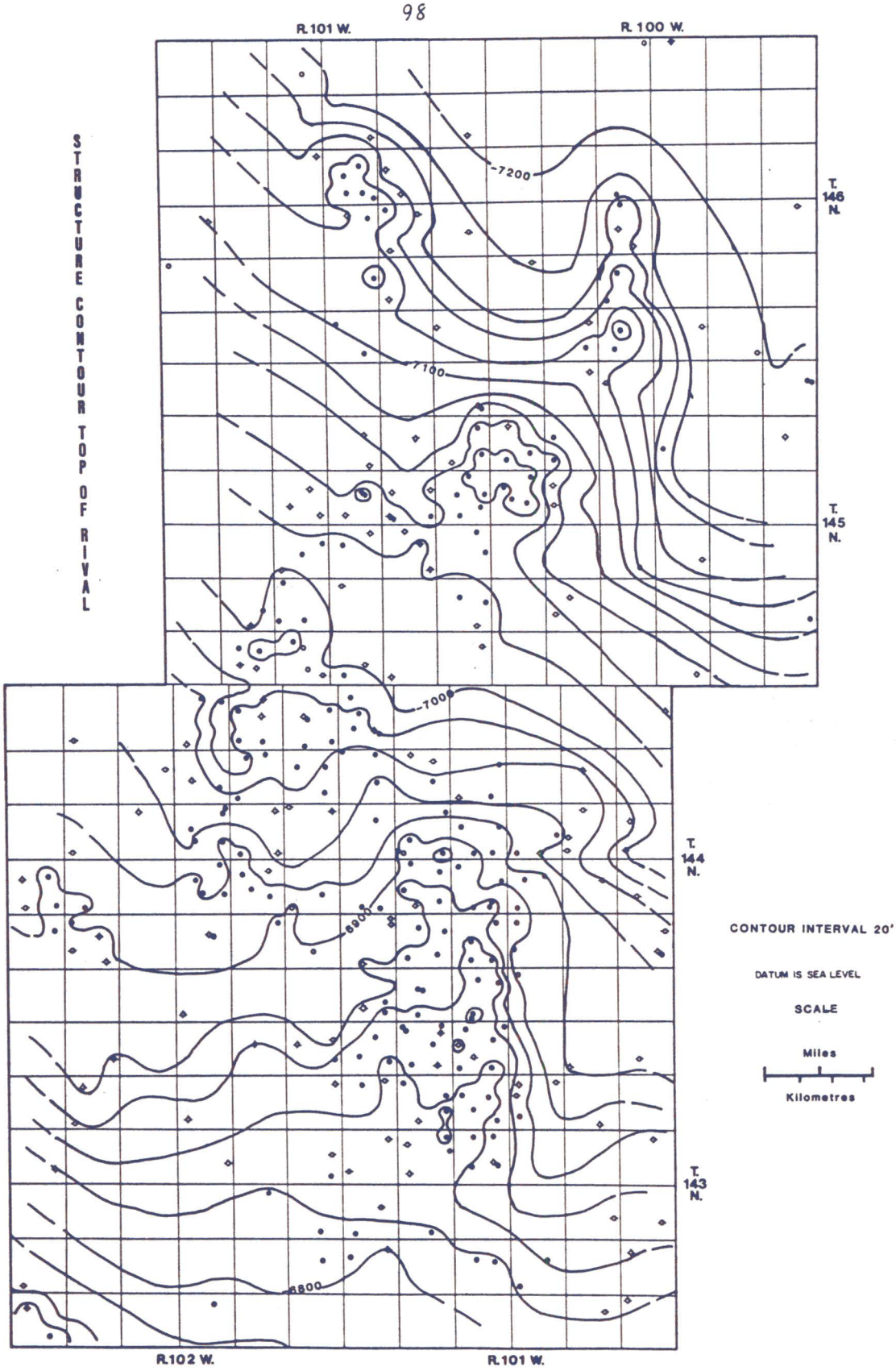
STRUCTURE CONTOUR TOP OF RIVAL
R.101 W.
R. 100 W.
T. 146 N.
T. 145 N.
T. 144 N.
T. 143 N.
R.102 W.
R.101 W.
7200
7100
7000
6900
6800
CONTOUR INTERVAL 20'
DATUM IS SEA LEVEL
SCALE
Miles
Kilometres

Figure 35. Structure contour map/ Top of Fryburg gamma-ray marker. Well symbols are those used on the North Dakota Geological Survey's field maps and are presented to show mapping control points.

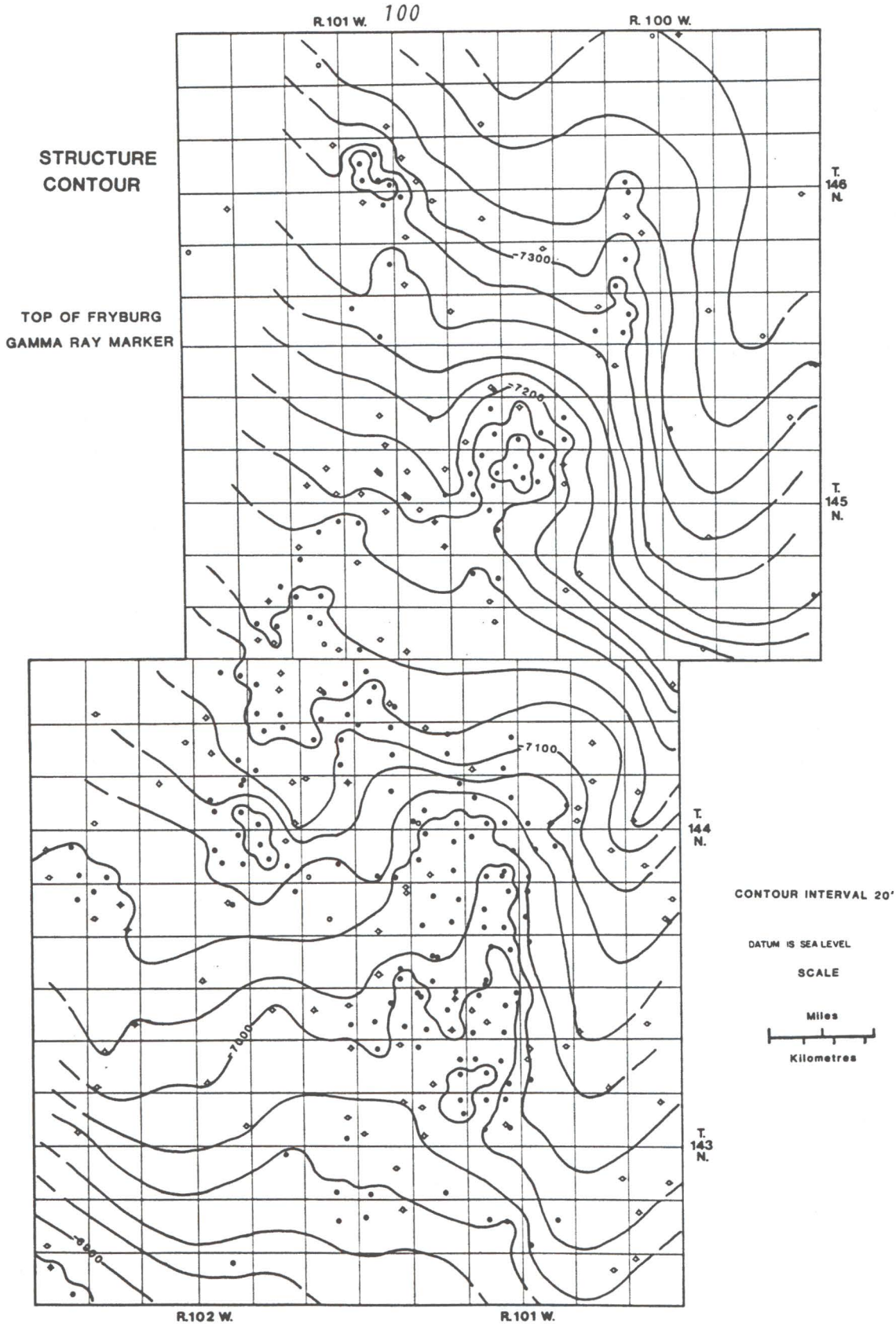
R.101 W.
R. 100 W.
STRUCTURE CONTOUR
TOP OF FRYBURG GAMMA RAY MARKER
T. 146 N.
T. 145 N.
T. 144 N.
T. 143 N.
7300
7200
7100
7000
6900
R.102 W.
R.101 W.
CONTOUR INTERVAL 20'
DATUM IS SEA LEVEL
SCALE
Miles
Kilometres

marine conditions prevailed through Frobisher-Alida time until a regressive phase dominated deposition as shown by a progradational sequence of littoral and supralittoral rocks. The progradational sequence culminated with Rival deposition of transgressive open marine carbonates (Fig. 5).

Lithofacies throughout the study area generally follow the same depositional sequence of thick units of sublittoral carbonates, followed by a thin sequence of littoral carbonates, and culminating in a thick unit of supralittoral evaporites (Fig. 4). Sublittoral rocks dominate the basal lithologies throughout the study area; skeletal packstones-wackestones are the common basal unit. These rocks (LT-1) were deposited in the normal marine environment. The thick uninterrupted sequence of these rocks indicates that carbonate production could keep up with basinal subsidence. These rocks are overlain by the skeletal wackestones of LT-2 and the burrowed mudstones of LT-3.

The skeletal wackestones of LT-2 indicate a normal to slightly restricted environment. This marginally restricted environment often is gradational to normal marine and is intercalated with rocks of LT-1. Shoreward of this environment, areas of restricted circulation due to increased dampening effects caused dysaerobic conditions to develop within isolated lows on the bottom. Deposition of carbonate mud (LT-3) occurred in the lows and skeletal wackestones (LT-2, LT-3) on the highs. These lithotypes became interbedded with the packstones of the normal marine LT-1 as the progradational phase caused lateral shifts of facies (Fig. 36).

Figure 36. Depositional model diagram showing the progradation of facies basinward.

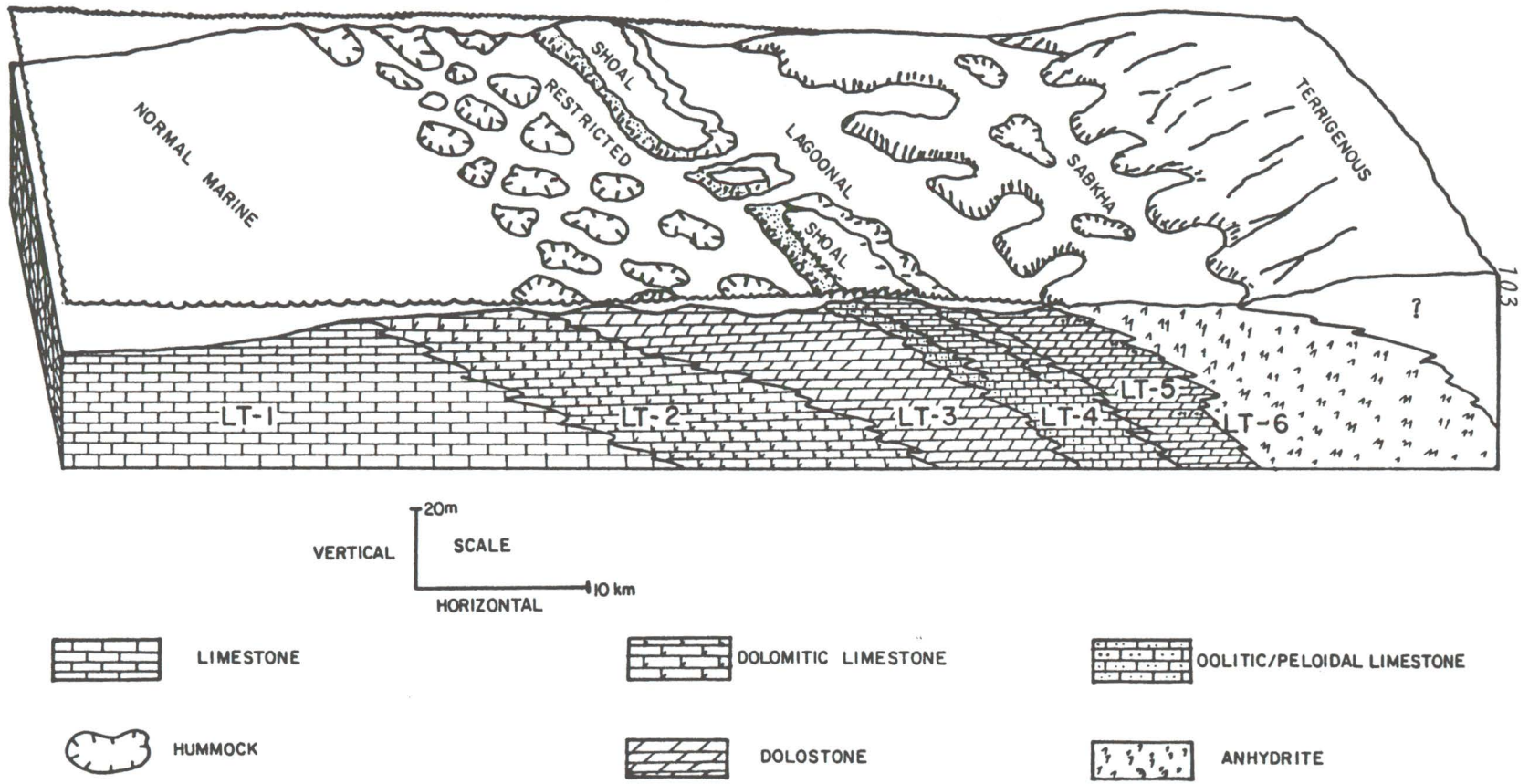
NORMAL MARINE
RESTRICTED
SHOAL
LAGOONAL
SHOAL
SABKHA
TERRIGENOUS
?
LT-1
LT-2
LT-3
LT-4
LT-5
LT-6
20m
VERTICAL
SCALE
10 km
HORIZONTAL
LIMESTONE
DOLOMITIC LIMESTONE
OOLITIC/PELOIDAL LIMESTONE
HUMMOCK
DOLOSTONE
ANHYDRITE

Littoral and related sublittoral rocks (LT-4 and LT-5) increase upward in the section. These reflect the progradation of a littoral to sublittoral complex of shoals. Oolith and pisolith grainstones (LT-4c) developed on shoals near or within wave base. Cross laminated packstones (LT-4a) developed seaward of the shoal as the shoal prograded or laterally shifted. Landward of the shoal accumulations of foram algal packstones (LT-4b) collected on the protected leeward side of the shoals.

A shoal complex dampened wave effects and restricted circulation landward of the shoals. This restriction created lagoonal conditions in which circulation was absent, except for breaches of the shoal barrier by storms and influxes of storm surge waters. Evaporitic conditions caused a drawdown of the lagoonal waters and an elevated salinity. Carbonate production there was generally limited to cryptalgal accumulations and peloidal and lime mud deposits (LT-5).

The progradational sequence culminated in sabkha deposition. Thick accumulations of nodular anhydrite developed on littoral flats, and massive anhydrites developed in areas of ponded waters. Missing from this sequence of carbonates and evaporites is the presence of terrigenous clastics. Paleoclimatic reconstruction of trade wind directions (Quinn, 1986) indicated that arid air moved westward over the ancestral seas. Mississippian terrigenous deposits are not preserved east of this area, so direct evidence of a landmass is absent. Trace amounts of quartz silt are pervasive in each of the lithotypes examined. Persistent marker beds within the study area

have higher proportions of quartz silt than surrounding units. Quartz sandstones occur in Frobisher-Alida marker beds in north central North Dakota (Fuller, 1956; LeFever and others, 1984). The western North Dakota area (this study) of the upper Frobisher-Alida beds must have been farther away from the terrigenous sources. Only wind-carried silts could reach this area, perhaps during sand storms such as are seen in modern sabkha environments of the Trucial Coast.

Diagenetic Processes

The rocks described in this study have undergone varying degrees of crystallization, diagenetic changes to crystal morphology and to chemical composition. The alteration of depositional fabrics has significantly changed the original textures of each of the lithotypes previously described (Fig. 37). Observation of petrographic relationships have allowed inferences to be made about the relative sequences of diagenetic events, using the terminology proposed by Choquette and Pray (1970).

Micritization

Micritization is a process by which crystalline carbonate material is converted to micrite. Depositionally, the original carbonate mud was composed of chemically unstable aragonite or fibrous magnesian-calcite. During lithification crystal growth is controlled by a change in the Mg/Ca ratio (Folk, 1974, p. 48) in which aragonite or magnesium-calcite inverts to equant micritic calcite.

Micritization can also occur through the actions of boring endolithic algae which chemically precipitate micrite in the vacated cavities (Bathurst, 1975, p.383). A micrite envelope often coats allochems and in some instances micritization has progressed to the point where the original microstructure is obliterated. In these instances the allochems resemble peloids or appear amorphous (Fig. 16).

Figure 37. Paragenesis diagram. Eogenetic refers to the time that processes were influenced by proximity to the surface. Mesogenetic refers to the time interval in which the rocks were buried below the influence of surface processes (Choquette and Pray, 1970). Major processes are marked with an asterisk (*).

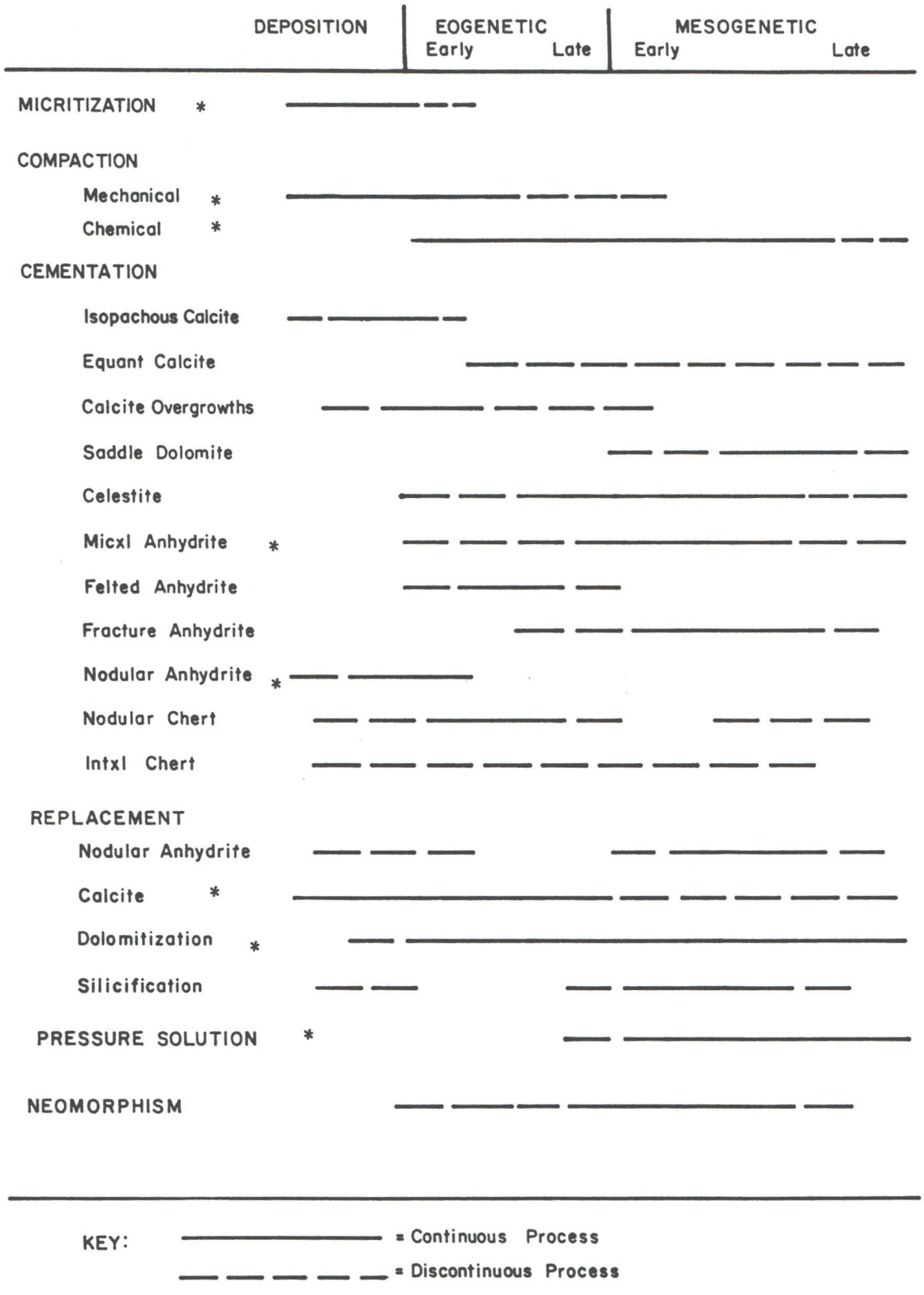
DEPOSITION
EOGENETIC
Early
Late
MESOGENETIC
Early
Late
MICRITIZATION *
COMPACTION
Mechanical *
Chemical *
CEMENTATION
Isopachous Calcite
Equant Calcite
Calcite Overgrowths
Saddle Dolomite
Celestite
Micxl Anhydrite *
Felted Anhydrite
Fracture Anhydrite
Nodular Anhydrite *
Nodular Chert
Intxl Chert
REPLACEMENT
Nodular Anhydrite
Calcite *
Dolomitization *
Silicification
PRESSURE SOLUTION *
NEOMORPHISM
KEY:
= Continuous Process
= Discontinuous Process

Micrite is common to abundant in all lithotypes except the nodular and bedded anhydrite lithotype (LT-6) (Table 2). Micritization in this study area occurred during a time interval from deposition to early eogenesis.

Compaction

Mechanical and chemical compaction features can be observed throughout the lithologies studied. Compaction of soft sediment prior to complete lithification is suggested by features such as collapsed or crushed allochems and by broken grains. These features are common in the skeletal lithotypes (LT-1, LT-2, and LT-3) (Figs. 7, 8 and 9). Also in these lithotypes are compacted or flattened burrows (Figs. 11 and 38), and draping laminae around dolomitic or silicified burrows (Fig. 10). Draping laminae or wispy microstylolites also surround allochems or bound packstone beds (Fig. 39). This indicates that the allochems are more resistant to compaction than the micritic matrix material.

These structures indicate a relationship to early cementation within the burrows prior to, or simultaneous with, matrix cementation. Figure 40 illustrates that compaction occurred in three basic stages or steps. Stage 1 was deposition and bioturbation of restricted lithotype LT-3, adjacent to the unrestricted LT-1 lithologies. Stage 2 was the preferential compaction of LT-1 due to burial by continued deposition. Indications are, that the cemented burrowed lithotype would resist mechanical compaction more than the

Figure 38. Core photograph of LT-1 showing flattened burrows (B), and spalled corallite (C). Bar scale is 1.0 in (2.5 cm). NDGS 4088 at 9375 ft (2850 m).

NDGS4088-9375

Figure 39. Core photograph of LT-1 showing horizontal burrows (B). Note the draping of compaction laminae (L) around burrows. Bar scale is 1.0 in (2.5 cm). NDGS 2853 at 9574 ft (2910 m).

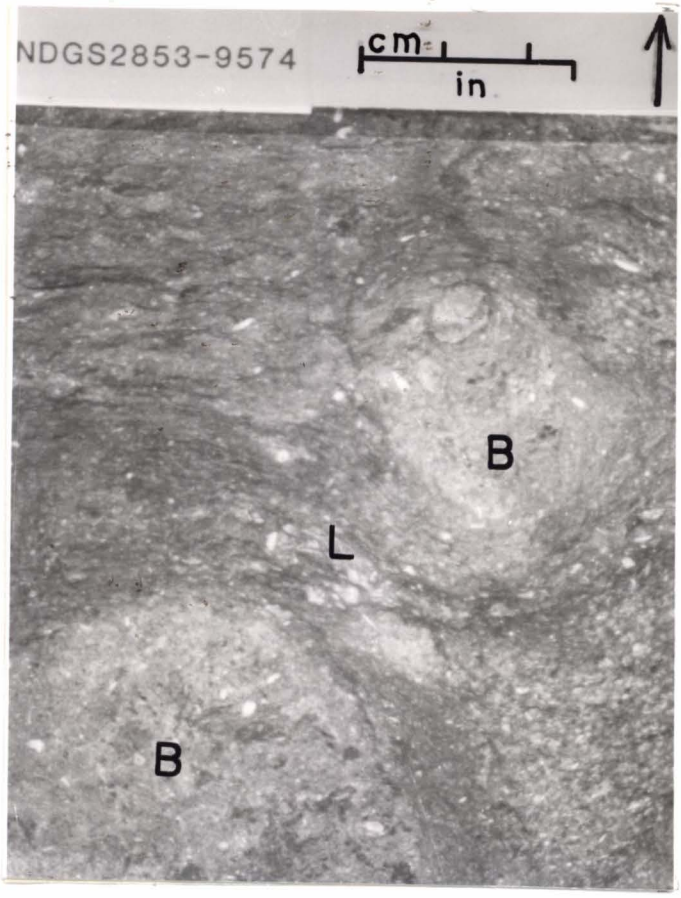
NDGS2853-9574
cm
in
B
L
B

Figure 40. Schematic compaction model. Darker lithologic shade represent burrowed lithotypes (LT-2 and LT-3), the lighter shade represents non-burrowed lithotype LT-1.

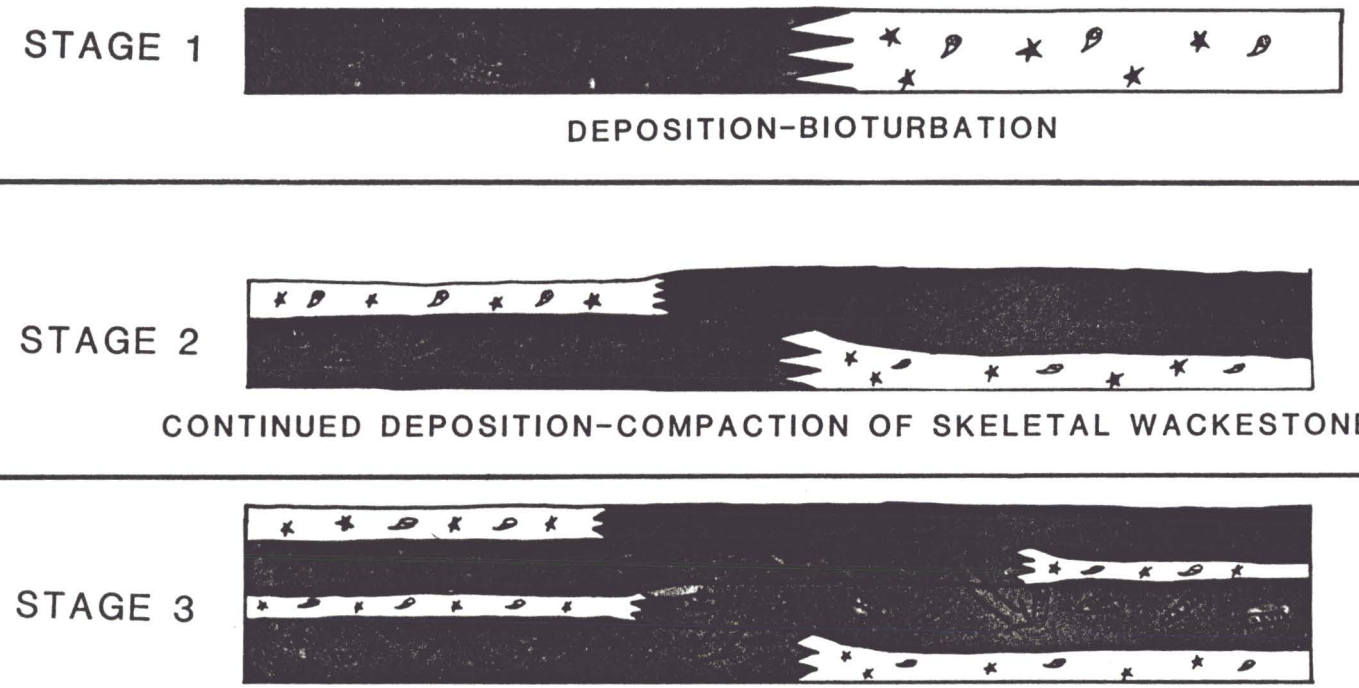

SCHEMATIC COMPACTION MODEL

surrounding non-burrowed carbonate of LT-1. Stage 3 was the formation of solution migration pathways in which interstitial fluids moved preferentially through the less compacted (more porous) rocks of LT-3.

As the sediments were buried through subsidence and continued sedimentation they became lithified and, thus, more resistant to mechanical compaction. At burial depths on the order of 1000 feet (305 m), mechanical compaction effects are diminished (Shinn and Robbin, 1983) and rocks respond to overburden stress through pressure solution. Pressure solution is a response to tectonic or overburden stresses (Wanless, 1979; Bathurst, 1975, p.462). Chemical compaction occurs as solution of carbonate at the points of stress causes diffusion of carbonate toward nearby porous areas. This results in a stratigraphic shortening as the net pore volume decreases.

Pressure solution or chemical compaction features such as offset contacts between allochem fragments along stylolites, as well as concentrations of less soluble allochems along these solution fronts, resulted in stratigraphic shortening. Concentrations of stylolites are suggestive of significant shortening of the rock record. Other chemical compaction features include spalled corals (Fig. 38) and sutured allochem contacts (Figs. 7 and 9).

Mechanical compaction occurred from burial to late eogenetic time. Chemical compaction commenced as overburden stresses increased. Chemical compaction is more important than mechanical compaction during mesogenesis.

Cementation

Cement in this study refers to chemically precipitated minerals which fill pores by growing from a surface within the pore (Bathurst, 1975). Five minerals form the bulk of the cements found in this study area. Calcite, dolomite, anhydrite, celestite and chert occur in each of the lithotypes described.

Calcite

Calcite or spar is a common cement in the rocks studied and occurs in equant, isopachous, or syntaxial forms. Equant calcite occurs in blocky habit which occludes pore spaces within skeletal lithotypes (LT-1, LT-2) and in intergranular voids within the grainstone lithotype (LT-4). Equant cement also occurs as fracture fills in fractured zones within LT-1 and LT-3. Equant cement also fills interparticle areas lined by isopachous calcite (Fig. 41). Equant cement is the product of slow crystallization in late eogenetic and mesogenetic diagenetic environments.

Isopachous calcite occurs in fibrous and bladed forms as a grain coating in the grainstone lithotype (LT-4). Isopachous cement was considered by Longman (1980, p. 464) to be an indicator of an agitated marine environment of deposition. Isopachous chert cements (discussed in the silicification section of this study) may have been replacements of marine calcite cements.

Figure 41. Photomicrograph of LT-1 showing interparticle calcite cement (C) between corallite dissepiments. Bar scale is 0.02 in (0.5 mm). NDGS 5258 at 9310 ft (2830 m).

Figure 42. Photomicrograph of crinoid columnal (C) with syntaxial overgrowths. Bar scale is 0.02 in (0.5 mm). NDGS 5383 at 9447 ft (2872 m).

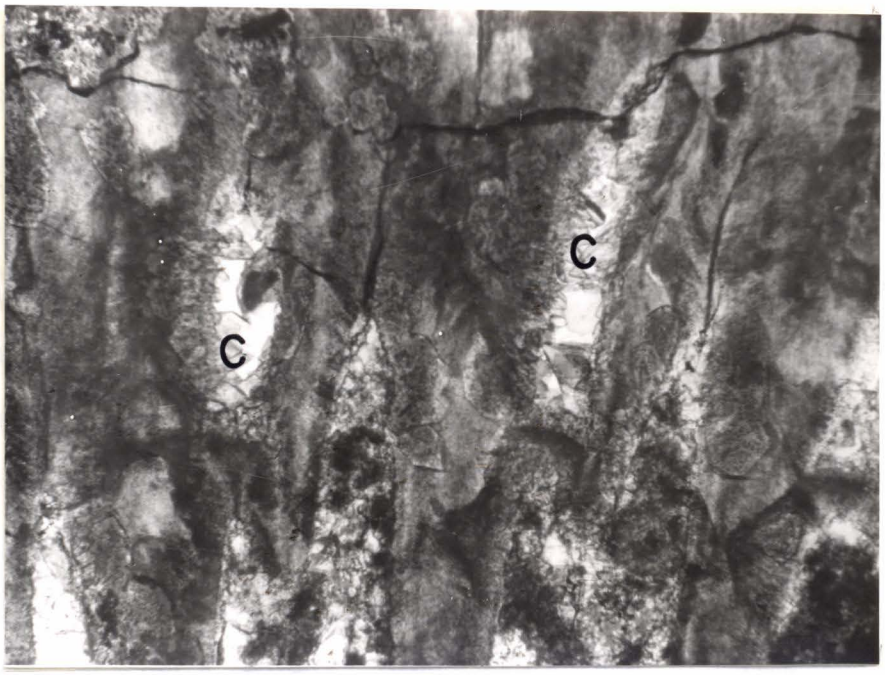
C
C

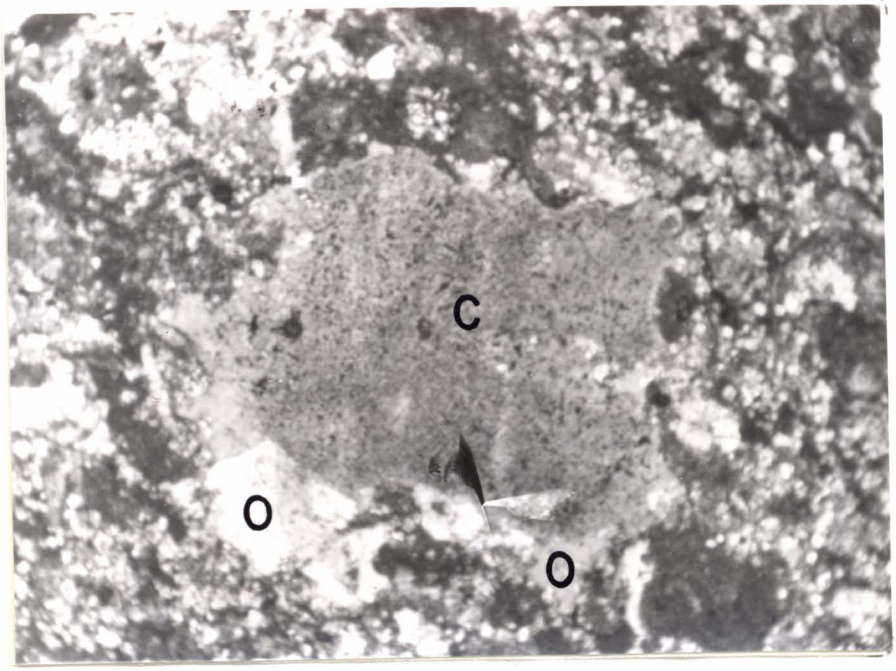
C
O
O

Calcite cement also occurs as overgrowths or enlargements on fossil allochems such as crinoid columnals (Fig. 42). These syntaxial cements are in optical continuity with the allochems. Bathurst (1975), p.423) considered that well-ordered calcite comprising crinoid columnals provided nucleation sites for the development of syntaxial overgrowths. Syntaxial cementation was limited by the size of the pore containing the columnal or the fringes of the carbonate cement around the pore. This suggests that syntaxial calcite cementation was insignificant following initial pore filling events.

Dolomite

In this study area dolomite cement occurs in the form of baroque, or saddle dolomite (Radke and Mathis, 1980). Trace amounts of saddle dolomite are common in LT-3 and lesser amounts occur in LT-1, LT-4 and LT-5 (Table 2). Saddle dolomite in these samples is a minor pore-filling cement that exhibits a characteristic sweeping extinction under crossed nichols. Saddle dolomite often occurs in the same pore spaces with celestite and anhydrite. Saddle dolomite is also present within some cloudy white anhydrite nodules of LT-3 (Fig. 15). Saddle dolomite is a late cement associated with late stage porosity occlusion and probably formed during a later mesogenetic event, possibly during dewatering of the overlying evaporites.

Celestite

Celestite is a minor cement and occurs as a void filling within LT-3 and LT-5. Trace amounts are present in LT-2, LT-4, and LT-1.

Clear subhedral to euhedral crystals of celestite rarely occlude pores without associated anhydrite cements. Celestite cementation was often the terminating phase of passive cementation in the lithotypes examined.

Anhydrite

Anhydrite is a major cement often associated with celestite, calcite, and saddle dolomite. Crystal morphologies are varied and include microcrystalline, subfelted, and felted. Microcrystalline anhydrite cementation occurs within intercrystalline pores of the muddier lithotypes (LT-2, LT-3, and LT-5). Where microcrystalline anhydrite is present in these lithotypes nearly all porosity is occluded. Mesogenetic or deep-burial movement of calcium sulfate-rich fluids is suggested by the pervasiveness of this anhydrite in these lithotypes. Mesogenetic timing is suggested by the association with saddle dolomite cement.

Subfelted and felted anhydrite cement occurs within the anhydrite lithotype (LT-6) and occurs in rare to trace amounts in the lithotypes adjoining massive and bedded anhydrites (LT-5). Blocky and lath shaped crystals may be due to differences in pH in the fluid from which it precipitated (Barta and Zemlicka, 1971). Precipitation of anhydrite in partially lithified carbonate sediments is indicated by the lath shape of the crystals (Fig. 25) in which crystal growth was not confined by lithified material. This type of anhydrite is suggestive of early eogenetic processes.

Anhydrite also occludes fractures and occurs along stylolitic

boundaries. The downward migration of sulfate-rich fluids along vertical fractures is suggested for mesogenetic time. The precipitation of anhydrite along stylolites is also attributed to mesogenetic movement of fluids. Anhydrite is also a common replacement mineral in the rocks studied and is discussed in the replacement chapter to follow.

Chert

Chert cement is a minor cement in the muddier lithotypes (LT-2, LT-3, and LT-5). Chert occurs as an intercrystalline cement scattered throughout pores in dolomitized sections. The burrowed wackestone-mudstone lithotype (LT-3) has numerous cherty nodules (Fig. 32). Lithologies containing cherty nodules include the burrrowed lithotypes (see Table 2). Many chert nodules have the shape resembling burrow structures and contain skeletal wackestone textures suggestive of burrow fills (Fig. 32). Chert is a common interparticle cement in the peloidal packstone lithologies (LT-5). The relationship between chert cement and silicification is discussed in the section concerning silicification.

Replacement

Replacement of one mineral by another is a common feature in the rocks studied. Several types of replacement minerals occur, including anhydrite, calcite, dolomite and chert.

Anhydrite

Anhydrite has replaced carbonate in all lithotypes examined. The form of replacement is non-fabric-selective, and anhydrite crystals cross-cut primary features. Allochem ghosts of ooids or other allochems are common within blocky anhydrite crystals. Anhydrite cementation was commonly accompanied by anhydrite replacement along pore walls or other calcite contacts.

Replacement anhydrite occurs with the growth of anhydrite nodules within sediments. This can be observed where primary laminations have been disrupted as well as partially replaced by anhydrite as in LT-5.

Pressure solution features are often accompanied by anhydrite nodules which may have replaced carbonate along the walls of the 'stylolite pore'. Anhydrite-filled pores and beds underlying evaporite beds are also affected by anhydrite replacement.

Anhydrite replacement is considered to be penecontemporaneous with deposition where nodular beds of anhydrite are present. Later stage anhydrite replacement is considered to be an eogenetic to mesogenetic process occurring together with pressure solution.

Calcite

Calcite has replaced dolomite by the process of dedolomitization (Lippman, 1973), whereby calcium-rich solutions convert dolomite to calcite. Dedolomite is rare in the study area but is a common minor mineral in the muddy lithotypes, LT-3 and LT-2. Corroded dolomite rhombohedra and replaced dolomite are present within pores.

Calcite replacement of dolomite may have occurred through neomorphism (Folk, 1965). Evidence for calcite replacement of dolomite includes corroded dolomite rhombohedra and calcite enclosed within dolomite. Replacement calcite often occurs along with pressure solution features such as stylolites. Euhedral dedolomite within dolomitized sections indicates a post-dolomitization timing for this replacement.

Dolomitization

Dolomitization has occurred in each lithotype except for the anhydrite lithotype (LT-6). Three types of dolomite were identified in this study: microcrystalline; coarsely crystalline; and saddle dolomite. Microcrystalline (<40 um) dolomite has a clear to cloudy appearance, subhedral to euhedral morphology and selectively replaces micritic matrix. Microcrystalline dolomite also replaces allochems where dolomitization is intense as in LT-3 and LT-5. Concentrations of microcrystalline dolomite also occur along stylolites. Wanless (1979) indicated that magnesium-rich fluids released during pressure solution would form dolomite.

Coarsely crystalline dolomite is predominant (Table 2) in LT-3 and LT-2 where mudstone lithotypes occur. Dolomite in these lithotypes is euhedral and ranges from 30 to 120 um in size. Coarse dolomite also occurs in LT-1 but is restricted in size to 60 to 80 um. This size restriction is probably a function of the lack of primary porosity in the crinoid packstone-wackestone lithotype (LT-1). This would restrict the movement of dolomitizing fluids necessary

for dolomite crystal growth. The third type of dolomite is saddle dolomite which is considered a cement and was discussed previously in the section on cements.

Dolomitization of these rocks is considered to have occurred through multiple movements of magnesium-rich fluids which interacted with previously precipitated calcium carbonate (Fig. 43). Figure 44 shows an isopach map generated from neutron porosity logs. Economic accumulations of hydrocarbons are present within these dolomitized sections. A discussion of dolomitization models is included in the diagenetic environments section.

Silicification

Chert replacement or silicification is common in the muddier lithotypes (LT-3 and LT-5). Chert replacement has occurred in light-colored nodules of the burrowed mudstone-wackestone lithotype (LT-3). It is not clear whether the chert is entirely due to replacement or is partially a cement. The preservation of skeletal components within silicified nodules indicates post-depositional replacement of a calcite precursor. There are occurrences of silicified burrows within otherwise unsilicified Ordovician limestone in Missouri (Shourd and Levin, 1976). Silicified trace fossils also occur in the Cretaceous chalks of Europe (Bromley and Ekdale, 1984).

The mucus linings of burrows, and the physical and biogenic

Figure 43. Photomicrograph of poikilitic dolomite in a micritic matrix. Note the replacement of anhydrite (A) by dolomite. Bar scale is 0.008 in (0.2 mm). NDGS 5380 at 9235.5 ft (2808 m).

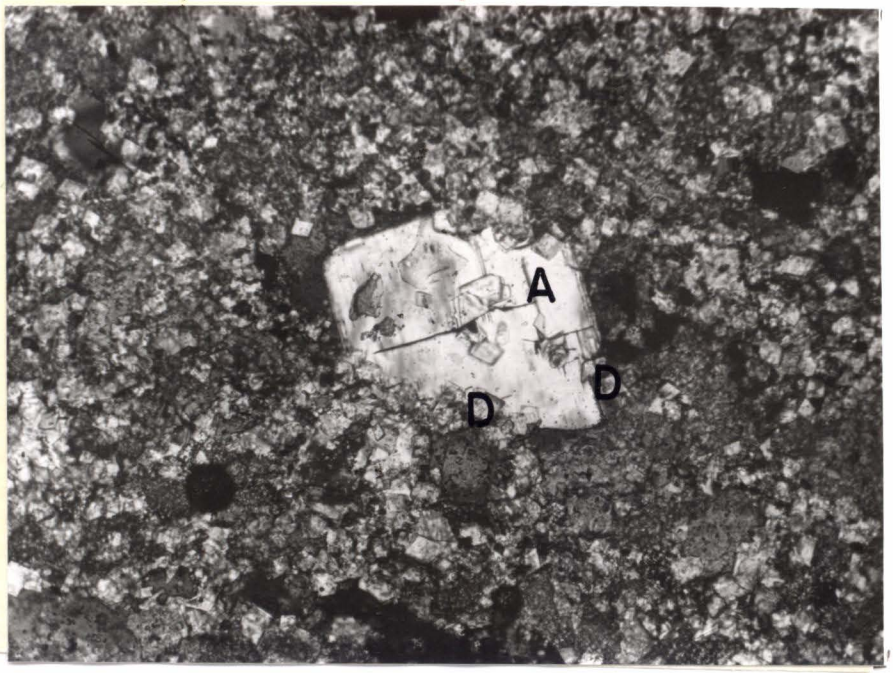
A
D
D

Figure 44. Isopach map of Elkhorn Ranch-Roughrider porosity. Well symbols are those used on the North Dakota Geological Survey's field maps and are presented to show mapping control points.

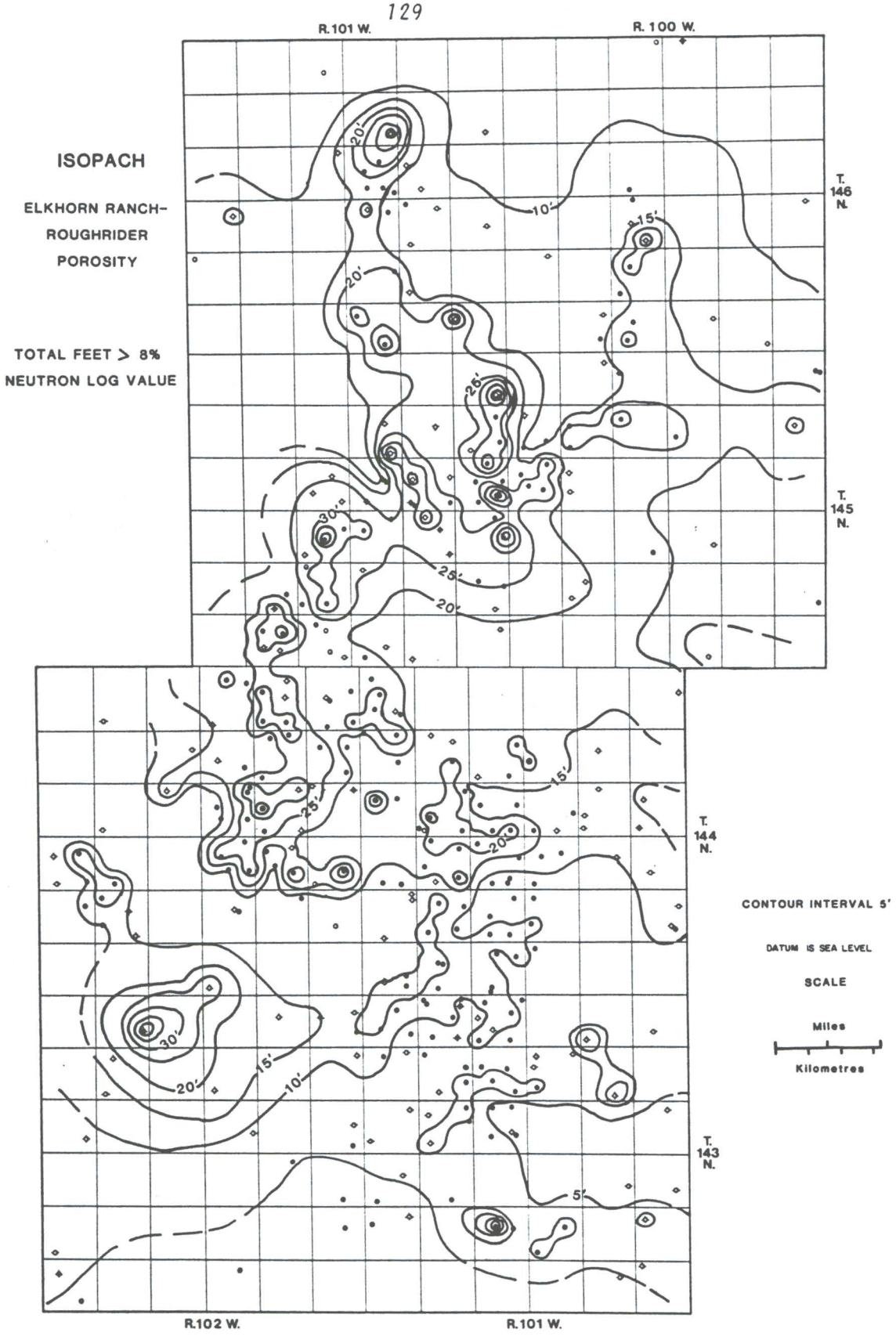
R.101 W.
R. 100 W.
ISOPACH
ELKHORN RANCH-
ROUGHRIDER
POROSITY
TOTAL FEET > 8%
NEUTRON LOG VALUE
T.
146
N.
T.
145
N.
T.
144
N.
T.
143
N.
R.102 W.
R.101 W.
20'
10'
15'
20'
25'
30'
25'
20'
15'
25'
20'
30'
20'
15'
10'
5'
CONTOUR INTERVAL 5'
DATUM IS SEA LEVEL
SCALE
Miles
Kilometres

activities contained within the burrows, had to have some effect on diagenetic processes. The porous sediment would have allowed for the movement of interstitial fluids. The chemistry of the interstices of the sediment may have been conducive to selective silicification of burrows.

The numerous quartz-rich marker beds or sandy carbonates reported by Quinn (1986, p.93) could have been a source for silica-rich fluids except that these beds do not occur in the study area. Siliceous organisms (such as sponge spicules) were not identified in thin-sections of the rocks studied, but may require different petrographic techniques for identification. The source of silica in the Frobisher-Alida beds of this study may have been the traces of eolian quartz silt that occur throughout the rocks described. Pressure solution has concentrated these silt-sized quartz grains within stylolites. Trace amounts of quartz silt may have been in solution during periods of increased pH, which is favorable for quartz dissolution (Blatt and others, 1980).

Pressure Solution

Pressure solution has affected the porosity, textures and crystal morphology of the rocks of this study area. Bathurst (1975, p.464; 1985) described pressure solution as the result of dissolution, diffusion and precipitation. Applied stress against carbonate minerals causes an increase in solubility along the stressed contact and results in the dissolution of the carbonate. The dissolved carbonate then diffuses away from the stress site and

subsequently precipitates in available pore space. Clays and insoluble materials accumulate along the solution "front" and result in development of stylolites.

Stylolites are common in LT-1 and LT-3, and less abundant in LT-2 and LT-5. The grainstone lithotype (LT-4), and the anhydrite lithotype (LT-6) rarely exhibit stylolites (see Table 2). Stylolites described are of three forms: 1) tooth and socket-type; 2) microstylolite-type; and 3) solution seam-type (Wanless, 1979).

Tooth and socket-type stylolites, or Type I of Wanless (1979), are common in the wackestones and mudstones of LT-1, LT-2 and LT-3. The Type I stylolites can be subdivided into two groups: the first are of low amplitude or distance between top of tooth and bottom of socket (0.5 to 4.0 cm); the second are high-amplitude stylolites (3.0 to 10.0 cm). The low-amplitude stylolites are more prevalent where there is a paucity of allochems such as in the wackestone/mudstones of LT-2, LT-3, and LT-5. The high-amplitude stylolites occur in carbonates with a greater skeletal component and are often bounded on top and bottom by resistant allochems or clay laminae. These insoluble materials represent the upper and lower limits to solution of carbonate while adjacent areas of the stylolite front represent selectively dissolved matrix carbonate. High-amplitude stylolites occur in LT-1, LT-2, and LT-3.

Microstylolites are thin lamina of insoluble materials that most commonly occur intercalated with matrix or micritic carbonate (Figs. 8 and 9). These were termed by Wanless (1979) Type II or non-sutured seam solution stylolites, which can occur singly or as composites

(microstylolite swarms)(Fig. 21). Swarms of microstylolites are found along with occurrences of tooth and socket stylolites and represent differences in structural response of the carbonate to solution. In some instances, the density of microstylolite swarms is such that the depositional texture of the rock is obliterated. In other instances, the texture of a mudstone is altered, so that a pseudo-mottled texture is apparent. Microstylolites occur most commonly in LT-1, LT-2, LT-3, and LT-5.

Solution seam stylolites are thick (0.8 to 2.0 cm) accumulations of insoluble material and commonly occur in the allochem-poor rocks of LT-3. Various gamma-ray marker beds such as the Fryburg gamma-ray marker (Fig. 45) are concentrations of stylolite seams. Petrographic examination reveals a composition of insoluble materials, clay, dolomite and detrital quartz silt. The clay in these beds, which Stephens (1986, p. 94) described as illite, give gamma-ray responses which can be correlated across the Williston Basin. Various workers (Harris and others, 1966; Shanley, 1983; Quinn, 1986) considered these beds to be isochronous in nature. Concentrations of microstylolites were shown by Schwartz (1987, p.136) to give distinctive responses on gamma-ray logs. Radioactive minerals within clays were concentrated by pressure solution, which would contribute to a gamma-ray deflection. Other pressure solution features include spalled or smeared corallites (Fig. 38).

Stylolitization or pressure solution was suggested by Shinn and

Figure 45. Core photograph of LT-1 showing gamma-ray marker bed. Note the accumulation of skeletal debris (D) along the stylolite seam (S) margins. Bar scale is 1.0 in (2.5 cm). NDGS 2853 at 9548 ft (2903 m).

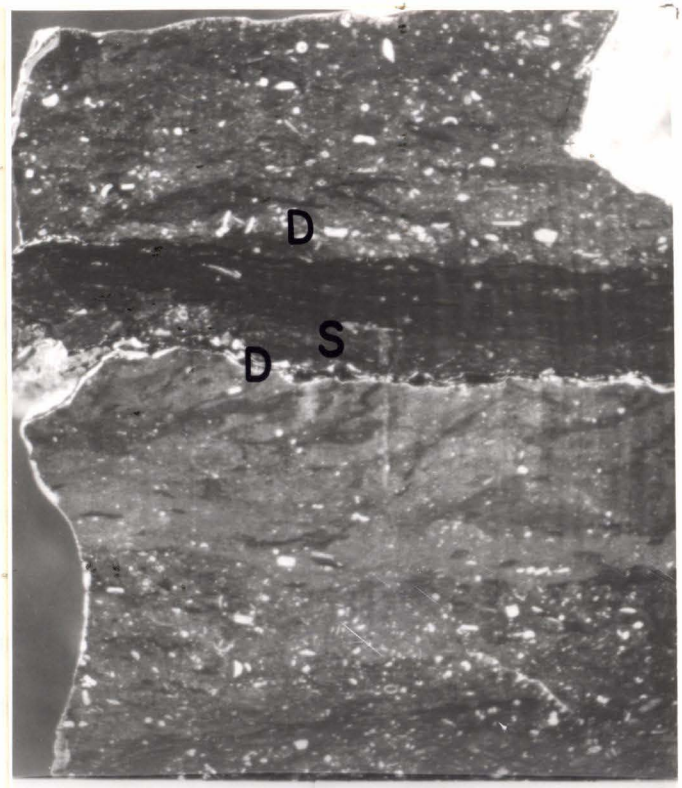

NDGS2853-9548

Robbin (1983) to begin prior to lithification. Stylolites in the study area do not cross-cut sedimentary structures in a way that would indicate onset prior to lithification. In this study the presence of stylolites also corresponds to intervals of low porosity which indicate post-lithification occlusion of pores by pressure solution. Pressure solution responses are considered to be a late eogenetic through mesogenetic diagenetic process.

Neomorphism

Neomorphism was proposed by Folk (1965, p.21) to include all forms of inversion or recrystallization between polymorphs of minerals or of the minerals themselves. Microspar is a neomorphic calcite with a range in crystal size from 4 to 30 um. Pseudospar is a neomorphic calcite with crystals greater than 30 um.

Much of the depositional carbonates were likely comprised of aragonite mud. These needle-shaped crystals normally invert to calcite in modern environments. Following the inversion of aragonite to calcite, the process of aggrading neomorphism (Folk, 1965) commenced. Micrite neomorphosed to microspar and the coarser equivalent pseudospar.

Microspar is common in the lithotypes containing larger mud or matrix fractions. The association of micritic lithologies with microspar is obvious because micrite is a precursor for microspar. The size difference between micrite and microspar is slight and the petrographic delineation between them is difficult. Therefore,

quantitative estimates of neomorphic calcite are unreliable with petrographic techniques. Neomorphism is considered to be a pervasive diagenetic process in the carbonates of the Frobisher-Alida. Some degree of neomorphism can be found in any lithology containing significant micritic matrix.

Pseudospar or coarser neomorphic calcite is rare and is due to continued inversion or recrystallization (Folk, 1965, p.43) to coarser grains. Pseudospar occurs in trace amounts and is limited to the crinoid, coral, brachiopod packstone-wackestone lithotype (LT-1) and the crinoid, brachiopod, skeletal wackestone lithotype (LT-2). Pseudospar is developed in small areas within larger areas of microspar in these lithotypes and is gradational in size to microspar. Neomorphism of the mud-supported carbonate rocks may have occurred during mesogenetic influxes of fresh water, which would have removed magnesium ions which retard neomorphism (Folk, 1974). If fresh water is needed for neomorphism, and since the presence of a deep fresh-water aquifer adjacent to the ancient saline epeiric sea is not likely, then eogenetic processes did not result in significant neomorphism. Also, there is no evidence of a significant rainfall recharge area from an ancient land-mass east of the basin. Episodes of neomorphism may have been due to the mesogenetic influx of fresh water from Madison aquifers to the west (Downey, 1984).

Stephens (1986), in a study of the Big Stick and T. R. fields on the Billings Anticline, suggested that neomorphism had an effect upon

different dolomitization phases. Geochemical analyses by Stephens showed that dolomites in this portion of the Frobisher-Alida may be a product of neomorphic transformation of "originally calcium-enriched" dolomites (p. 134).

SUMMARY OF DIAGENETIC ENVIRONMENTS

The rocks of the upper Frobisher-Alida beds in this study area were subjected to varying and complex diagenetic processes and environments. The relative timing and distribution of diagenetic processes are summarized in Figure 37. An interpreted paragenesis for this study area is presented.

Depositional

Diagenetic processes during sediment deposition were limited to mechanical compaction, micritization and early calcium carbonate cementation.

Eogenetic

Early eogenetic diagenetic features were the result of the movement of hypersaline brines which infiltrated supralittoral areas downward to produce features such as displacive nodular anhydrites. Anhydrite cementation and replacement were also eogenetic features.

In sublittoral areas, early cementation by calcite was followed by differential compaction. Sublittoral areas of normal marine waters were conducive to significant mechanical compaction. More restricted areas contained varying burrow structures which were selectively cemented by early calcite. This early cementation provided a rigidity to the sediments containing them.

Refluxing hypersaline brines (Adams and Rhodes, 1960) moved readily through the more rigid burrowed sediments than through the

adjoining compacted wackestones (Fig. 39), because of differential compaction. These migration pathways for overlying hypersaline phreatic waters allowed extensive dolomitization of the burrowed units while effectively bypassing the compacted, less porous normal marine wackestones. Silicification of burrows accompanied dolomitization and reflect localized changes in pH or other factors related to chert nucleation.

Mesogenetic

Deep burial environments had a dynamic hydrologic regime which produced a series of complex diagenetic features. Physical compaction features become overshadowed by chemical compaction as burial depth increased. Chemical compaction features were a result of pressure solution. Pressure solution features (Wanless, 1979), which overprint earlier textures and features in all lithotypes, illustrate that periods of pore fluid movement were active throughout mesogenetic diagenesis.

Mesogenetic movements of magnesium-rich fluids resulted in multiple dolomitization episodes. Coarser crystalline dolomite was formed due to movements of dolomitizing fluids liberated by pressure solution. Episodes of dedolomitization and neomorphism may have been a result of the influx of fresh water from Madison aquifers to the west (Downey, 1984).

The distribution of porosity was influenced by the primary sedimentary characteristics of the lithotypes as well as

dolomitization events. Early resistance to compaction created solution migration pathways through which early dolomitizing fluids moved. Secondary intercrystalline porosity is a result of the degree of dolomitization in the rock. Late-stage cementation by anhydrite and calcite partially or completely occludes dolomitized beds in some areas.

CONCLUSIONS

1) Six distinct, yet related lithotypes are represented in this study area: 1) crinoid, coral, packstone-wackestone (LT-1); 2) brachiopod, skeletal wackestone (LT-2); 3) skeletal, burrowed mudstone-wackestone (LT-3); 4) intraclast, peloid packstone-grainstone (LT-4); 5) peloid, intraclast, ostracode packstone-wackestone (LT-5); and 6) nodular and bedded anhydrite (LT-6).

2) Deposition of upper Frobisher-Alida sediments in this area of the Williston Basin was in a broad, shallow epeiric sea. The sediment surface was of low relief and restricted circulation conditions prevailed through much of the interval studied.

3) Lithofacies generally follow a sequence of thick sublittoral units overlain by a thin sequence of littoral carbonates and culminating in a thick unit of supralittoral evaporites.

4) Due to the movements of currents and storm surge events lateral shifting of environments prevailed rather than regressive-transgressive movements.

5) Active carbonate production overtook subsidence and caused a progradational sequence of normal marine carbonates to arid evaporitic deposits.

6) Early diagenetic cementation of burrowed carbonates inhibited compaction of the rocks containing them, and thus allowed for migration of dolomitizing fluids. Sediments without early cementation of burrows would more readily compact and inhibit movement of

dolomitizing fluids.

7) Burrowed carbonate lithofacies (LT-3, LT-2 and LT-5) were preferentially dolomitized, and resulted in greater porosity development than the other lithotypes.

8) Deep-burial environments were dominated by multiple episodes of dolomitization and overprints of pressure solution features.

9) The preservation of skeletal components within silicified nodules indicates diagenetic replacement of early calcite-cemented burrows. The physical and biogenic conditions within burrows may have caused selective nucleation of chert.

APPENDICES

APPENDIX A

NAME AND LOCATION OF WELLS USED IN THIS STUDY

Wells are listed in increasing numerical order by township, range and quarter section. Locations are based on the standard Land Office Grid System. In describing the locations, Q/Q stands for first and second quarters of the section; S, T, and R stand for section, township and range respectively; C in the Q/Q column stands for center of quarter section. All townships in North Dakota are north and all ranges are west of the principal baseline and meridian. Well numbers in the third column are those of the North Dakota Geological Survey. Operator and well names may not be complete legal names for brevity.

Q/Q	S-T-R	Number	Operator	Well Name (Cored intervals in feet)
	Billings County			
SW/SW	2-143-101	7113	Samson Resources	Federal 1-2
NE/NW	4-143-101	9428	Cenex	Fuce-Federal 4-4
SW/NW	4-143-101	5690	Farmers Union	U.S. 5-4
NE/SW	4-143-101	6724	Farmers Union	Fuce-Federal 11-4
SW/SW	4-143-101	6912	Apache Corp.	Federal 13-4
SW/SE	4-143-101	6937	Apache Corp.	Federal 15-4
SW/NE	4-143-101	8929	Cenex	Fuce-Federal 2-4
NE/NE	4-143-101	9594	Nucorp Energy	Federal 34-1
NW/NW	5-143-101	6686	Gulf Oil	Federal 2-5
C-NW	5-143-101	5964	Gulf Oil	Elkhorn-U. S. 1-5
SE/SW	5-143-101	6013	Gulf OIl	Gulf-Sunbehm-U.S. 1-5
SW/SE	5-143-101	6292	Gulf Oil	Elkhorn-U.S. 2-5
SW/NE	5-143-101	5948	Farmers Union	Federal 7-5
C-NE	5-143-101	2853	Shell Oil	Gov't 41X-5-1 (9459-9489, 9492-9639)
NE/NE	5-143-101	5168	Cenex	Federal 16-32
NE/SW	6-143-101	5664	Farmers Union	Federal 7-6
NE/SW	6-143-101	9121	Nucorp Energy	Federal 6-1
SW/NE	6-143-101	5789	Farmers Union	Federal 9-6
NE/NW	7-143-101	8705	Nucorp Energy	Federal 7-1
NW/NW	8-143-101	6158	Farmers Union	Fuce-Kordon 4-8
SE/SW	8-143-101	7364	Farmers Union	Federal 14-8
NE/SE	8-143-101	6856	Apache Corp	Evoniuk 1-8
SE/NE	8-143-101	7118	Farmers Union	Kordon 8-8
SW/NW	9-143-101	7250	Farmers Union	Fuce-Federal 5-9
NE/SW	9-143-101	6905	Apache Corp	Federal 1-9
SE/SE	9-143-101	7439	Farmers Union	Federal 16-9
SW/NE	9-143-101	7165	Apache Corp	Federal 2-9
NW/NW	10-143-101	9247	Cenex	Fuce-Federal 4-10
NW/SW	10-143-101	8068	Cenex	Federal 12-10
SW/SE	11-143-101	6346	Farmers Union	Whitetail Creek 14-11
NW/NE	13-143-101	8022	Gulf Oil	Spear-Federal 1-13-2A
NE/NW	16-143-101	6999	Apache Corp	State 2-16
NE/SW	16-143-101	6938	Apache Corp	State 1-16

Q/Q	S-T-R	Number	Operator	Well Name
			(Cored intervals in feet)	
NW/SE	16-143-101	7225	Apache Corp	State 4-16
NW/NE	16-143-101	7143	Apache Corp	State 3-16
SW/SW	17-143-101	7131	Apache Corp	Federal 4-17
SE/NE	17-143-101	7070	Apache Corp	Federal 2-17
NE/NE	17-143-101	6258	Apache Corp	Federal 1-17
NE/NE	18-143-101	4455	Shell Oil	Gov't 41X-18
			(9238-9394, 9442-9501)	
SE/SW	19-143-101	7690	Chambers Exploration	Blacktail-Federal 3-19
SW/SE	20-143-101	7128	Jerry Chambers	Blacktail-Federal 1-20
SW/NW	25-143-101	6169	Tenneco Oil	BN 1-25
SW/SW	27-143-101	8962	Chambers Exploration	Blacktail 2-27
SW/NE	27-143-101	8465	Chambers Exploration	Blacktail 1-27
SE/NW	28-143-101	7082	Chambers Exploration	Blacktail-Federal 1-28
SE/NE	28-143-101	9122	Chambers Exploration	Blacktail-Federal 2-28
SW/NW	30-143-101	8723	Chambers Exploration	Blacktail-Federal 1-30
NE/NE	30-143-101	9329	Axem-Chambers	Federal 2-30
NW/NW	36-143-101	10074	W.H. Hunt Trust	State 1-36
SW/NW	1-143-102	7399	Cenex	Fuce 7-5
NE/SE	1-143-102	5711	Farmers Union	BN 9-1
SE/NW	2-143-102	7761	Cenex	Cenex-Connell 6-2
NE/SE	5-143-102	6957	Apache Corp	Federal 1-5
SE/NW	8-143-102	9224	Apache Corp	Federal 8-1
SW/SW	10-143-012	10474	Basic Earth Systems	Mikkelson-Mosser 14-10
NE/NE	12-143-102	5816	Diamond Shamrock	S.U.D.S-Federal 1-12
SE/SE	13-143-102	8487	Conoco	Conoco-Federal-Blacktail 13-1
NE/SE	15-143-102	9340	Chambers Exploration	Mosser Bros. 9-15
NE/SE	18-143-102	11109	Cities Service	Federal-D.K. 1-18
NW/NE	23-143-102	8363	Al-Aquitaine	Al-Aquitaine-BN 1-23
SW/SE	24-143-102	8251	Jerry Chambers	Chambers-Citgo 1-24
SW/NE	25-143-102	7984	Jerry Chambers	Chambers-BN 1-25
SE/NW	31-143-102	7451	Gas Enterprises	BN 1-31
NW/SE	31-143-102	7792	Al-Aquitaine	U.S. 2-31
NW/NE	34-143-102	10475	Basic Earth Systems	Mikkelson-Short 31-34
SE/NE	1-144-101	9516	Koch Exploration	Federal 8-1
SW/NW	6-144-101	8155	Supron Energy	Federal 2-6
SE/NW	6-144-101	6310	Supron Energy	Federal 1-6
NW/SE	6-144-101	9351	Supron Energy	F-6-144-101-3
NW/NW	7-144-101	10065	Florida Exploration	Federal 7-3
NW/SE	7-144-101	8651	Supron Energy	F-7-144-101-2
NW/NE	7-144-101	8564	Supron Energy	F-7-144-101-1
NE/NW	8-144-101	9524	Florida Exploration	F-8-144-101-3
NW/SE	8-144-101	9607	Florida Exploration	F-8-144-101-2
SW/SW	9-144-101	10222	Cenex	Cenex-Federal 13-9
SE/NE	9-144-101	11240	Cenex	Cenex-Federal 8-9
NW/SW	10-144-101	11621	Tenneco Oil	Panos-U.S.A. 1-10
SE/NW	11-144-101	7600	Koch Exploration	Federal 6-11
SE/NW	13-144-101	10451	Amoco Production	U.S.A.-Amoco-Magpie 13-1

Q/Q	S-T-R	Number	Operator	Well Name
			(Cored intervals in feet)	
SW/SW	13-144-101	7308	Amoco Production	Northrup-Federal A-1-13
SW/SW	15-144-101	10303	Apache Corp	Federal 15-13
SW/SE	15-144-101	7291	Amoco Production	Amoco-U.S.A.-Federal 2-15
SE/NE	15-144-101	9641	R.T. Duncan	Duncan-Federal 15-43
SW/NW	16-144-101	10215	Tenneco Oil	Amerada-State 2-16
SE/SW	16-144-101	9578	Tenneco Oil (9469-9564)	Amerada-State 1-16
SW/SE	16-144-101	9577	Tenneco Oil	Amerada-State 3-16
SE/NE	16-144-101	9856	Tenneco Oil	Amerada-State 4-16
NE/SW	17-144-101	9626	Tenneco Oil	Martin-U.S.A. 2-17
SW/SW	17-144-101	10177	Florida Exploration	Federal 3-19
SE/SE	17-144-101	9561	Tenneco Oil	Martin-U.S.A. 3-17
NE/NE	17-144-101	9990	Florida Exploration	Magpie-Federal 1-17
SW/NE	18-144-101	9386	Florida Exploration	Federal 1-18
SE/SW	19-144-101	9492	Florida Exploration	Federal 1-19
SW/SE	19-144-101	9900	Florida Exploration	Magpie-Federal 2-19
NE/NW	20-144-101	9581	Tenneco Oil	Childs-U.S.A. 2-20
NW/SE	20-144-101	10915	Tenneco Oil	Childs-U.S.A. 5-20
SE/SW	20-144-101	9294	Tenneco Oil	Childs-U.S.A. 1-20
C/SE	20-144-101	9215	Tenneco Oil	Childs-U.S.A. 3-20
C/NE	20-144-101	9295	Tenneco Oil	Childs-U.S.A. 4-20
NW/NW	21-144-101	9772	Koch Exploration	Federal 4-21
SE/SW	21-144-101	9743	Koch Exploration	Federal 14-21
NW/SE	21-144-101	11079	Koch Exploration	Federal 16-21A
SE/NE	21-144-101	9756	Koch Exploration	Federal 8-21
SE/NW	22-144-101	8422	Koch Exploration	Federal 6-22
SW/SW	22-144-101	8128	Koch Exploration	Federal 13-22
C/NE	22-144-101	9079	Tenneco Oil	Childs-U.S.A. 1-22
NW/SE	25-144-101	7629	Koch Exploration	Federal 15-25
C/NW	27-144-101	8853	Amoco Production	Northrup-Federal D-1-27
NW/SW	27-144-101	10114	Koch Exploration (9274-9301)	Federal 12-27
SE/NW	28-144-101	8671	Tenneco Oil	Hamilton-U.S.A. 1-28
SE/SW	28-144-101	8430	Tenneco Oil	Hamilton-U.S.A. 2-28
SW/SE	28-144-101	8490	Tenneco Oil	Childs-U.S.A. 2-28
NE/NE	28-144-101	8429	Tenneco Oil	Childs-U.S.A. 1-28
SE/NW	29-144-101	9216	Tenneco Oil	Hamilton-U.S.A. 2-29
C/SW	29-144-101	9183	Tenneco Oil	Hamilton-U.S.A. 1-29
C/SE	29-144-101	9182	Tenneco Oil (9204-9332)	Hamilton-U.S.A. 3-29
SE/NE	29-144-101	9214	Tenneco Oil	Hamilton-U.S.A. 4-29
SE/SW	30-144-101	5811	Diamond Shamrock	S.U.D.S.-Federal 1-30
NE/NE	30-144-101	9711	Donald Slawson	Elkhorn Ranch-Federal 1-30
NE/SW	31-144-101	5588	Farmers Union	Federal 14-31
SE/SE	31-144-101	5554	Farmers Union	Federal 16-31
SE/NW	32-144-101	8579	Nucorp Energy	Anderson-Federal 32-2
SW/NE	32-144-101	9113	Petrolewis	Federal 3-32
SE/SW	32-144-101	5423	Farmers Union	Federal 14-32

Q/Q	S-T-R	Number	Operator	Well Name
			(Cored interval in feet)	
NE/NW	33-144-101	9585	Tenneco Oil	Hamilton-U.S.A. 2-33
SE/SW	33-144-101	10229	Tenneco Oil	U.S.A.-U.V.I. 1-33
			(9295-9391)	
SE/SW	33-144-101	8024	Tenneco Oil	Tenneco-U.S.A.-U.V.I. 3-33
SE/NE	33-144-101	9567	Tenneco Oil	U.S.A.-U.V.I. 4-33
NW/NW	34-144-101	9432	Ladd Petroleum	Ladd-Federal 34-11
SE/NW	1-144-102	9616	MGF Oil	BN 22-1
SE/SW	1-144-102	10457	Milestone	BN 24-1
SE/SE	1-144-102	8710	MGF Oil	MGF-BN 44-1
SE/NE	1-144-102	9007	MGF Oil	MGF-BN 42-1
SW/NW	2-144-102	8472	Apache Corp	Federal 2-2
SW/SW	2-144-102	8869	Apache Corp	Federal 2-4
SW/SE	2-144-102	8695	Apache Corp	Federal 2-3
SW/NE	2-144-102	9145	Apache Corp	Federal 2-5
NW/NE	2-144-102	5328	Texacota Oil	Federal 1-2
			(9296-9318)	
SE/NW	3-144-102	9889	Apache Corp	Federal 3-4
SW/SW	3-144-102	8609	Apache Corp	Federal 3-2A
SE/NE	3-144-102	7833	Apache Corp	Federal 3-1
SW/NE	4-144-102	11705	Apache Corp	Easy Rider-Federal 4-8
NW/SW	10-144-102	10596	Basic Earth Systems	Fantail-Federal 23-10
NE/SE	10-144-102	8874	Supron Energy	Federal 1-10
NW/NE	11-144-102	9425	Supron Energy	Federal 1-11
SW/SW	11-144-102	9443	Florida Exploration	Federal 2-11
NW/NE	11-144-102	10077	Florida Exploration	Federal 4-11
SE/NW	12-144-102	10989	Milestone	Federal 12-12
NW/SE	12-144-102	9426	Florida Exploration	Federal 12-1
SW/NE	12-144-102	8542	Tenneco Oil	Graham-U.S.A. 1-12
NE/NE	13-144-102	9442	Florida Exploration	Federal 13-1
SW/SW	14-144-102	8007	Apache Corp	Gulf-Federal 2-14
SE/SE	14-144-102	4419	Shell Oil	Shell-NP-Gov't 44-14
			(9300-9350, 9393-9443)	
NE/NE	14-144-102	8417	Apache Corp	Federal 14-4
SE/NW	15-144-102	8903	Basic Earth Systems	Buckhorn-Federal 22-15
NE/SW	15-144-102	8474	Tenneco Oil	Graham-U.S.A. 1-15
NE/SE	15-144-102	8192	Apache Corp	Federal 1-15
NE/NE	15-144-102	8931	Apache Corp	Federal 2-15
NE/NE	15-144-102	9861	Apache Corp	Federal 3-15
NE/NW	16-144-102	9943	Apache Corp	Moore 3-16
SE/NW	19-144-102	10085	Coastal	Coastal-BN 3-19
SE/SE	19-144-102	8070	Coastal	Big Elk Creek-BN 1-19
SW/NE	19-144-101	9598	Coastal	Coastal-BN 2-19
SE/SW	20-144-102	9078	Tenneco Oil	Coulam-U.S.A. 1-20
SE/NW	22-144-102	9271	Axem Resources	Connell-Fee 6-22
NE/SW	22-144-102	9902	Axem Resources	Connell-Fee 11-22
NE/SE	22-144-102	8291	Apache Corp	Connell 2-22
NE/NE	22-144-102	7567	Apache Corp	Federal 1-22

Q/Q	S-T-R	Number	Operator	Well Name (Cored interval in feet)
C/NW	23-144-102	8008	Apache Corp	Federal 2-23
NE/SW	23-144-102	8829	Chambers Exploration	Buckhorn-Federal 3-23
NW/SE	23-144-102	10576	Nance Petroleum	Federal 10-23
SW/SW	24-144-102	11231	Nance Petroleum	Federal 13-24
NW/SE	24-144-101	11184	Petroleum Inc	Masters-Federal 1-24
SE/NW	26-144-102	11784	Nance Petroleum	Federal 6-26
NE/NE	26-144-102	10713	Nance Petroleum	Federal 1-26
SW/NE	27-144-102	8037	Apache Corp	Connel 27-1
NW/Nw	29-144-102	8234	Coastal	Coastal-Al Aquitaine 1-29
SW/NE	30-144-102	10935	Milestone	Federal 42-30
SW/SW	34-144-102	10212	Adobe Oil and Gas	Adobe-Western-Connell 14-34
	(McKenzie County)			
SE/NE	1-145-100	9762	Belco Petroleum	Sheep Creek-Storm 2-1
SE/NE	1-145-100	8013	Amoco Production	Storm 1-1
SE/NW	7-145-100	7555	Belco Petroleum	Edgar-BN 6-7
SE/SW	7-145-100	6552	Belco Petroleum	Edgar-BN 3-7
NW/SE	7-145-100	7098	Belco Petroleum	Edgar-Bn 12-7
SW/NW	8-145-100	7808	Sinclair	Sinclair-Federal 2-8
C/SW	8-145-100	7705	Sinclair	Federal-RR 1-8
SW/NW	9-145-100	11727	Meridian	Meridian 12-9
NW/SW	10-145-100	11275	Meridian	Federal-Sharptail 13-10
SE/NW	12-145-100	8064	Adobe Oil-Western Exploration	Roughrider-Federal 22-12
SW/NW	17-145-100	8782	Belco Petroleum	Sheepcreek-BN 19-17
NW/NE	18-145-100	7483	Sinclair	Federal-RR 2-18
NW/SE	18-145-100	8854	Sinclair	Sinclair-Federal 4-18
NE/SW	18-145-100	8811	Sinclair	Federal-RR 5-18
SW/NW	18-145-100	7224	Sinclair	Federal 1-18
SW/SE	21-145-100	9005	Gulf Oil	Roughrider-Federal 1-21-3D (9584-9596.5, 9601-9647)
NE/SE	25-145-100	7501	Amoco Production	Federal "B" 1-25
SE/NW	29-145-100	7518	Pennzoil	Outback-Federal 29-22
C/SE	34-145-100	9569	Cities Service	Federal-DG 1-34
SE/SE	1-145-101	7525	Belco Petroleum	Edgar-BN 10-1
SW/NE	10-145-101	2723	Hunt Oil	U.S.A. "A" 1-10
SW/SE	10-145-101	6550	Belco Petroleum	Roughrider-Federal 10-10
SW/NE	11-145-101	6077	Belco Petroleum	BN-Sheepcreek 1-11
NE/NE	12-145-101	6926	Belco Petroleum	Edgar-Federal 5-12
NE/SE	12-145-101	6566	Belco Petroleum	Edgar-Federal 4-12
NW/NE	13-145-101	6403	Belco Petroleum	Edgar-BN 2-13
SE/NW	13-145-101	9643	Belco Petroleum	Edgar-BN 13-13
SE/SW	13-145-101	9379	Belco Petroleum	Edgar 9-13
NE/SE	13-145-101	6083	Belco Petroleum	Edgar-BN 1-13

Q/Q	S-T-R	Number	Operator	Well Name
SE/NE	13-145-101	8340	Belco Petroleum	Edgar-BN 11-13
SE/NE	14-145-101	2757	Texaco	Gov't "A" NCT 12-14
SW/NW	14-145-101	7251	Exeter Exploration	Federal 5-14
SW/SW	14-145-101	2611	Texaco	Gov't "A" NCT 11-14
SE/SE	14-145-101	7300	Exeter Exploration	Federal 16-14
SE/SW	14-145-101	5383	Belco Petroleum (9449.5-9480)	BN 5-15
SW/NE	15-145-101	6282	Petro Lewis	BN 32-15R
SW/NE	16-145-101	2584	Shell-NP (9540-9574)	State 32-16-1
NE/SW	16-145-101	10940	Belnorth Petroleum	Deer Draw-State 1-16
SE/SE	16-145-101	6132	Belco Petroleum	Roughrider-State 9-16
SW/SW	21-145-101	4088	Farmers Union (9338-9387, 9404-9445)	NP-RR 14-21
NW/SE	21-145-101	5994	Belco Petroleum-BN	Roughrider 8-21
SE/NE	21-145-101	5870	Belco Petroleum-BN	BN 7-21
NE/NE	22-145-101	2987	H.L. Hunt	U.S.A. "B" 1-22
SE/NW	22-145-101	5632	Belco Petroleum	Federal 6-22
NE/NW	23-145-101	10319	Koch Exploration	Koch-RR-BN 16-23
SW/NE	23-145-101	2678	Shell-NP (9453-9556)	NP 32X-23-1
SE/SE	23-145-101	10882	Milestone	BN 44-23
NE/NW	24-145-101	10818	Conoco	Halvorson 31-5
NE/SW	24-145-101	10817	Petroleum Inc	Arithson D-2
NE/SE	24-145-101	9865	Union Texas	Federal 24-2
NE/NE	24-145-101	8162	Union Texas	Federal 24-1
SE/NW	25-145-101	9288	Belco Petroleum	Sheep Creek-BN 22-25
SW/SE	25-145-101	9453	Belco Petroleum	Sheep Creek-BN 24-25
SE/NE	25-145-101	7314	Belco Petroleum	Sheep Creek-BN 16-25
NW/NW	27-145-101	9399	Depco	Forest-Depco-BN 11-27
NW/NW	28-145-101	11178	Belnorth Petroleum	Roughrider-Federal 12-28
SW/SW	28-145-101	5214	Belco Petroleum	Roughrider 1-28
SW/SE	28-145-101	5263	Davis Oil-Tiger Oil	Roughrider-Federal 4-28
SW/SE	29-145-101	5268	Davis Oil-Tiger Oil	Roughrider-Federal 1-29
SE/NE	29-145-101	11257	Beartooth Oil	Federal 1-29
SE/SE	31-145-101	11307	Sage Energy	Buckhorn-Federal 44-31
SE/NW	32-145-101	5380	Belco Petroleum (9241-9267)	Roughrider-Federal 1-32
NE/SW	32-145-101	5297	Tiger Oil (9246-9264)	Roughrider-Federal 2-32
NW/SE	32-145-101	9297	Grace Petroleum	Magpie-Federal 1-32
SW/NE	32-145-101	5258	Tiger Oil (9276-9291, 9309-9353)	Roughrider-Federal 3-32
NE/NW	33-145-101	5346	Lone Star Producing (9172-9196)	BN 1-33
SW/NE	33-145-101	5254	Belco Petroleum	Roughrider-BN 2-33
NW/SE	33-145-101	8602	Milestone	BN 33-33
SE/SW	34-145-101	8733	Belco Petroleum	Roughrider-Federal 14-34

Q/Q	S-T-R	Number	Operator	Well Name
SW/SW	35-145-101	2707	Shell-NP (9460-9608)	NP 14-35-1
NE/NW	3-146-100	8604	Pennzoil	Pennzoil-Depco-Trailside 3-21F
NE/NE	4-146-100	7823	Amoco Production	Federal-C 1-4
SE/SW	16-146-100	7496	Pennzoil	Roughrider 16-24
NE/NW	21-146-100	8937	Belco Petroleum	Sheep Creek-BN 9-21
NE/SW	21-146-100	9874	Belco Petroleum	Sheep Creek-BN 26-21
SW/SE	21-146-100	6786	Belco Petroleum	Sheep Creek-BN 4-21
SE/NW	28-146-100	10460	Belnorth Petroleum	Sheep Creek-Federal 27-28
SW/SW	28-146-100	7481	Pennzoil	Pennzoil 28-14
SE/SE	32-146-100	6985	Belco Petroleum	Sheep Creek-Federal 7-32
SE/NW	33-146-100	6698	Belco Petroleum	Sheep Creek-BN 2-33
NE/SW	33-146-100	7313	Belco Petroleum	Sheep Creek-BN 10-33
NW/SE	4-146-101	11384	Milestone	Milestone-Federal 33-4
SE/SE	10-146-101	8219	Pennzoil	Pennzoil-Depco 10-44-F
SW/SE	12-146-101	8199	Belco Petroleum	Sheep Creek-Federal 17-12
SE/SW	14-146-101	7435	Kerr-McGee Corp	Federal 1-14
SW/NW	14-146-101	2667	Texaco (9465-9548, 9582-9640)	Gov't-M. Pace 1-14
SW/NE	15-146-101	9253	Pennzoil-Depco	BN 15-32
SE/NW	15-146-101	7494	Pennzoil-Depco	BN 15-22
SE/SW	15-146-101	7495	Pennzoil-Depco	BN 15-24
NW/SE	15-146-101	8668	Pennzoil	BN 15-34
SE/SE	15-146-101	6846	Pennzoil	Pennzoil-Depco-BN 15-44
NE/NE	16-146-101	9872	Depco	State 41-16
SE/NE	19-146-101	8568	Amerada Hess	Roughrider-Federal 1-19
NE/NW	22-146-101	7512	Kerr-McGee	Federal 1-22
SE/NE	22-146-101	8086	Kerr-McGee	Federal 2-22
NW/NW	23-146-101	4520	Belco Petroleum	Sheep Creek 8-23
SW/SW	26-146-101	9186	Pennzoil	Beicegel Creek-Federal 26-14
SE/NE	27-146-101	8468	Pennzoil-Depco	Beicegel Creek-BN 27-42
C/NW	34-146-101	9982	Basic Earth System	Beicegel-Carson 1-34
SW/SE	34-146-101	10548	Basic Earth System	Beicegel-Federal 34-34
SW/NW	36-146-101	6503	Belco Petroleum	Edgar-State 2-36

APPENDIX B

WELL LOG DATA

Subsurface data was acquired from mechanical well logs recorded in wells throughout the study area. Deviated borehole data was not included. Well numbers are those of the North Dakota Geological Survey. The KB column represents the elevations measured at the top of the drilling rig's kelly bushing, from which all depths are measured and presented below as subsea elevations. RIVAL represents the top of the Rival subinterval. STATE"A" represents the top of the State "A" log marker beds. FRYBURG represents the top of the Fryburg gamma-ray marker bed. ER-RR"PAY" represents total cumulative feet of porosity greater than or equal to 8% Neutron log value. NR indicates a log marker that was not reached by the logging tools. NA indicates that mechanical logs were not available over that interval. A "?" indicates that interval was unable to be determined from mechanical logs. Wells are listed in the same order as Appendix A.

Well No.	KB	RIVAL	/ STATE"A"	/ FRYBURG	/ ER-RR"PAY"
7113	2392	-6922	-6948	-7079	13
9428	2452	-6846	-6872	-7002	13
5690	2527	-6833	-6857	-6985	5
6724	2428	-6842	-6864	-6994	10
6912	2361	-6843	-6872	-6997	11
6937	2409	-6837	-6864	-6988	8
8929	2450	-6840	-6867	-6994	11
6686	2474	-6838	-6860	-6993	NA
5964	2334	-6849	-6878	-7107	4 (Sonic)
6013	2477	-6841	-6859	-6991	11 (Sonic)
6292	2408	-6854	-6875	-7008	23 (Sonic)
5948	2453	-6845	-6869	-7002	14
2853	2572	-6850	-6873	-7006	NA
5664	2453	-6847	-6869	-7000	11
9121	2303	-6856	-6883	-7011	15
5789	2311	-6831	-6853	-6987	8
8705	2413	-6864	-6888	-7015	14
6158	2371	-6831	-6857	-6989	6
7364	2405	-6829	-6853	-6983	4
6856	2443	-6817	-6843	-6973	10
7118	2435	-6842	-6865	-6997	9
7250	2467	-6827	-6849	-6984	6
6905	2445	-6829	-6851	-6980	11
7439	2515	-6848	-6874	-7007	13

Well No.	KB	RIVAL /	STATE"A" /	FRYBURG /	ER-RR"PAY"
7165	2405	-6834	-6856	-6989	8
9247	2448	-6876	-6900	-7032	9
8068	2476	-6870	-6894	-7028	10
6346	2517	-6881	-6897	-7040	14
8022	2725	-6870	-6894	-7030	4
6999	2502	-6834	-6856	-6988	2
6938	2493	-6847	-6858	-7001	6
7225	2501	-6859	-6881	-7011	0
7143	2526	-6850	-6876	-7006	0
7131	2444	-6829	-6850	-6982	13
6258	2448	-6819	-6842	-6970	11
4455	2468	-6828	-6852	-6980	NA
7690	2373	-6813	-6832	-6959	8
7128	2382	-6809	-6832	-6964	NA
6169	2555	-6841	-6873	-7002	10
8962	2480	-6828	-6850	-6991	11
8465	2741	-6850	-6872	-7009	13
7082	2416	-6814	-6837	-6973	29
9122	2423	-6794	-6819	-6955	5
8723	2352	-6807	-6826	-6954	2
9329	2396	-6796	-6814	-6944	2
10074	2684	-6821	-6842	-6980	6
7399	2283	-6867	-6885	-7015	16
5711	2285	-6857	-6879	-7009	15
7761	2278	-6842	-6861	-6992	19
6957	2155	-6873	-6885	-7020	44
9224	2266	-6896	-6906	-7035	17
10474	2450	-6858	-6869	-7002	21
5816	2445	-6847	-6865	-6993	13
8487	2344	-6827	-6844	-6972	6
9340	2283	-6838	-6851	-6981	7
11109	2359	-6814	-6830	-6950	9
8363	2287	-6815	-6831	-6955	5
8251	2334	-6807	-6824	-6950	3
7984	2342	-6810	-6828	-6956	6
7451	2574	-6738	-6750	-6876	8
7792	2398	-6730	-6746	-6872	4
10475	2181	-6797	-6809	-6934	2
9516	2538	-7046	-7070	-7202	15
6310	2198	-6962	-6982	-7114	25
9351	2203	-6983	-7000	-7133	24
8651	2372	-6931	-6950	-7083	15
8564	2250	-6956	-6978	-7114	27
9524	2261	-6971	-6993	-7129	18
9607	2296	-6959	-6980	-7113	23
10222	2284	-6958	-6976	-7103	16
11240	2288	-6960	-6982	-7112	23

Well No.	KB	RIVAL	STATE"A"	FRYBURG	ER-RR"PAY"
11621	2309	-6947	-6968	-7097	22
7600	2325	-6952	-6976	-7108	12
10451	2352	-6968	-6991	-7122	5
7308	2356	-7020	-7047	-7164	10
10303	2343	-6924	-6941	-7071	18
7291	2297	-6979	-7003	-7134	10
9641	2355	-6929	-6952	-7080	10
10215	2361	-6916	-6933	NR	14
9578	2515	-6887	-6907	-7040	18
9577	2507	-6905	-6921	-7047	22
9856	2427	-6916	-6939	NR	10
9626	2577	-6891	-6914	-7048	25
9561	2559	-6879	-6901	-7035	22
9492	2247	-6916	-6935	-7067	9
9900	2272	-6884	-6904	-7034	12
9581	2476	-6889	-6912	-7036	22
10915	2340	-6878	-6902	-7037	19
9294	2286	-6895	-6922	-7048	13
9215	2359	-6868	-6893	-7025	21
9295	2451	-6887	-6904	-7036	19
9772	2463	-6881	-6897	-7031	23
11079	2476	-6866	-6886	-7020	6
8422	2363	-6909	-6931	-7061	13
8128	2589	-6881	-6901	-7031	6
9079	2387	-6913	-6932	-7061	12
7629	2633	NA	NA	-7083	13
8853	2574	-6890	-6912	-7043	5
10114	2345	-6910	-6932	NR	14
8671	2295	-6845	-6865	-6993	8
8430	2270	-6857	-6879	-7009	13
8490	2285	-6856	-6878	-7007	13
9216	2274	-6887	-6908	-7039	18
9183	2310	-6872	-6892	NR	17
9182	2308	-6872	-6894	-7024	9
9214	2268	-6870	-6892	-7021	12
5811	2537	-6873	-6894	NR	10
9711	2243	-6879	-6899	-7032	10
5588	2255	-6873	-6877	-7009	19
5554	2562	-6848	-6866	-6994	19
8579	2519	-6872	-6891	-7023	19
5423	2486	-6852	-6868	-7008	12
9585	2354	-6847	-6872	-7000	7
10229	2392	-6835	-6861	-6992	11
9567	2417	-6859	-6878	-7004	13
9432	2318	-6906	-6926	-7055	8
9616	2378	-6975	-6992	-7124	22

Well No.	KB	RIVAL /	STATE"A" /	FRYBURG /	ER-RR"PAY
10547	2520	-6966	-6986	-7116	22
8710	2307	-6965	-6984	-7117	27
9007	2233	-6965	-6989	-7121	22
8472	2304	-6970	-6986	-7123	31
8869	2520	-6973	-6992	-7122	33
8695	2514	-6975	-6996	-7127	31
9145	2421	-6976	-6990	-7116	29
5328	2254	-6970	-6991	-7120	29
9889	2405	-6955	-6974	-7106	29
8609	2234	-6956	-6972	-7100	20
7833	2377	-6982	-6993	-7123	22
10596	2284	-6957	-6971	-7100	24
8874	2547	-6961	-6973	-7105	22
9425	2522	-6988	-7002	-7130	20
9443	2545	-6958	-6975	-7105	28
10077	2520	-6968	-6984	-7116	34
10989	2486	-6978	-6992	-7124	27
9426	2602	-6948	-6966	-7098	24
8542	2543	-6941	-6958	-7087	8
9442	2660	-6946	-6964	-7097	15
8007	2236	-6907	-6924	-7050	25
4419	2341	-6960	-6978	-7106	NA
8417	2604	-6958	-6976	-7106	38
8474	2173	-6935	-6949	-7077	16
8192	2264	-6911	-6926	-7052	26
8931	2523	-6949	-6963	-7094	32
9943	2129	-6935	-6947	-7077	25
10085	2308	-6900	-6910	-7040	10
8070	2300	-6894	-6906	-7031	14
9598	2427	-6899	-6913	-7040	24
9078	2444	-6894	-6910	-7036	23
9271	2324	-6922	-6936	-7063	30
9902	2160	-6940	-6955	-7081	14
8291	2295	-6917	-6935	-7064	29
7567	2176	-6932	-6946	-7069	27
8008	2176	-6896	-6914	-7042	19
8829	2184	-6912	-6926	-7056	15
10576	2197	-6917	-6935	-7065	25
11231	2252	-6898	-6924	-7048	24
11184	2231	-6913	-6929	-7059	32
11784	2485	-6920	-6932	-7062	14
10713	2439	-6895	-6911	-7043	14
8037	2203	-6913	-6927	-7057	14
8234	2239	-6903	-6915	-7042	22
9515	2450	-6886	-6902	-7026	14
10935	2279	-6877	-6889	-7015	16

Well No.	KB	RIVAL / STATE"A" / FRYBURG / ER-RR"PAY"			
10212	2413	-6887	-6903	-7032	29
9762	2445	-7197	-7217	-7343	13
8013	2442	-7196	-7222	-7350	10
7555	2312	-7024	-7050	-7177	16
6552	2346	-7012	-7032	-7160	14
7098	2366	-7032	-7050	-7182	14
7808	2332	-7064	-7084	-7212	20
7705	2339	-7034	-7060	-7189	21
11727	2255	-7109	-7140	-7269	28
11275	2282	-7182	-7200	-7330	24
8064	2545	-7190	-7208	-7338	21
8782	2341	-7060	-7081	-7207	17
7483	2330	-7019	-7043	-7176	26
8854	2379	-7011	-7032	-7163	27
8811	2398	-7004	-7022	-7151	27
7224	2359	-7032	-7050	-7179	23
9005	2361	-7139	-7166	-7295	17
7501	2556	-7112	-7131	-7271	11
7518	2535	-7057	-7087	-7221	22
9569	2585	-7059	-7083	-7216	5
7525	2443	-7051	-7079	-7207	42
6550	2320	-7044	-7063	-7196	39
6077	2324	-7074	-7089	NR	22
6926	2285	-7037	-7055	-7185	34
6566	2351	-7014	-7043	-7173	30
6403	2387	-7019	-7042	-7177	38
9643	2397	-7036	-7051	-7187	18
9379	2424	-7033	-7050	-7192	18
6083	2405	-7024	-7044	-7177	44
8340	2410	-7002	-7030	-7153	9
2757	2402	-7036	-7056	NR	NR
7251	2380	-7055	-7076	NR	35
2611	2335	-7025	-7049	NR	NR
7300	2398	-7055	-7067	-7200	26
5383	2350	-7028	-7049	-7178	NA
6282	2303	-7019	-7045	NR	11
2584	2463	-7028	-7053	-7185	NA
10940	2452	-7030	-7048	-7175	29
6132	2391	-7037	-7054	-7183	28
4088	2305	-6985	-7015	-7143	27
5994	2496	-7008	-7024	NR	41
5870	2559	-7017	-7032	NR	31
2987	2381	-7023	-7043	-7172	NA
5632	2400	-7008	-7027	-7156	32
10319	2346	-7035	-7061	-7191	38
2678	2401	-7019	-7051	-7168	NA

Well No.	KB	RIVAL	STATE"A"	FRYBURG	ER-RR"PAY"
10882	2441	-7036	-7055	-7179	25
9865	2463	-7027	-7052	-7187	40
8162	2440	-7026	-7046	-7178	12
9288	2401	-7009	-7027	-7155	26
9453	2368	-7003	-7018	-7148	23
7314	2353	-7007	-7033	-7163	NA
9399	2499	-7012	-7028	-7157	27
5214	2197	-6989	-7001	-7136	11
5263	2177	-6991	-7004	-7135	33
5268	2117	-7005	-7019	-7147	32
11307	2407	-6973	-6987	-7115	22
5380	2173	-6997	-7017	-7145	33
5297	2193	-6981	-6999	-7129	31
9297	2237	-7001	-7020	-7151	25
5258	2210	-6973	-6997	-7128	38
5346	2148	-6964	-6984	-7116	23
5254	2162	-6982	-6994	-7128	NA
8602	2166	-6982	-7001	-7132	22
8733	2214	-6992	-7009	-7140	21
2707	2218	-7002	-7018	-7152	NA
8604	2123	-7216	-?	-7388	25
7823	2116	-7168	-?	-7338	17
7496	2621	-7161	-7183	-7311	14
8937	2614	-7151	-7178	-7305	10
9874	2575	-7155	-7175	-7305	11
6786	2590	-7170	-7184	-7318	28
10460	2668	-7138	-7160	NR	24
7481	2563	-7122	-7145	-7273	9
6985	2527	-7117	-7131	NR	NR
6698	2536	-7094	-7072	NR	15
7313	2574	-7116	-7148	NR	24
11384	2141	-7167	-7184	-7319	3
8219	2443	-7140	-7166	-7303	37
8199	2412	-7210	-7226	-7358	3
7435	2612	-7137	-7158	-7299	12
2667	2382	-7146	-7183	-7312	NA
9253	2442	-7112	-7127	-7271	28
7494	2557	-7101	-7115	-7258	21
7495	2492	-7104	-7126	-7260	19
8668	2453	-7103	-7124	-7267	11
6846	2443	-7101	-7121	-7251	14
9872	2628	-7127	-7146	NR	15
7512	2616	-7114	-7134	-7271	1
8086	2477	-7134	-7159	-7295	22
9186	2318	-7110	-7128	-7260	15
8468	2357	-7095	-7111	-7250	20
9982	2171	-7109	-7129	-7260	26
10458	2234	-7096	-7117	-7246	32
6503	2256	-7126	-7144	-7274	35

APPENDIX C

CORE AND THIN SECTION DESCRIPTIONS

The following sample descriptions are arranged alphabetically by county and numerically by North Dakota Geological Survey well number within each county. Depths given are those footages marked on each individual box of core. Core depths which have been corrected to electric log depths are given in parentheses. Core descriptions include the following: the gross rock textures of Dunham (1962), and Maiklem and others (1969); color from the GSA Rock Color Chart (Goddard, 1963); gross mineralogy; stratification (McKee and Weir, 1953); significant sedimentary structures; significant bioturbation structures; allochems in decreasing abundance; diagenetic features; stylolites (with amplitudes in parentheses); visual estimates of porosity; and estimate of any oil staining. Lithotype designations are assigned to each core description at the end of the description and are denoted by the symbols LT (e.g. LT-5) as defined in the text.

Thin section descriptions are inserted between the core descriptions and are denoted by TS preceding the sample depth. Thin section descriptions include the following: the classification of Dunham (1962), or Maiklem and others (1969); mineralogic modifiers; allochems in decreasing abundance; sorting; particle packing and particle contacts after Taylor (1950) and Kahle (1966); orthochems and accessory minerals in decreasing abundance; visual estimates of porosity after Choquette and Pray (1970); diagenetic features; and comments (if any).

Shell, Government 41x-5-1 (NDGS-2853)
C-NE 5-143N-101W Billings County, North Dakota
Core Depths: 9460-9490, 9497-9647
Log Depths: 9459-9489, 9492-9642

9460-9461.3 Packstone; dark yellowish brown; dolostone; non-laminated, massive; intraclasts, ooliths, bioclasts; anhydritic cement; tight; (LT-4).

9461.3-9470.1 Mudstone; pale yellowish brown; dolostone; laminated; fenestral; anhydritic cement; tight; interbedded with: Very light gray and medium gray; distorted massive and bedded massive anhydrite; (LT-5,6).

9470.1-9477.2 Mudstone; dusky yellowish brown; limestone; laminated and massive; vertical and horizontal burrows (Chondrites); blocky and lath crystallotopic anhydrite; (LT-5).

9477.2-9482.3 Bedded massive anhydrite; pale yellowish brown; anhydrite; (LT-6).

9482.3-9482.8 Mudstone-wackestone; dark yellowish brown; dolostone; laminated; fenestral; ostracodes; anhydritic cement; tight; (LT-5).

9482.8-9484.8 Bedded massive anhydrite; pale yellowish brown; anhydrite; (LT-6).

9484.8-9488.4 Finely crystallotopic anhydrite; brownish black; dolostone; fenestral; mudstone; tight; (LT-5).

TS9485 Mudstone; massively bedded anhydrite; rounded intraclasts, ostracodes; well sorted; no packing; microcrystalline to subfelted replacement anhydrite, aligned displacive anhydrite, trace microspar, trace saddle dolomite; tight; allochem ghosts.

9488.4-9489.3 Wackestone-packstone; pale yellowish brown; dolomitic limestone; massive; peloids, bioclasts; fine crystallotopic anhydrite; tight; anhydrite replacement of allochems; (LT-2).

TS9489 Packstone; calcitic dolostone; peloids, calcispheres, bioclasts, ostracodes; very well sorted; point packed; microcrystalline dolomite, microcrystalline replacement anhydrite, saddle dolomite; cement filled interparticle porosity; possible algal tubules.

9489.3-9490 Mudstone; brownish gray; limestone; massive; horizontal burrows (Chondrites); peloids; tight; (LT-5).

9497-9497.7 Mudstone; brownish black; limestone; laminated; abundant crystallotopic anhydrite; tight; (LT-5,6).

9497.7-9500 Bedded nodular anhydrite; brownish black, very light gray; limestone; tight; (LT-6).

9500-9504 Packstone; dark yellowish brown; limestone; stromatolitic with interbedded nodular anhydrite; crystallotopic anhydrite; peloids; tight; peloid grainstone lense at 9501.5; (LT-4).

9504-9508.4 Bedded massive anhydrite; pale yellowish brown; anhydrite; relict gypsum sand at 9505, black organic laminae at 9504.5; tight; (LT-6).

9508.4-9511.3 Packstone; dark yellowish brown; limestone; laminated; peloids, intraclasts; stylolite at 9510 (3 cm); poor intercrystalline and moldic porosity; even oil stain; (LT-4).

TS9509 Grainstone-packstone; dolomitic limestone; peloids, ooliths, intraclasts, bioclasts, calcispheres, forams; variably sorted; point and longitudinally packed; microcrystalline interparticle dolomite, isopachous chert, replacive microcrystalline anhydrite; no porosity.

TS9510 Grainstone; dolostone; ooliths, intraclasts, bioclasts; very well sorted; point packed, concavo-convex packed; interparticle dolomite, calcspar; solution-enlarged moldic porosity.

9511.3-9522 Mudstone-wackestone; dusky yellowish brown; limestone; massive; corals (Vesiculophyllum); stylolites (0.5-2.0 cm); microfractured at 9518, tight; (LT-1).

9522-9527 Mudstone; pale yellowish brown; limestone; massive; core rubble; (LT-3).

9529-9539 Mudstone; brownish gray; limestone; massive; burrow relief at 9534; stylolites (0.5-2.0 cm); tight; (LT-3).

9539-9540.3 Wackestone; dusky yellowish brown; limestone; massive; corals (Sychnoelasma, Syringopora, fragments); tight; (LT-1).

9540.3-9545 Mudstone; pale yellowish brown; limestone; massive; stylolites at 9541.7, 9542.1 (1.5 cm); poor intercrystalline porosity; oil stain; (LT-3).

9545-9557 Wackestone; brownish black; limestone; massive; crinoids, coral fragments; stylolite seam at 9548 (1.5 cm); tight; (LT-1).
TS9548 Packstone; limestone; crinoids, brachiopods, trilobite fragments; variably sorted; point, concavo-convex packed; microspar, pseudospar, dolomite; tight; stylolite seams and swarms.

9557-9559 Mudstone; dark yellowish brown; calcitic dolostone; massive; stylolite at 9558.5 (10 cm); tight; (LT-3,2).

9559-9566.5 Mudstone, massive; moderate yellowish brown; dolostone; fair intercrystalline porosity; oil stain; (LT-2,3).
TS9562 Mudstone; dolostone; dolomite, bitumen; solution enlarged intercrystalline porosity.

9566.5-9573.2 Wackestone-mudstone; pale yellowish brown; limestone; massive; coral fragments and corals (Vesiculophyllum, Sychnoelasma); spalled allochems; tight; (LT-2).

9573.2-9577 Wackestone; brownish black, dark gray; limestone; horizontal burrows (3 cm) at 9574; coral fragments, corals (Vesiculophyllum, Syringopora); stylolites at 9573.3, 9575.2, 9575.4; tight; burrows resistant to compaction; (LT-1).

9577-9588 Mudstone; pale yellowish brown; calcitic dolostone; massive; horizontal and inclined indistinct burrows (Zoophycos?); anhydrite nodules (2.0-8.0 cm), trace pyrite; brecciated zone at 9586.5; tight; (LT-3).
TS9586.5 Mudstone; dolostone; dolomite, calcspar; cementation reduced intercrystalline porosity; microstylolite swarms.

9588-9591.4 Wackestone; dark yellowish brown; limestone; massive; coral fragments, corals (Vesiculophyllum); silicic nodules at 9590.7,

9590.9; tight; (LT-1).

TS9591 Wackestone; silicified dolostone; crinoids, brachiopods; well sorted; no packing; dolomite, chert; tight; silicified crinoids.

9591.4-9601.5 Mudstone; dark yellowish brown; dolomitic limestone; massive; scattered anhydrite nodules (1.0-2.0 cm), pyrite; stylolite seam at 9601 (0.8 cm); tight; (LT-3).

TS9593 Mudstone; anhydritic dolostone; intraclasts, forams, ostracodes; well sorted; no packing; dolomite, subfelted-felted anhydrite, calcspar, celestite, pyrite; cementation filled intercrystalline porosity.

TS9596 Wackestone; calcitic dolostone; crinoids, brachiopods; well sorted; no packing; dolomite, calcspar, microspar, pseudospar, pyrite; tight.

TS9601.5 Wackestone; dolostone; crinoids, bioclasts, ostracodes; well sorted; no packing; dolomite, saddle dolomite, trace calcspar, pyrite; cementation reduced intercrystalline porosity; stylolite swarms.

9601.5-9607 Wackestone; brownish gray; limestone; massive; vertical to inclined indistinct burrows (Chondrites?, Planolites?); crinoids, bioclasts, brachiopods, corals; stylolite at 9606 (9.0 cm); tight; (LT-1).

9607-9622 Wackestone; brownish gray; limestone; massive; peloids, bioclasts; stylolites (0.2-6.0 cm); tight; (LT-1).

9622-9639 Packstone-wackestone; brownish gray; limestone; massive; horizontal burrows at 9635; peloids, crinoids, brachiopods (Schelwienella), brachiopod zone at 9630; stylolites (0.5 cm), trace anhydrite nodules; tight; burrows resist compaction; (LT-2).

TS9630 Packstone; limestone; crinoids, brachiopods, molluscs, trace corals; variably sorted; concavo-convex, sutured packed; micrite, microspar, dolomite, trace saddle dolomite; tight; wispy microstylolites.

9639-9642.4 Wackestone; brownish gray; limestone; discontinuously laminated; horizontal and inclined burrows (Zoophycos); bioclasts, peloids; compaction laminae around burrows; trace intercrystalline porosity; (LT-3).

9642.4-9647 Wackestone, local packstones; dark gray; limestone; massive; crinoids, bioclasts, coral fragments; wispy microstylolites, stylolites (0.2-2.5 cm); tight; (LT-1).

TS9643 Packstone; limestone; crinoids, brachiopods, molluscs, trilobite fragments, corals, stony bryozoans; poorly sorted; point packed, sutured allochems; micrite, microspar, dolomite, chert, trace pyrite, bitumen; tight.

Shell, Government 41x-18 (NDGS 4455)
NE/NE 18-143N-101W Billings County, North Dakota
Core Depths: 9238-9394, 9442-9501
Log Depths: 9238-9362, 9364-9394, 9442-9501

9296-9299.4 Wackestone, local packstones; grayish black; limestone; indistinctly laminated; possible contact with Midale subinterval; crinoids, corals; tight; compacted allochems; (LT-1).

9299.4-9304.2 Wackestone, local mudstone; dusky yellowish brown; limestone; burrow mottled; brachiopods, algal clasts, bioclasts, (brachiopod zone at 9300); stylolite (1.0 cm) at 9302.4; tight; (LT-2).

TS9300 Packstone; dolomitic limestone; crinoids, brachiopods, peloids, pellets, forams, ostracods, calcispheres, stoney and fenestrate bryozoans, gastropods; well sorted; point packed; micrite, microspar, dolomite, saddle dolomite, anhydrite; poor cementation reduced moldic porosity; early breakage of brachiopods and ostracodes (compaction).

9304.2-9305.3 Packstone; dark yellowish brown; limestone; peloids; 30% crystallotopic anhydrite; microstylolites at 9305; tight; (LT-5).

9305.3-9306.8 Wackestone; light olive gray; dolomitic limestone; local ostracode packstones; tight; (LT-5).

9306.8-9307.5 Mudstone; pale yellowish brown; dolomitic limestone; laminated, disrupted laminated clasts, teepee structure at 9307; tight; (LT-5).

9307.5-9317 Nodular mosaic anhydrite interbedded with nodular bedded anhydrite; medium gray; clay laminae and seams; tight; (LT-6).

9317-9320 Packstone; light gray to brownish gray; nodular mosaic anhydrite interbedded with laminated dolostone; peloids, intraclasts; pyritic; dolomitized algal crusts; tight; (LT-6,5).

9320-9331 Mudstone; olive gray; calcitic dolostone; thickly laminated, clay laminae at 9324; intercrystalline porosity; oil florescence; (LT-5).

9334-9335 Wackestone, local mudstones; dusky yellowish brown; limestone; thickly laminated; peloids; 15% crystallotopic anhydrite; tight; (LT-5).

9335-9339 Nodular mosaic anhydrite; light gray; dolomitic clayey seams; tight; (LT-6).

9339-9340 Wackestone; dark yellowish brown; dolostone; thinly laminated, algal laminae; peloids; tight; (LT-5).

9340-9347 Massively bedded anhydrite; medium dark gray and brownish gray; thin algal laminae at 9344.5-9345; dolomitic clay seams; tight; (LT-6).

9347-9349 Mudstone; light olive gray; dolomitic limestone; thickly laminated; enterolithic layer at 9347.3; Chondrites zones at 9347.5, 9348.0; tight; (LT-5).

9349-9353 Packstone; pale yellowish brown and dusky yellowish brown; limestone; thickly laminated, subareal dolomitic laminae between packstones; codiacean algae, pisoids, intraclasts, ooliths; 30% crystallotopic anhydrite and trace framboidal pyrite at 9351-9353; tight; (LT-5,6).

9353-9361 Massive anhydrite and bedded nodular anhydrite; medium gray; distorted clay laminae; tight; (LT-6).

9361-9364 Packstone; pale yellowish brown; dolostone; thickly laminated; dolomitic laminae and peloid packstone interlaminated; peloids; tight; (LT-5).

9364-9372 Packstone, locally wackestone; dusky yellowish brown; limestone; bedded nodular anhydrite at 9364-9365, 9371.8-9372; intraclasts, pisoliths, codeacean algal clasts at 9368-9369.3, brachiopods; 20% crystallotopic anhydrite at 9371-9371.8; tight; (LT-4b).

9372-9376 Grainstone-packstone; pale yellowish brown; dolomitic limestone; cross laminated and thinly laminated; intraclasts, ooliths, peloids; anhydrite nodules at 9373; tight; (LT-4c).

9376-9378 Bedded massive anhydrite; light brownish gray; wispy dolomitic laminae; tight; (LT-6).

9378-9381.8 Grainstone, local packstone; pale yellowish brown; calcitic dolostone; cross laminated and thinly laminated; peloids, intraclasts, pisoliths, bioclasts at 9381-9381.8; anhydrite nodules at 9380, anhydritic cement at 9381-9381.8; tight; (LT-4).

9381.8-9385.8 Wackestone, mudstone; dark yellowish brown; limestone; peloids, ostracodes, brachiopods; stylolite seam at 9385.2, scattered stylolites (1.5-2.5 cm), 1% pyrite; tight; (LT-2).

9385.8-9397 Packstone; dusky yellowish brown and dark yellowish brown; limestone; peloids; stylolite seam at 9390, scattered stylolites (1.0-6.0 cm); poor intercrystalline porosity; light brown oil stain at 9390-9397; (LT-4).

9440-9446 Wackestone; dusky yellowish brown; dolomitic limestone; indistinctly burrow mottled; corals at 9440-9441 (Vesiculophyllum),

bioclasts; tight; (LT-1).

9446-9450.8 Mudstone; olive gray; dolomitic limestone; vertical burrow at 9448; bioclasts; stylolite seam (2.0 cm) at 9449, scattered anhydrite nodules and pyrite crystals at 9448.8, 9450.7; tight; (LT-3).

9450.8-9457.5 Wackestone; Brownish black; limestone; crinoids, abundant corals (Vesiculophyllum, Stelechophyllum banfense, Sychnoelasma), brachiopods; cherty nodules at 9451-9452, 9455; tight; (LT-1).

9457.5-9461 Mudstone-wackestone; brownish gray; dolomitic limestone; indistinctly horizontal burrow mottled; bioclasts; scattered anhydrite nodules, stylolite seam (0.3 cm) at 9460.5, stylolite (2.5 cm) at 9458.7; tight; (LT-3).

9461-9473 Wackestone-mudstone; dusky yellowish brown; limestone; indistinctly burrowed; bioclasts, corals (Sychnoelasma); stylolite seam (0.3 cm) at 9470, microstylolitic, abundant stylolites (0.1-2.0 cm), cherty nodules at 9463, 9465, 9469; tight; (LT-3).

9473-9493 Wackestone-packstone; brownish gray; limestone; peloids, crinoids, coral fragments; abundant stylolites (0.2-4.5 cm), anhydrite at stylolite sutures at 9478.5, 9482.3; tight, vertical microfractures at 9488-9490.2; (LT-2).

9493-9498 Wackestone; brownish gray; limestone; crinoids, intraclasts; scattered stylolites (0.3-1.0 cm); tight; (LT-3).

Amerada, State 1-16 (NDGS-9578)
SE/SW 16-144N-101W Billings County, North Dakota
Core Depths: 9460-9556
Log Depths: 9469-9564

9460-9464 Packstone; dark yellowish brown; dolomitic limestone; thick dolomitic subaereal laminae; peloids, bioclasts; anhydrite nodules at 9461, 9461.8, 9463.7, microstylolites at 9460.4-9464.6; tight; (LT-7).

TS9461 Packstone; dolomitic limestone; peloids, pellets, calcispheres, intraclasts, ostracodes; well sorted; point packing; micrite, microspar, dolomite, microcrystalline anhydrite; no porosity.

TS9463 Packstone; calcitic dolostone; intraclasts, peloids, bioclasts, brachiopods, calcispheres; well sorted; point and longitudinal packing; dolomite (matrix selective), subfelted anhydrite (early selective replacement of intraclasts); no porosity; multi-stage dolomitization (dolospar growth into anhydrite).

9464-9471.6 Wackestone; dark yellowish brown; dolomitic limestone; massive; ostracodes, bioclasts; abundant anhydrite nodules (0.5-2.0 cm) at 9466, 9468, 9470, crystallotopic anhydrite at 9467, stylolite (4.0 cm) at 9468, microstylolites at 9471; tight; (LT-7).

TS9465 Packstone; dolostone; angular and rounded intraclasts, peloids, brachiopod fragments, calcispheres, ostracodes, crinoids; very well sorted; longitudinal and concavo-convex packing; dolomite, microcrystalline anhydrite; no porosity; multi-stage dolomitization (dolospar growth into replacive anhydrite).

TS9466 Packstone; dolostone; peloids, rounded intraclasts; very well sorted; longitudinal and concavo-convex packing; dolomite, interparticle and mold-filling anhydrite, celestite; 15% cementation reduced moldic porosity; thickly laminated.

TS9467 Packstone; calcitic dolostone; intraclasts (0.5-4.0 mm), pellets, peloids; variable sorting; point and concavo-convex packing; dolomite, micrite, replacive anhydrite, pore filling and replacive celestite; no porosity; tooth-in-socket stylolites cut across anhydrite, dolomite growth into anhydrite.

TS9469 Packstone; anhydritic limestone; intraclasts, peloids, pellets, calcispheres; variable sorting; point packing; subfelted anhydrite (replacive nodular, displacive and interparticle infill), micrite; cementation filled moldic porosity.

TS9471 Packstone; dolomitic limestone; intraclasts (0.3-4.0 mm), peloids, brachiopods; well sorted; longitudinal and concavo-convex packing; dolomite, micrite, celestite (replacive), subfelted anhydrite (infill); no porosity; allochem ghosts in celestite.

9471.6-9474.7 Rudstone-grainstone; medium gray to brownish gray; dolomitic limestone; pisoliths, ooliths, bioclasts, coral fragments (Syringopora); stylolite seam at 9472.5 (0.2 cm), anhydrite cemented; tight; (LT-4).

9474.7-9479 Packstone; moderate yellowish brown; dolomitic limestone; massively bedded; brachiopods, peloids, forams; scattered crystallotopic anhydrite, stylolite seam (0.5 cm) at 9478.5; tight; (LT-4).

TS9475 Packstone-rudstone; limestone; rounded and angular intraclasts (0.3-5.0 mm), peloids, bioclasts (including: gastropods, molluscs, crinoids, brachiopods, forams, coralline algae); poorly sorted; longitudinal and concavo-convex packing; bladed calcite, equant mosaic calcite, micrite; cementation filled interparticle porosity; micrite envelopes.

TS9478 Packstone; limestone; intraclasts, peloids, bioclasts (including: brachiopods, crinoids, calcispheres, forams, molluscs); well sorted; point and longitudinal packing; micrite, microspar, dolomite, anhydrite; no porosity.

9479-9487 Packstone; brownish gray; dolomitic limestone; peloids, crinoids; abundant stylolites (1.0-3.0 cm), closed vertical fractures; (LT-4).

TS9482 Packstone; dolomitic limestone; rounded intraclasts, peloids, crinoids, pellets, brachiopods and spines, bioclasts; well sorted; concavo-convex packing; microspar, micrite, dolomite, anhydrite (allochem replacive), celestite; no porosity; micrite envelopes.

9487-9489 Packstone-rudstone; pale yellowish brown; calcitic dolostone; crinoids, intraclasts; tight; (LT-4).

TS9488 Packstone-rudstone; calcitic dolostone; intraclasts (0.5-3.0 mm), peloids, crinoids, forams, brachiopods, bioclasts; very well sorted; longitudinal, concavo-convex and sutured packing; dolomite (<40 um), micrite, microspar, saddle dolomite (replaces crinoids), bitumen; no porosity.

9489-9491 Packstone; pale yellowish brown; dolomitic limestone; cross-laminated; vertically burrowed laminations; peloids, intraclasts, crinoids; tight; (LT-4).

9491-9496 Wackestone; dark yellowish brown; dolomitic limestone; indistinctly burrowed; crinoids, coral fragments; stylolite (8.0 cm) at 9494; tight; (LT-2).

TS9492 Mudstone; dolostone; microcrystalline dolomite, subhedral pyrite, microcrystalline anhydrite; 6% cementation enlarged intercrystalline porosity.

TS9493 Packstone; dolomitic limestone; angular intraclasts, crinoids, brachiopods, coralline algae; very well sorted; point and longitudinal packing; dolomite (<80 um), trace subhedral pyrite; 3% cementation enlarged intercrystalline porosity.

TS9496 Wackestone; calcitic dolostone; crinoids, ostracodes; well sorted; no packing; dolomite, calcspar, microcrystalline anhydrite, subhedral pyrite; 5% cementation enlarged intercrystalline porosity; mud replacment by dolomite, late calcspar.

9496-9501 Wackestone-packstone; dark yellowish brown; limestone; inclined and horizontal burrows (Zoophycos); peloids, brachiopods (Schelwienella), crinoids; stylolite (5.0 cm) at 9497, anhydrite in stylolite teeth; tight; (LT-2).

TS9497 Wackestone; calcitic dolostone; crinoids; well sorted; no packing; microcrystalline dolomite, microcrystalline anhydrite; 8% cementation enlarged intercrystalline porosity.

TS9498 Mudstone; calcitic dolostone; trace crinoids; dolomite (<100 um), micrite, trace microcrystalline anhydrite, trace framboidal pyrite, trace bitumen; no porosity.

TS9500 Packstone; dolomitic limestone; crinoids, angular intraclasts, brachiopods, molluscs; well sorted; concavo-convex and sutured packing; micrite, microcrystalline dolomite,

subhedral and framboidal pyrite; no porosity; overgrowths on crinoids.

9501-9502 Packstone-rudstone; brownish gray; limestone; intraclasts, ooliths, bioclasts; tight; (LT-4).

9502-9503 Wackestone; brownish gray; limestone; crinoids, gastropods, ostracodes; tight; (LT-2).

9503-9506 Packstone-rudstone; brownish gray; limestone; intraclasts, bioclasts (crinoids, brachiopods, coral fragments), ooliths, pisoliths; silicified from 9503-9504, stylolite (3.0 cm) at 9504.4; tight; (LT-4).

9506-9515 Wackestone; dark yellowish brown; dolomitic limestone; indistinctly burrowed, bioclast packstone-wackestones at 9507, 9511.4-9512.3; wackestone to mudstone; bioclasts, peloids; chert nodules at 9509-9510.5; tight; (LT-3).

TS9511 Wackestone; dolomitic limestone; crinoids, brachiopods; well sorted; no packing; dolomite (<40 um), micrite, framboidal pyrite, oil stain; 1% cementation enlarged intercrystalline porosity.

TS9514 Wackestone; calcitic dolostone; brachiopods, crinoids; well sorted; no packing; dolomite micrite, trace anhydrite filled mold; 3% cementation enlarged intercrystalline porosity.

TS9515 Mudstone; dolostone; dolomite (<100 um), saddle dolomite, trace intercrystalline anhydrite, trace celestite, trace oil stain; 3% cementation reduced intercrystalline porosity.

9515-9523 Wackestone; medium gray to brownish gray; limestone; Zoophycos at 9521; crinoids, corals (Vesiculophyllum); stylolitic from 9521-9523 (2.0-4.0 cm), chemically resistant coral clasts accumulated along solution interfaces; (LT-1).

9523-9532 Wackestone; dusky yellowish brown; dolostone; crinoids; dolomitized, anhydrite nodules (<3.0 cm); poor porosity; even dark brown oil stain; (LT-2).

TS9524 Mudstone; dolostone; dolomite (<20 um), microcrystalline anhydrite, celestite, saddle dolomite, framboidal pyrite; 10% cementation enlarged intercrystalline porosity.

TS9527 Mudstone; dolostone; dolomite (<20 um), framboidal and subhedral pyrite, microcrytalline anhydrite; 2% cementation enlarged intercrystalline porosity.

TS9528 Mudstone; dolostone; crinoid ghosts; dolomite (<20 um), dolomite (<100 um), intercrystalline anhydrite, celestite, trace framboidal pyrite; 3% cementation enlarged intercrystalline porosity.

TS9529 Mudstone to wackestone; dolostone; crinoids; very well sorted; no packing; dolomite (<100 um), celestite, trace microcrystalline anhydrite, bitumen; 8% cementation enlarged intercrystalline porosity.

TS9531 Wackestone; calcitic dolostone; crinoids, brachiopods; well sorted; no packing; dolomite (<100 um), anhydrite, celestite, trace bitumen; 1% cementation filled moldic porosity.

9532-9537 Wackestone; dark yellowish brown; indistinctly burrowed, Zoophycos at 9535.5; crinoids; stylolite seams (1.0 cm) at 9532, 9533.3, 9533.9, siliceous between stylolite seams, microstylolites at 9533.9-9534, zoned anhydrite nodule at 9532.5; tight; (LT-3).

TS9533 Packstone; calcitic dolostone; crinoids, brachiopods; very well sorted; point and longitudinal packing; dolomite (<100 um), celestite (pore filling and crinoid replacement), intercrystalline anhydrite, trace bitumen; no porosity.

TS9536 Wackestone to packstone; calcitic dolostone; crinoids, brachiopods; well sorted; point packing; dolomite (<40 um), celestite, microcrystalline anhydrite; no porosity.

9537-9538 Wackestone; dark yellowish brown; corals (Vesiculophyllum, Syringopora), brachiopods (Schelwienella); microstylolites, anhydrite filled vertical microfractures; (LT-2).

9538-9542 Wackestone-packstone; brownish black; dolomitic limestone; corals (Stelechophyllum banfensse, Vesiculophyllum, Sychnoelasma), crinoids, brachiopods; tight; (LT-1).

TS9539 Wackestone; calcitic dolostone; brachiopods, corals, crinoids, molluscs; poorly sorted; point packing; dolomite, celestite; no porosity; bladed calcspar and celestite replacement within coral.

TS9541 Packstone; calcitic dolostone; crinoids, brachiopods; very well sorted; longitudinal packing; dolomite (80-120 um), trace bitumen; no porosity.

9542-9547 Wackestone; dark yellowish brown; dolomitic limestone; massively bedded, cross-laminated at 9545-9546; bioclasts; anhydrite nodules (0.5-2.5 cm), black insolubles collect with pyrite and calcite around nodules; tight; (LT-2).

TS9544 Wackestone; dolostone; crinoids, brachiopods, ostracodes; well sorted; no packing; dolomite, microcrystalline anhydrite, celestite, framboidal pyrite, insolubles; 5% cementation enlarged intercrystalline porosity, 0% occluded moldic porosity.

TS9546 Wackestone to packstone; dolostone; crinoids, ostracodes, calcispheres; well sorted; point packing; dolomite (20-120 um), subfelted laths anhydrite, traces celestite, framboidal pyrite,and insolubles; 5% cementation enlarged intercrystalline and 0% cementation filled moldic porosity.

9547-9552.3 Packstone-wackestone; dark yellowish brown; dolomitic limestone; indistinctly burrowed, halo burrows at 9551, bioclast packed burrow at 9552; pellets, bioclasts; stylolite seam (2.0 cm) at 9548, (1.0 cm) at 9549, anhydrite nodules (0.2 to 2.0 cm) between seams, calcitic nodule (2.0 cm) with anhydrite core and pyrite at 9547.6; tight; (LT-3).

TS9549 Packstone; calcitic dolostone; pellets, brachiopods, crinoids, ostracodes, molluscs, codiacean algae; well sorted; point packing; dolomite, calcspar, microcrystalline to subfelted anhydrite, celestite, framboidal pyrite; 0% cementation filled moldic porosity; recrystallized ostracodes.

9552.3-9556.2 Wackestone; dark yellowish brown; dolomitic limestone; crinoids, corals; stylolites (8.0 cm) at 9556; tight; (LT-1).

Koch Exploration, Federal 12-27 (NDGS-10114)
NW/SW 27-144N-101W Billings County, North Dakota
Core Depths: 9268-9295
Log Depths: 9274-9301

9268-9269.5 Bedded massive and distorted bedded massive anhydrite; medium light gray; tight; (LT-6).

9269.5-9273.4 Mudstone; olive gray; limestone; laminated; interlaminated with intraclast wackestone-packstone; abundant crystallotopic anhydrite 9269.5-9270.7; poor porosity; (LT-5).

9273.4-9279.2 Mudstone; pale yellowish brown; limestone; interlaminated with packstones at 9275 and 9276.4; ostracodes, gastropods, intraclasts; crystallotopic anhydrite, pyritized intraclasts; tight; (LT-5).

9279.2-9280 Mudstone; light olive gray; dolostone; massive; tight; (LT-5).

9280-9281.7 Mudstone; pale yellowish brown; dolomitic limestone; thickly laminated, dolomitic laminae; tight; (LT-5).

9281.7-9286 Mudstone; dusky yellowish brown; limestone; thinly laminated, dewatering plume at 9282; abundant crystallotopic anhydrite; tight; (LT-5).

9286-9288.8 Distorted bedded mosaic anhydrite; medium light gray; thick lamina of dolomite at 9287; tight; (LT-6).

9288.8-9289.5 Wackestone; dark yellowish brown; dolostone; thinly laminated, stromatolitic laminae, gypsum rip-up clasts and sand; peloids, pellets; tight; (LT-5).

9289.5-9295 Bedded massive and massive anhydrite; light olive gray, dark yellowish brown; thin bedded intraclast packstones at 9291, 9294 and 9294.5; tight; (LT-6).

Tenneco, Hamilton-U.S.A. 3-29 (NDGS-9182)
C/SE 29-144N-101W Billings County, North Dakota
Core Depths: 9195-9323
Log Depths: 9204-9332

9195-9197 Packstone; dusky yellowish brown; limestone; laminated and cross-laminated; peloids, bioclasts; crystalltopic anhydrite; tight; (LT-4).

TS9197 Packstone; dolomitic limestone; bioclasts, crinoids, brachiopods, ostracodes; well sorted; concavo-convex packing; micrite, microspar, dolomite (<40 um); no porosity.

9197-9206 Mudstone; light olive gray; slightly dolomitic limestone; thinly laminated; tight; (LT-5).

TS9199 Mudstone; limestone; calcispheres; clotted micrite, microspar, trace microcrystalline anhydrite, subhedral anhydrite, bitumen; no porosity.
TS9201 Mudstone; limestone; calcispheres; clotted micrite, microspar, subhedral pyrite, trace bitumen; no porosity.
TS9206 Mudstone; limestone; micrite, bitumen, trace intercrystalline anhydrite; no porosity.

9206-9210.5 Packstone; dusky yellowish brown; dolomitic limestone; thinly laminated, cross-laminated; peloids; scattered intercrystalline anhydrite, trace bitumen; tight; (LT-4).

9210.5 9214 Massive anhydrite; light gray, brownish gray; tight; (LT-6).

9214-9215.3 Wackestone; brownish gray; limestone; peloids; crystallotopic anhydrite; tight; (LT-5).

9215.3-9216.7 Nodular mosaic anhydrite; light gray; tight; (LT-6).

9216.7-9220.4 Packstone; brownish gray, pale yellowish brown; dolostone; thickly laminated, cross-laminated peloidal packstones interbedded with massively bedded anhydrite; tight; (LT-5,6).

TS9218 Wackestone; limestone; calcispheres, ostracodes, gastropods; very well sorted; no packing; microspar, micrite, microcrystalline anhydrite; no porosity.

9220.4-9227.3 Packstone; brownish gray; thinly laminated; burrowed at 9220.4-9221 (Chondrites, Planolites); peloids; scattered crystallotopic anhydrite; tight; (LT-5).

TS9223 Packstone; limestone; brachiopods, crinoids, fenestrate bryozoans, forams, calcispheres; well sorted; concavo-convex packing; micrite, microspar, bitumen; no porosity; micrite envelopes on crinoids, mosaic calcite in brachiopod.

9227.3-9234 Massive to bedded massive anhydrite; brownish gray; tight; (LT-6). TS9228 Packstone to wackestone; anhydritic limestone; pellets, calcispheres (100-150 um), ostracodes; very well sorted; point packing; felted anhydrite, celestite, micrite, wavy microlamina of bitumen; no porosity.

TS9233 Mudstone; anhydrite; calcispheres (100 um), ostracodes (1.0 mm); microcrystalline anhydrite, spalled wispy clay partings; no porosity.

9234-9237.5 Mudstone-wackestone; dark yellowish brown; calcitic dolostone; thinly laminated, massively bedded anhydrite at 9234.9-9235, 9236.8-9237.4; burrowed (Chondrites) at 9235-9236.8; bioclasts, ooliths; tight; (LT-5).

9237.5-9240.3 Packstone-rudstone; pale yellowish brown, light bluish gray; calcitic anhydritic dolostone; pisoliths, ooliths, peloids; scattered anhydrite nodules (1.0-2.0 cm) grading up to massive anhydrite; tight; (LT-4,5).

TS9238 Mudstone; anhydrite; ostracodes; microcrystalline anhydrite, subfelted anydrite allochem mold fill, spalled wispy clay, bitumen; no porosity; dolomite rhomb ghosts in anhydrite.

9240.3-9245 Packstone; dark yellowish brown; dolomitic limestone; thinly laminated; peloids grading to intraclasts and pisoliths at 9242.5; spalled allochems, diagenetic mottling; tight; (LT-5).

TS9243 Wackestone; calcitic dolostone; angular intraclasts, brachiopods; poor sorting; concavo-convex packing; dolomite (<30 um), blocky laths anhydrite; no porosity; spalled intraclasts.

9245-9248 Packstone; dusky yellowish brown; dolostone; peloids; scattered anydrite nodules (0.2-2.0 cm); trace intercrystalline porosity; oil stain; (LT-4).

TS9245 Packstone; dolostone; pellets; well sorted; point packing; dolomite, trace anhydrite; 15% interparticle and cementation enlarged intercrystalline porosity.

TS9247 Wackestone; calcitic dolostone; calcispheres, crinoids, ostracodes; well sorted; no packing; dolomite (30-50 um), celestite; 10 % cementation enlarged intercrystalline and cementation reduced interparticle porosity; dolomitized crinoids.

9248-9257 Packstone; dark yellowish brown; dolomitic limestone; thinly laminated with massive interbeds; rudstone at 9248-9249; peloids ooliths, intraclasts, pisoliths at 9248-9251; stylolites (0.5-2.0 cm), crystallotopic anhydrite at 9253.5-9255.2; tight; (LT-5).

TS9252 Wackestone; limestone; calcispheres (100-200 um), ostracodes, peloids, ooliths; no packing; micrite, calcspar, anhydrite within stylolite teeth; no porosity; stylolites (4.0-6.0 cm).

TS9256 Packstone; limestone; pellets, calcispheres, brachiopods, crinoids; well sorted; point packing; microspar, dolomite, micrite, bitumen; no porosity; neomorphism.

9257-9287.3 Packstone; dark yellowish brown; limestone; massive to indistinctly laminated; peloids, scattered thin beds of bioclastic packstones (Schelwienella) at 9263, 9277, 9287, corals (Vesiculophyllum) at 9257, 9272, (Syringopora) at 9272, gastropod at 9286; tight; (LT-2,3).

TS9261 Packstone; limestone; pellets, bioclasts, calcispheres; calcspar, microspar, trace micrite; 0% cementation filled interparticle porosity.

TS9265 Packstone; limestone; pellets, brachiopods, rounded intraclasts, crinoids, calcispheres, forams; well sorted; point packing; micrite, microspar, dolomite, anhydrite; 5% solution enlarged intraparticle porosity; neomorphism.

TS9268 Packstone; limestone; pellets, intraclasts, crinoids; well sorted; point packing; micrite, microspar, anhydrite; 5% cementation reduced interparticle porosity; overgrowths on crinoids.

TS9271 Mudstone; calcitic anhydrite; calcispheres; thick wavy laminated; microcrystalline to subfelted anhydrite nodule, blocky celestite, dolomite (20-40 um), micrite, chert; microstylolites; no porosity.

TS9272 Wackestone; dolomitic limestone; peloids, crinoids, brachiopod spines, intraclasts, calcispheres; variably sorted; no packing; micrite, dolomite, microspar; no porosity.

TS9278 Packstone; limestone; pellets, crinoids, clotted intraclasts (0.2-1.5 mm), brachiopods (0.1-1.5 mm), benthic forams, coralline algae; well sorted; point packing; pseudospar, anhydrite; overgrowths on crinoids, crinoids ghosts; no porosity.

TS9284 Packstone; dolomitic limestone; crinoids, intraclasts, peloids; well sorted; concavo-convex and sutured packing; microspar, micrite, calcspar, dolomite (50 um); no porosity; dedolomite as rhomb ghosts in calcspar.

9287.3-9295 Wackestone; dark yellowish brown; dolomitic limestone; bioturbated (Chondrites at 9289); packstone at 9288.5-9289; crinoids, bioclasts, corals (Syringopora); stylolite seam at 9291 (0.5 cm), microstylolites at 9292-9295; fair to good intercrystalline porosity at 9290-9295, oil stain at 9290-9293; (LT-3).

TS9289 Packstone; dolomitic limestone; crinoids, brachiopods, bioclasts; well sorted; point packing; micrite, microspar, dolomite, trace anhydrite; no porosity.

TS9295 Packstone; limestone; brachiopods (0.5-2.0 mm), brachiopod spines, bioclasts (0.1-0.3 mm), crinoids, peloids, fenestrate and encrusting bryozoans, forams; well sorted; longitudinal and sutured packing; microspar, micrite; no porosity; peloids neomorphosed to microspar, microstylolites.

9295-9296, 9296-9301 Packstone; dusky yellowish brown; limestone; crinoids, corals, bioclasts; microstylolitic; tight; (LT-1).
TS9299 Packstone; limestone; brachiopods (0.5-5.0 mm), bioclasts (0.1-0.8 mm), crinoids (0.1-3.0 mm), trilobite fragments, gastropods, molluscs; poorly sorted; longitudinal and concavo-convex packing; micrite, dolomite, bitumen; no porosity.

9301-9307.5 No core found.
TS9302 Mudstone; dolostone; crinoids, brachiopods; dolomite, anhydrite, bitumen; 7% cementation enlarged intercrystalline and cementation reduced (anhydrite) moldic porosity.

9307.5-9314 Packstone-wackestone; dark yellowish brown; dolostone; bioturbated, indistinct horizontal to inclined burrows; crinoids, bioclasts, corals, gastropod at 9311; stylolite seam (1.2 cm) at 9308.8, microfractured at 9310.5-9311, stylolite (5.0 cm) at 9314; tight; (LT-1).
TS9304 Mudstone; dolostone; crinoids, brachiopods; dolomite (100 um), calcspar, bitumen; 10% cementation enlarged intercrystalline and solution enlarged moldic porosity.
TS9306 Packstone; dolomitic limestone; intraclasts, crinoids, brachiopods, brachiopod spines, bioclasts; well sorted; point packing; micrite, dolomite, microcrystalline anhydrite, celestite, bitumen; 5% cementation enlarged intercrystalline and cementation reduced moldic porosity.
TS9312 Packstone; calcitic dolostone; crinoids, brachiopods, molluscs, ostracodes, calcispheres, coralline algae; variably sorted; point packing; dolomite (100 um), microspar, bitumen, trace subhedral pyrite; 3% cementation enlarged intercrystalline and cementation reduced moldic porosity.

9314-9319.6 Wackestone, local packstone; medium gray; limestone; crinoids, corals (0.5-3.0 cm)(Vesiculophyllum, Sychnoelasma), gastropod at 9315.5; stylolite (3.0 cm) at 9315.7; tight; (LT-1).
TS9316 Wackestone-packstone; limestone; bioclasts, intraclasts, crinoids, brachiopods, ostracodes, molluscs, forams; poorly sorted; local point packing; microspar, micrite, dolomite, saddle dolomite, bitumen, subhedral pyrite; 2% solution enlarged moldic porosity; saddle dolomite biomold fills, coarse dolomite within biomolds.

9319.6-9323 Mudstone-wackestone; dark yellowish brown; dolomitic limestone; bioturbated; bioclasts; anhydrite nodules (0.2-2.0 cm), vertical burrow at 9320, microstylolites at 9321.5, stylolites at 9321.9- 9323; fair intercrystalline porosity; (LT-3).
TS9320 Mudstone; dolostone; crinoids, brachiopods; well sorted; no packing; dolomite (100-120 mu), microcrystalline anhydrite; 15% cementation enlarged intercrystalline porosity.

Tenneco, U.S.A.- UVI 1-33 (NDGS-10229)
SE/SW 33-144N-101W Billings County, North Dakota
Core Depths: 9289.5- 9387
Log Depths: 9295- 9391

9289.5-9291 Massively bedded anhydrite; pale yellowish brown; tight; (LT-6).

9291-9300 Wackestone-packstone; pale yellowish brown; thickly laminated, anhydrite nodule and mud chips at 9292, mosaic anhydrite at 9292.6-9293, teepee at 9294; peloids, crinoids; tight; (LT-5).

TS9292 Packstone; calcitic dolostone; peloids, ostracodes; well sorted; concavo-convex and sutured packing; dolomite (<30 um), microcrystalline anhydrite, microspar, celestite, clay; no porosity; microstylolites.

TS9294 Packstone; calcitic dolostone; peloids, ostracodes, calcispheres; well sorted; point packing; dolomite (<30 mu), microcrystalline anhydrite, celestite; no porosity; early compacted peloids, ostracodes replaced by anhydrite and celestite.

TS9296 Packstone; dolostone; intraclasts, ostracodes, calcispheres; well sorted; point and longitudinal packing; dolomite (<30 um), microcrystalline anhydrite, celestite, calcspar; 2% cementation enlarged intercrystalline and trace cementation filled moldic porosity; neomorphosed intraclasts, trace dedolomite, late calcspar.

TS9297 Wackestone; dolostone; calcispheres, gastropods, ostracodes; well sorted; no packing; dolomite (<30 um), microcrystalline anhydrite, celestite; 8% cementation reduced moldic and cementation enlarged intercrystalline porosity.

TS9298 Wackestone; dolostone; ostracodes, crinoids; well sorted; no packing; dolomite (<30 mu), subfelted laths anhydrite, celestite, calcspar; 5% cementation reduced moldic and cementation enlarged intercrystalline porosity; dedolomite in latest calcspar.

TS9299 Wackestone; dolostone; ostracodes, crinoids; well sorted; no packing; dolomite, subfelted anhydrite, celestite; 7% cementation enlarged intercrystalline and cementation reduced moldic porosity.

9300-9302.3 Nodular mosaic anhydrite; light gray; tight; (LT-6).

9302.3-9304 Mudstone; dusky yellowish brown; dolostone; laminated; tight; interbedded with bedded nodular and nodular mosaic anhydrite; (LT-6).

9304-9308 Wackestone; dusky yellowish brown; dolomitic limestone; thickly laminated peloids packstones anf thinly laminated mudstones, mud-chips, dolomitic subaereal laminae; peloids, ooliths; tight; (LT-5).

TS9306 Grainstone; dolomitic limestone; angular and discoidal intraclasts, brachiopods, peloids, forams, crinoids, ostracodes, molluscs, calcispheres; variably sorted; point, sutured packing; dolomite (20-30 um), anhydrite laths, dolomite (>100 um), celestite; 5% cementation reduced interparticle porosity; dolomitized isopachous cement.

9308-9311.5 Nodular mosiac anhydrite; medium light gray and pale yellowish brown; tight; (LT-5,6).

TS9309 Grainstone; dolomitic limestone; intraclasts, peloids, brachiopods; well sorted; longitudinal and concavo-convex packing; dolomite (50-100 um), celestite, anhydrite, trace subhedral pyrite; 12% cementation reduced interparticle porosity; micrite envelopes, dolomitized isopachous cement, intraclast ghosts in celestite.

TS9310 Grainstone; anhydritic dolostone; intraclasts, peloids; well sorted; point and longitudinal packing; dolomite, subfelted laths anhydrite, celestite; no porosity; dolomitized intraclasts.

9311.5-9312.5 Packstone-rudstone; pale yellowish brown; limestone; wavy thinly bedded; intraclasts, gastropods, ostracodes; anhydrite cement; tight; (LT-4).

9312.5-9314.7 Packstone; pale yellowish brown; limestone; thickly laminated, mudchips at 9313; intraclasts, ooliths, peloids; microstylolites, stylolites (2.0-3.0 cm) at 9314-9314.7; tight; (LT-5).

TS9314 Packstone; dolomitic limestone; peloids, clotted intraclasts. peloids, brachiopods, micritized ooliths, gastropods, coralline algae, forams; poor sorted; longitudinal and concavo-convex packing; dolomite (<60 um), micrite, felted laths anhydrite, saddle dolomite, celestite; 10% cementation reduced and solution enlarged moldic porosity; dolomitized allochem cores.

9314.7-9321.7 Mudstone; moderate yellowish brown; limestone; massively bedded, thickly laminated at 9316-9317, Chondrites at 9320; microstylolites at 9319, nodular chert bed at 9316.7-9317, stylolites (1.0-3.0 cm) at 9317.5 and (5.0 cm) at 9321; tight; (LT-5).

TS9319 Mudstone; dolostone; ostracodes, crinoids; well sorted; no packing; dolomite (<20-30 um), calcspar, anhydrite; no porosity; ostracode molds filled with anhydrite.

TS9321.5 Mudstone-wackestone; calcitic dolostone; crinoids; dolomite, calcspar, trace anhydrite, celestite; no porosity; dedolomite (corroded dolomite in calcite).

9321.7-9322.5 Packstone-rudstone; dark yellowish brown; limestone; massive; ooliths, pisoliths, intraclasts; tight; (LT-4).

9322.5-9332.8 Packstone; dark yellowish brown; limestone; massive; indistinctly burrowed, Chondrites at 9324; crinoids, peloids, brachiopods (Schelwienella) at 9323; stylolites (2.0-4.0 cm) at 9323.5; tight; (LT-3).

TS9324 Packstone; dolomitic limestone; intraclasts, peloids, crinoids, brachiopods, trace calcispheres; well sorted; longitudinal packing; dolomite (<30 um), subhedral pyrite, saddle dolomite, trace anhydrite; no porosity.

TS9327 Packstone; calcitic dolostone; crinoids, brachiopods; well sorted; point packing; dolomite, calcspar; no porosity; recrystallized brachiopods, overgrowths on crinoids.

TS9330 Packstone; calcitic dolostone; crinoids, brachiopods, rounded intraclasts, forams; well sorted; point packing; dolomite, laths of microcrystallline anhydrite, trace celestite; 6% cementation enlarged intercrystalline and solution enlarged intraparticle (forams) porosity; micrite envelopes (brachiopods).

9332.8-9339 Packstone-rudstone; dark yellowish brown; limestone; massive; intraclasts, ooliths; tight; interbedded with pale yellowish brown; limestone; bioturbated; packstone; peloids; cherty at 9334.8-9335.1; tight; (LT-4).

TS9339 Wackestone-packstone; dolomitic limestone; crinoids, rounded intraclasts, brachiopods; well sorted; point packing; microspar, micrite, dolomite, trace subhedral pyrite; no porosity; recrystallized brachiopods.

9339-9342.4 Wackestone-packstone; pale yellowish brown; limestone; bioturbated; crinoids, brachiopods (Schelwienella), corals; stylolites (<1.0 cm) at 9340; tight; (LT-3).

9342.4-9354.4 Wackestone-packstone; brownish black; limestone; massive; crinoids, corals (Vesiculophyllum), brachiopods, bioclasts; microstylolites, spalled corals; tight; (LT-1).

TS9350 Packstone; limestone; brachiopods and spines (0.1-4.0 mm long), crinoids (0.3-2.0 mm); poorly sorted; concavo-convex and sutured packing; micrite, dolomite; no porosity; stylolites, microstylolites, dolomite rhombs in stylolites.

9354.4-9360.4 Mudstone; dusky yellowish brown; dolostone; burrowed (Chondrites); peloids; stylolites (1.0- 2.0 cm) at 9355, (1.0 cm) at 9358; poor intercrystalline porosity; oil stain; (LT-3).

TS9357 Mudstone; calcitic dolostone; brachiopods; dolomite, trace anhydrite, pyrite; 3% cementation enlarged intercrystalline porosity.

TS9358 Wackestone; calcitic dolostone; bioclasts, dolomite, calcspar, trace subhedral pyrite; no porosity; recrystallized allochems, dedolomite.

TS9359 Mudstone; dolostone; dolomite, trace subhedral pyrite; 9% cementation enlarged intercrystalline porosity.
TS9359.3 Mudstone; dolostone; dolomite (<30 um), calcspar, subhedral pyrite; 5% cementation enlarged intercrystalline porosity; dedolomite.
TS9360 Mudstone; dolostone; dolomite (20-120 um), calcspar, subhedral pyrite; 6% intercrystalline porosity.
TS9360.3 Mudstone; dolostone; dolomite (20-120 um), calcspar, trace pyrite; 5% cementation enlarged intercrystalline porosity.

9360.4-9373 Wackestone-mudstone; dark yellowish brown; limestone; corals (Vesiculophyllum, Syringopora, Sychnoelasma, Stelechophyllum banffense (at 9371.5), crinoids, bioclasts; stylolite seams (2.0 cm) at 9362.4 and (0.3 cm) at 9364, microstylolites; tight; (LT-1).
TS9361 Wackestone; calcitic dolostone; crinoids, bioclasts, brachiopods; no packing; well sorted; dolomite, microspar, trace framboidal pyrite; no porosity.
TS9361.3 Mudstone-wackestone; calcitic dolostone; bioclasts; dolomite, microspar, pseudospar, trace pyrite, celestite; 5% cementation enlarged intercrystalline porosity.
TS9367 Wackestone; dolomitic limestone; crinoids, brachiopods; well sorted; point packing; dolomite (20-100 um), microspar, trace oil stain; 5% cementation enlarged intercrystalline porosity.
TS9371 Packstone; dolomitic limestone; crinoids; well sorted; point and longitudinal packing; dolomite (cloudy, 40-120 um), microspar, trace oil stain; no porosity.

9373-9383 Wackestone; dark yellowish brown and brownish gray; dolomitic limestone; indistinctly burrowed; crinoids; pressure solution breccia at 9379, stylolite seams at 9380-9380.9, anhydrite nodules at 9375, 9379 and 9379.7; tight; Fryburg Gamma Ray Marker at 9380-9380.8; (LT-3).
TS9376 Mudstone; calcitic dolostone; crinoids; dolomite, microspar, saddle dolomite; 10% cementation enlarged intercrystalline porosity.
TS9380 Wackestone; dolostone; crinoids, brachiopods; dolomite (20-50 um), celestite (with dolomite inclusions), trace anhydrite; 5% cementation enlarged intercrystalline porosity.

9383-9387.5 Wackestone-packstone; dusky yellowish brown; limestone; crinoids, coral fragments; chert nodules at 9386, 9387, stylolites (1.0-3.0 cm) at 9383-9384; tight; (LT-1).
TS9385 Packstone-wackestone; dolomitic limestone; crinoids (0.3-1.0 cm), brachiopods (pseudopunctates); well sorted; point and longitudinal packing; dolomite (30-100 um), microspar, chert, trace anhydrite, pyrite; no porosity; chert replacement of crinoids, microstylolites.

Texacota, Federal 1-2 (NDGS-5328)
NW/NE 2-144N-102W Billings County, North Dakota
Core Depths: 9290-9313
Log Depths:9296-9318

9290-9291.5 Mudstone; moderate yellowish brown; calcitic dolostone; thickly laminated (algal); light bluish gray anhydrite nodules; tight;
(LT-5).

TS9291.5 Mudstone; dolostone; dolomite (10-30 um), laths of microcrystalline anhydrite, calcspar, trace bitumen; no porosity.

9291.5-9294.6 Mudstone; dark yellowish brown; calcitic dolostone; burrowed (Chondrites); coral fragments; poor intercrystalline porosity; (LT-3).

TS9294 Mudstone; calcitic dolostone; brachiopods, discoidal intraclasts; no packing; well sorted; dolomite (10-120 um, average 40 um), calcspar, microspar, dedolomite, bitumen; 5% cementation reduced intercrystalline porosity.

9294.6-9297.8 Wackestone; dusky yellowish brown mottled with brownish black; dolomitic limestone; packstone at 9295; brachiopods, bioclasts, corals; anhydrite cement at 9295; tight; (LT-4).

TS9295 Packstone-rudstone; limestone; rounded to discoidal intraclasts (0.5-4.0 mm), crinoids, peloids, pellets, forams; poorly sorted; point and concavo-convex packing; isopachous marine calcite, micrite, microspar, dolomite, blocky anhydrite laths; no porosity.

9297.8-9299.7 Wackestone; dark yellowish brown; calcitic dolostone; massive, indistinctly burrowed, Zoophycos at 9298.5, Chondrites at 9298; brachiopods, corals, crinoids; fair intercrystalline porosity; (LT-2).

TS9298.3 Wackestone; dolomitic limestone; intraclasts, bioclasts, crinoids, corals, codiacean algae (tubular rods), ostracodes, calcispheres; well sorted; no packing; micrite, dolomite (20-30 um), blocky microcrystalline anhydrite, bitumen; no porosity; oil filled ostracode molds.

9299.7-9301 Wackestone; brownish black; dolomitic limestone; brachiopods, bioclasts, crinoids; chert nodule (burrow) at 9300, microstylolites, stylolites (1.0-4.0 cm); poor intercrystalline porosity; (LT-1).

TS9300 Packstone; cherty calcitic dolostone; angular and discoidal intraclasts, pellets, brachiopods, crinoids, molluscs, ostracodes; well sorted; no packing; micrite, dolomite (20-50 um), chert; 5% solution enlarged interparticle porosity; chert nodule.

TS9300.8 Wackestone; dolomitic limestone; bioclasts, crinoids, brachiopods; well sorted; no packing; micrite, dolomite; no porosity.

9301-9305 Wackestone; light olive gray; calcitic dolostone; chert nodule (burrow) at 9302.5, Teichichnus, Chondrites at 9320.5-9303, vertical burrow at 9304, brachiopods at 9303; brachiopods; anhydrite filled burrow molds at 9304; fair intercrystalline porosity; (LT-3).

TS9302.5 Mudstone-wackestone; cherty dolomitic limestone; ostracodes, calcispheres; well sorted; no packing; clotted micrite, chert, dolomite; no porosity.

TS9303.3 Wackestone; calcitic dolostone; angular intraclasts, bioclasts; well sorted; no packing; dolomite, microspar, calcspar; no porosity.

TS9305 Wackestone; dolomitic limestone; rounded intraclasts, bioclasts; well sorted; no packing; dolomite, microspar, calcspar; no porosity; stylolites (100 um).

9305-9306.5 Packstone-wackestone; dusky yellowish brown; dolomitic limestone; graded bedding at 9306, occassionally cross laminated; bioclasts, intraclasts, brachiopods; isopachous marine cement, stylolite (10.0 cm); fair vugular porosity; (LT-4).

TS9305.5 Packstone; dolomitic limestone; rounded intraclasts, peloids, crinoids; well sorted; point packing; micrite, dolomite, laths of subfelted anhydrite; 5% solution enlarged interparticle porosity; dolomitized isopachous cement.

TS9306 Packstone-wackestone; dolomitic limestone; angular intraclasts, bioclasts, crinoids, brachiopods; well sorted; point packing; micrite, dolomite, laths of microcrystalline anhydrite; no porosity.

9306.5-9311 Wackestone; dark yellowish brown; dolomitic limestone; burrowed, Planolites, Chondrites, vertical protrusive burrow at 9309, halo burrows at 9310; bioclasts; cherty burrow zones at 9307 and 9310; microstylolites; 10% intercrystalline and vuggy porosity; trace oil stain; (LT-3).

TS9307.4 Packstone; cherty dolostone; bioclasts, pellets; well sorted; point packing; dolomite, chert; no porosity; chert nodule.

TS9309.5 Mudstone; dolostone; brachiopods; dolomite (20-40 um), calcspar, bitumen; no porosity; recrystallized brachiopods and calcspar filled biomolds.

TS9310 Wackestone; calcitic dolostone; bioclasts, ostracodes, codiacean algae, crinoids, brachiopods; well sorted; no packing; dolomite (15-40 um), chert; no porosity.

TS9311 Packstone; dolomitic limestone; bioclasts, crinoids, brachiopods, intraclasts, codiacean algae, peloids; well sorted; point packing; dolomite (20-70 um), micrite, microcrystalline anhydrite, bitumen; no porosity.

9311-9312.8 Wackestone; dusky yellowish brown; dolomitic limestone; brachiopods, crinoids, bioclasts; anhydrite filled biomolds, stylolites (2.0-5.0 cm); poor intercrystalline porosity; (LT-2).

Shell-Northern Pacific, Gov't 44-14 (NDGS-4419)
SE/SE 14-144N-102W Billings County, North Dakota
Core Depths: 9280-9331, 9375-9425
Log Depths: 9300-9350, 9393-9443

9280-9283 Packstone-wackestone; dusky yellowish brown; limestone;corals (Syringopora), crinoids, brachiopods; tight; Base of Midale; (LT-1).

9283-9286 Mudstone; dusky yellowish brown; limestone; thinly laminated; abundant crystallotopic anhydrite; tight; (LT-5).

9286-9289 Mosaic anhydrite; pale blue; tight; (LT-6).

9289-9290.3 Mudstone; dusky yellowish brown; limestone; thickly laminated; scattered crystallotopic anhydrite; tight; (LT-5).

TS9289 Mudstone; anhydritic limestone; micrite, laths of microcrystalline anhydrite, subfelted anhydrite nodules (3.0 cm), trace fluorite; no porosity; thick wavy laminated.

9290.3-9295.7 Nodular mosaic and distorted nodular mosaic anhydrite; pale blue; tight; (LT-6).

9295.7-9301.4 Mudstone; pale yellowish brown and pale blue; limestone; thinly bedded; algal laminae, thin interbeds of distorted mosaic anhydrite, crusts with desiccation cracks, gypsum sand at 9300 and 9300.8; tight; (LT-5).

TS9300.3 Wackestone; limestone; peloids, pellets; well sorted; no packing; micrite, laths of microcrystalline anhydrite, chert; no porosity.

9301.4-9311 Mudstone; light olive gray; thickly laminated; stylolite (8.0 cm) at 9310.5, crystallotopic anhydrite at 9310.5-9311; good intercrystalline and pin-point porosity; oil stain; (LT-5).

TS9307 Mudstone; dolomitic chert; chert, dolomite, subhedral pyrite; no porosity; thinly laminated; no porosity.

9311-9313.5 Distorted mosaic, highly distorted mosaic and nodular mosaic anhydrite; pale blue and pale yellowish brown; wavy dolomitic laminae; tight; (LT-6).

9313.5-9317.5 Mudstone; dusky yellowish brown; limestone; laminated, distorted laminae at 9316, desication cracks at 9314; scattered crystallotopic anhydrite at 9314.6-9315.5; tight; (LT-5).

TS9316 Wackestone; dolomitic limestone; pellets, calcispheres, bioclasts, ostracodes; poorly sorted; no packing; micrite, dolomite (<20 um), microspar, chert; no porosity; even wavy thinly laminated.

9317.5-9323.8 Wackestone-mudstone; limestone at 9317.5-9320.5, anhydrite at 9320.5-9321, dolomitic anhydrite at 9321-9323.8; pale yellowish brown and pale blue; laminated and algal laminated, distorted mosaic anhydrite at 9321-9322, bedded nodular anhydrite at 9323-9323.8, gypsum sand at 9319-9319.6; peloids, intraclasts; tight; (LT-5,6).

TS9317.8 Wackestone; limestone; bioclasts, calcispheres, pellets, peloids; poorly sorted; no packing; micrite, laths of felted anhydrite; no porosity.

TS9318.4 Packstone; anhydritic limestone; ooliths, rounded intraclasts; well sorted; longitudinal and concavo-convex packing; laths of microcrystalline anhydrite, micrite; no porosity.

9323.8-9325.4 Wackestone; pale yellowish brown; dolostone; laminated and disupted laminated, nodular anhydrite; peloids, intraclasts; tight; (LT-5).

9325.4-9331 Mudstone; dusky yellowish brown; burrowed, burrows disrupting laminations, Chondrites at 9327 and 9329; crystallotopic anhydrite, anhydrite nodules (0.2-1.0 cm), stylolite seam at 9327 (2.0 cm); tight; (LT-5).

TS9325.5 Wackestone; limestone; calcispheres, pellets, bioclasts, codiacean algae; well sorted; no packing; micrite, laths of microcrystalline anhydrite; no porosity.

9375-9378 Wackestone; dark yellowish brown; dolomitic limestone; crinoids, bryozoans; microstylolites; 10% moldic porosity; (LT-3).

9378-9388 Mudstone; dark yellowish brown and brownish gray; dolomitic limestone and dolostone interbedded; burrowed, Teichichnus at 9379 and 9383, Planolites at 9383-9384, Zoophycos at 9383-9384; microstylolites at 9380-9381 with cherty boundaries, stylolite at 9383 (2.0 cm), scattered anhydrite nodules (1.0-3.0 cm); 10% intercrystalline and vuggy porosity; (LT-3).

TS9380.5 Mudstone-wackestone; dolomitic limestone; crinoids; micrite, dolomite, bitumen; 4% cementation reduced intercrystalline porosity; stylolitic.

TS9384.3 Mudstone; dolostone; trace forams; dolomite, dedolomite, calcspar, trace microcrystalline anhydrite, framboidal and subhedral pyrite; cementation filled intercrystalline porosity.

9388-9398 Wackestone; pale yellowish brown; limestone; crinoids, corals (Sychnoelasma, Syringopora), gastropod at 9396.5, brachiopods at 9394-9395; stylolites (0.7-3.0 cm); 9% moldic porosity; (LT-2).

9398-9405 Wackestone-packstone; grayish black; limestone; corals (Vesiculophyllum, Sychnoelasma, Siphonodedron oculinum (at 9302), Syringopora), crinoids, brachiopods; tight; (LT-1).

9405-9413.3 Wackestone; grayish black; limestone; bioclasts; stylolite (2.0 cm) at 9409; 12% moldic porosity; (LT-1).
TS9413 Packstone; limestone; crinoids, bioclasts; well sorted; point packing; microspar, micrite; 2% solution enlarged intraparticle (corals, crinoids) porosity; stylolite.

9413.3- 9423.5 Wackestone; brownish black and grayish black; limestone; crinoids, bioclasts, corals (Vesiculophyllum, Sychnoelasma, Syringopora), gastropods; stylolites; tight; (LT-1).

9423.5-9425 Mudstone-wackestone; dark yellowish brown; limestone; bioclasts; 9% intercrystalline porosity; (LT-2).

Gulf Oil, Roughrider-Federal 1-21-3D (NDGS-9005)
SW/SE 21-145N-100W McKenzie County, North Dakota
Core Depths: 9558-9569, 9571-9616
Log Depths: 9584-9586.5, 9601-9647

9558-9563.8 Mudstone; pale yellowish brown; limestone; burrow mottled; stylolites (<3.0 cm), diagenetic mottling at 9558-9558.5, burrow replaced by anhydrite at 9562-9563; 5% intercrystalline porosity; (LT-3).
TS9558.5 Wackestone; calcitic dolostone; intraclasts, bioclasts, trilobite spines, crinoids, forams; well sorted; trace sutured packing; microspar, dolomite, (20-30 um), calcspar; no porosity; dolomite rhombs in cores of intraclasts, bladed intraparticle (foram) calcspar.
TS9562 Mudstone-wackestone; limestone; calcispheres, dasycladacean algal tubules, ostracodes, trace trilobite spines; well sorted; no packing; microspar, micrite, calcspar, pseudospar, microquartz (25 um); no porosity.
TS9562.3 Wackestone; limestone; rounded intraclasts (1.0-2.0 mm), double walled calcispheres (0.15 mm), ostracodes, bioclasts (<0.2 mm); well sorted; no packing; micrite, laths of anhydrite (0.5-4.0 mm); no porosity; allochem ghosts in anhydrite.

9563.8-9569 Wackestone-packstone; dark gray and yellowish brown; dolomitic limestone; burrow mottled at 9566-9569; corals, brachiopods, crinoids; chert nodule at 9569.3; 2% intercrystalline porosity; (LT-1).
TS9564 Packstone; limestone; peloids, crinoids, intraclasts, forams, ostracodes, brachiopods; well sorted; no packing; microspar, clotted micrite, pseudospar, dolomite (10-30 um), microquartz, trace anhydrite, bitumen; 2% solution enlarged

intraparticle and biomoldic porosity; micritized crinoids, neomorphosed peloids, corroded dolomite rhombs in calcite (dedolomite).

TS9567 Packstone; limestone; peloids, forams, crinoids, rounded intraclasts (0.25-2.0 mm), molluscs, calcispheres, ostracodes; well sorted; point and longitudinal packing; microspar, micrite, pseudospar, dolomite (10-30 um), bitumen, trace anhydrite, celestite; 5% cementation reduced moldic porosity; clotted intraclasts, geopetal micrite, recrystallized peloids, ostracodes.

TS9569 Packstone; limestone; intraclasts, crinoids, pellets, calcispheres, brachiopods; well sorted; point packing; micrite, pseudospar, calcspar, dolomite, bitumen, trace anhydrite; no porosity; crinoid overgrowths.

9570-9572.5 Mudstone; dusky yellowish brown; dolomitic limestone; burrow mottled, Planolites; dolomite; tight; (LT-3).

TS9571 Mudstone; dolostone; dolomite (10-40 um), calcspar, saddle dolomite, anhydrite, bitumen; 8% cementation reduced intercrystalline porosity.

9572.5- 9574 Mudstone; dusky yellowish brown; dolostone; cross laminated, laminated; stylolites, microstylolites; tight; (LT-4).

TS9573.6 Wackestone-packstone; dolostone; angular intraclasts, crinoids, calcispheres; well sorted; point and sutured packing; dolomite, micrite, trace clay, anhydrite, celestite; no porosity; microstylolites.

TS9573.9 Wackestone; dolostone; bioclasts, calcispheres (0.2 mm); well sorted; no packing; dolomite (10-100 um), saddle dolomite, trace bitumen; 8% cementation reduced intercrystalline and moldic porosity.

9574-9577.5 Mudstone; dusky yellowish brown; dolostone; indistinctly burrowed with Planolites, Chondrites; trace bitumen; scattered laths of anhydrite; 10% intercrystalline porosity; (LT-3).

TS9574.5 Mudstone; dolostone; bioclasts;well sorted; no packing; dolomite (20-30 um), dolomite (50-100 um), saddle dolomite, calcspar, dedolomite, trace anhydrite, bitumen; 7% solution enlarged intercrystalline porosity.

TS9575 Mudstone; dolostone; crinoids; dolomite (10-30 um), dolomite (30-50 um), calcspar, saddle dolomite, bitumen; 7% cementation reduced intercrystalline porosity.

TS9576 Mudstone; dolostone; dolomite (20 um), saddle dolomite, calcspar, trace anhydrite, bitumen; 8% cementation reduced intercrystalline porosity.

TS9576.5 Mudstone; dolostone; dolomite (20 um), saddle dolomite, trace laths anhydrite; 2% cementation reduced intercrystalline porosity.

TS9577 Wackestone; dolostone; bioclasts, crinoids, brachiopods; dolomite, chert, framboidal pyrite; no porosity; silicified allochems and chert filled microfractures.

9577.5-9583 Wackestone; brownish black; calcitic dolostone; burrow mottled, Planolites, Chondrites, cherty burrow zones at 9579, 9580, 9581.5 (filled with bioclastic packstones); crinoids, bioclasts; 3% intercrystalline porosity; (LT-3).

TS9579 Mudstone; dolostone; dolomite (20-50 um), calcspar, bitumen; no porosity.

TS9581 Mudstone-wackestone; calcitic dolostone; crinoids; dolomite (20-50 um), microspar, calcspar, bitumen; no porosity,

TS9581.4 Wackestone; dolomitic limestone; crinoids, brachiopods; well sorted; no packing; microspar, dolomite (20-80 um), calcspar, trace anhydrite, bitumen; no porosity; anhydrite predates dolomite, late dedolomitization.

9583-9591.2 Wackestone. local packstone; pale yellowish brown; calcitic dolostone; massive; brachiopods (Schelwienella) (1.0- 6.0 cm); 12% intercrystalline porosity; (LT-2).

TS9583 Packstone; dolomitic limestone; rounded intraclasts, crinoids, brachiopds; well sorted; sutured packing; microspar, dolomite (30-60 um), calcspar, bitumen, trace dedolomite; no porosity; tooth and socket stylolites (0.5 mm).

TS9585 Packstone; dolomitic limestone; rounded intraclasts, crinoids, brachiopods; well sorted; point packing; dolomite, microspar, calcspar, anhydrite, celestite; no porosity.

TS9587.5 Packstone; dolomitic limestone; crinoids, brachiopods (2.0-10.0 mm), rounded intraclasts, bryozoans, pellets, gastropods, molluscs, forams; variable sorting; point packing; micrite, microspar, dolomite (30-70 um), pseudospar, saddle dolomite; no porosity.

TS9588 Wackestone; dolomitic limestone; crinoids, brachiopods; microspar, dolomite, pseudospar; 5% solution enlarged moldic porosity; dedolomite.

TS9591 Packstone; dolomitic limestone; crinoids, brachiopods, molluscs; well sorted; point packing; micrite, microspar, dolomite, trace microcrystalline anhydrite, bitumen; no porosity.

9591.2-9595.5 Mudstone; dark yellowish brown; dolomitic limestone; burrow mottled, Planolites; bioclasts; tight: (LT-3).

TS9594 Mudstone; dolostone; crinoids; dolomite (cloudy 30-80 um and clear 80-150 um), microcrystalline anhydrite, bitumen; no porosity.

9595.5-9603.4 Wackestone-packstone; grayish black, dusky brown; dolomitic limestone; thick wavy laminae; crinoids, bioclasts, corals (Sychnoelasma, Syringopora), brachiopods; microstylolites, stylolite (3.0 cm) at 9600.3; tight; (LT-1).

TS9596 Wackestone-packstone; dolomitic limestone; brachiopods, crinoids, ostracodes, trilobites; variably sorted; point packing; microspar, dolomite (30-80 um), calcspar, bitumen, microcrystalline anhydrite; no porosity.
TS9600 Packstone; dolomitic limestone; bioclasts, brachiopods, crinoids; well sorted; point packing; dolomite, microspar, calcspar, bitumen, trace anhydrite; no porosity.
TS9603 Packstone; dolomitic limestone; bioclasts (0.1-0.4 mm), brachiopods (<0.4 mm), crinoids, bryozoans; well sorted; longitudinal packing; microspar, dolomite (10-50 um), bitumen, trace anhydrite; 1% cementation reduced intercrystalline porosity.

9603.4-9610 Mudstone; dusky yellowish brown; dolostone; burrow mottled, inclined and horizontal burrows; coral at 9604.5 (Syringopora); stylolites (4.0 cm) at 9604-9604.4; fair intercrystalline porosity; oil stain; (LT-3).
TS9604.5 Mudstone; dolostone; dolomite (20-100 um), trace bitumen, microcrystalline anhydrite; 12% cementation enlarged intercrystalline porosity.

9610-9616 Wackestone-mudstone; dusky yellowish brown; dolostone; burrowed, Planolites, Teichichnus, Zoophycos; crinoids; zoned anhydrite nodules at 9612, 9616; stylolite (2.0 cm) at 9613.5; fair intercrystalline porosity; (LT-3).
TS9611.5 Mudstone; dolostone; crinoids; dolomite (10-80 um), trace anhydrite, bitumen; 10% cementation reduced moldic and enlarged intercrystalline porosity.
TS9614 Mudstone; dolostone; dolomite (10-50 um), saddle dolomite, micrite, trace anhydrite; 8% cementation reduced intercrystalline porosity.
TS9615.5 Mudstone; dolostone; dolomite (30-100 um), calcspar, saddle dolomite, subfelted nodular anhydrite (<10 cm); 12% cementation reduced intercrystalline porosity; corroded anhydrite within calcite and saddle dolomite.

Belco Petroleum, Burlington Northern 5-15 (NDGS-5383)
SE/SW 15-145N-101W McKenzie County, North Dakota
Core Depths: 9447-9477
Log Depths: 9449.5-9480

9447-9448.3 Packstone; dark gray; cherty limestone; burrowed, packstone burrow fills; bioclasts; chert replacement; stylolite (6.0 cm) at 9447.6; tight; (LT-3).
TS9447 Packstone; dolomitic limestone; peloids, crinoids, pellets, brachiopods, corals, molluscs, trace trilobites; well sorted; longitudinal packing; dolomite (10-25 um). micrite; no porosity; overgrowths on crinoids.

TS9448 Wackestone-packstone; cherty dolomitic limestone; rounded intraclasts, corals, crinoids, brachiopods, trace forams; well sorted; point packing; cloudy dolomite (<20 um), microspar, chert, calcspar, framboidal pyrite; no porosity; early grain silicification (cloudy yellowish chert-dolomite mix), late interparticle silicification (clear chert).

9448.3-9455.5 Mudstone; brownish gray; dolostone; burrow mottled, Chondrites, cross laminated packstone at 9454.5-9455.3; bioclasts; crystallotopic anhydrite at 9451.4-9454.4, concretionary nodule at 9453.3, stylolite (5.0 cm) at 9455; poor intercrystalline porosity; (LT-3,4).

TS9452 Mudstone; dolostone; dolomite (<20 um), calcspar, trace framboidal pyrite, bitumen; 7% cementation reduced fenestral porosity.

TS9455 Packstone; calcitic dolostone; peloids, intraclasts, crinoids, brachiopods, bryozoans, corals; well sorted; point packing; no porosity; sutured seam stylolite (>10 mm).

9455.5-9458.9 Mudstone; pale yellowish brown; dolomitic limestone; burrow mottled, Zoophycos, Chondrites; brachiopods; good intercrystalline porosity; (LT-3).

9458.9-9461.5 Wackestone; dusky yellowish brown; dolomitic limestone; bioclasts, corals; stylolites (2.0 cm); corals cut by stylolites; tight; (LT-3)

TS9459 Mudstone; limestone; micrite, microspar; no porosity.

TS9461 Mudstone; calcitic dolostone; crinoids; dolomite (20-50 um), calcspar; 12% cementation reduced fenestral porosity.

9461.5-9463.4 Mudstone; pale yellowish brown; dolomitic limestone; burrow mottled; tight; (LT-3).

9463.4-9464.1 Wackestone; dusky yellowish brown; limestone; corals, crinoids, bioclasts; stylolites (2.0 cm); tight; (LT-1).

9464.1-9467.3 Wackestone; pale yellowish brown; dolomitic limestone; burrow mottled, Zoophycos; bioclasts, brachiopods, corals; fair intercrystalline porosity; (LT-2).

TS9467 Wackestone; dolomitic limestone; crinoids, molluscs, peloids; well sorted; no packing; micrite, dolomite (<40 um), microspar, anhydrite laths; no porosity.

9467.3-9470 Wackestone; dusky yellowish brown; dolomitic limestone; indistinctly burrow mottled; bioclasts; tight; (LT-2).

TS9469 Packstone; dolomitic limestone; crinoids (0.3-2.0 mm), brachiopods (<4.0 mm), bioclasts, molluscs, forams; poorly sorted; point packing; dolomite (10-30 um), calcspar, microspar; no porosity.

9470-9474.2 No core found; (LT-4).
TS9473 Packstone; dolomitic limestone; crinoids, brachiopods, codiacean algae, calcispheres, forams; well sorted; point packing; calcspar, dolomite (20-50 um), saddle dolomite, bitumen; cementation filled moldic porosity.
TS9474 Packstone-wackestone; dolomitic limestone; crinoids, (0.3-1.5 mm), coral fragments, trace ostracodes; well sorted; point and longitudinal packing; microspar, dolomite (30-50 um), calcspar; no porosity; stylolites (2.5 mm), microstylolites.

9474.2-9477 Mudstone; dusky yellowish brown; calcitic dolostone; burrow mottled, Zoophycos, Teichichnus; fair intercrystalline porosity; (LT-3).
TS9476 Mudstone; calcitic dolostone; crinoids, brachiopods; dolomite (10-30 um), calcspar; 5% cementation reduced moldic porosity.

Shell- Northern Pacific, State 32-16-1 (NDGS-2584)
SW/NE 16-145N-101W McKenzie County, North Dakota
Core Depths: 9524-9587 (Core Unavailable)
Log Depths: Unconfirmed

TS9540 Mudstone; limestone; ostracodes, bioclasts; micrite, dolomite (10-20 um); no porosity; poor quality thin section.
TS9544 Mudstone; dolostone; dolomite (5-15 um); no porosity.
TS9546 Mudstone; dolostone; dolomite (5-10 um), bitumen; no porosity; corroded centers of dolomite rhombs; (LT-3).

TS9548 Packstone; dolomitic limestone; peloids, ostracodes, calcispheres, crinoids; well sorted; point and concavo-convex packing; micrite, calcspar, dolomite (10-40 um), microspar, chert; no porosity; (LT-4).

TS9550 Packstone; dolomitic limestone; peloids, bioclasts; microspar, dolomite (10-35 um), chert, bitumen; no porosity.
TS9552 Wackestone; dolomitic limestone; peloids, bioclasts, intraclasts; poor sorting; no packing; dolomite (10-30 um), micrite, calcspar; no porosity.
TS9554 Wackestone; dolomitic limestone; intraclasts, bioclasts, peloids; well sorted; no packing; dolomite, micrite; 10% moldic porosity; poor quality thin section; (LT-4).

TS9556 Packstone; limestone; peloids, bioclasts, calcispheres; well sorted; point packing; micrite; 5% solution enlarged moldic porosity.
TS9558 Packstone; limestone; peloids, intraclasts, ostracodes, calcispheres; well sorted; point packing; micrite, microspar, pseudospar, dolomite, anhydrite laths; 8% solution enlarged

interparticle porosity.
TS9560 Packstone; limestone; peloids, bioclasts, intraclasts, crinoids, calcispheres, codiacean algae, forams; variably sorted; point packing; micrite, calcspar, celestite; no porosity; (LT-5).

TS9566 Packstone; dolomitic limestone; peloids, crinoids, intraclasts; well sorted; point packing; micrite, dolomite (20-40 um), calcspar, microspar; no porosity.
TS9568 Packstone; dolomitic limestone; peloids, crinoids, forams, codiacean algae, pellets, molluscs, brachiopods; poorly sorted; point packing; dolomite (20-60 um), microspar, calcspar, pseudospar, micrite, anhydrite, celestite; no porosity.
TS9574 Packstone; dolomitic limestone; peloids, bioclasts, pellets, intraclasts, crinoids, ostracodes; well sorted; point packing; dolomite (10-70 um), calcspar, microspar, pseudospar, bitumen; 5% cementation reduced interparticle and intraparticle porosity; (LT-5).

Farmers Union, Northern Pacific 14-21 (NDGS-4088)
SW/SW 21-145N-101W McKenzie County, North Dakota
Core Depths: 9344-9394, 9407-9449
Log Depths: 9338-9387, 9404-9445

9344-9347.8 Wackestone; light brownish gray; dolomitic limestone; interlaminated anhydrite and dolostone, dewatering plumes at 9346.5 within massive anhydrite; intraclasts, peloids, bioclasts; massive anhydrite at 9344.3-9344.7, 9346-9346.5, nodular mosaic anhydrite at 9344-9344.3, 9346.5-9347; tight; (LT-5,6).
TS9344 Packstone; dolomitic limestone; peloids, intraclasts, bioclasts, ostracodes, calcispheres; well sorted; point packing; dolomite, celestite, anhydrite; no porosity; poor quality thin section.

9347.8-9348 Mudstone; pale yellowish brown; dolomitic limestone; wavy thickly laminated, stromatolitic, anhydrite nodules at 9347.5; tight; (LT-5).

9348-9350 Packstone; pale yellowish brown; dolomitic limestone; current laminated; intraclasts, peloids; tight; (LT-4).
TS9348.1 Packstone-wackestone; dolomitic limestone; peloids, calcispheres, ostracodes, forams; well sorted; no-point packing; dolomite (10 um), micrite, calcspar, saddle dolomite, microcrystalline laths of anhydrite, bitumen; no porosity.

9350-9351 Packstone; pale yellowish brown; limestone; peloids, intraclasts; diagenetically mottled, microstylolites; tight; (LT-2).
TS9350.5 Packstone; dolomitic limestone; intraclasts, peloids,

crinoids, impunctate brachiopods; poorly sorted; point packing; dolomite, microspar, micrite, pseudospar, blocky anhydrite, pyrite, microquartz (20-50 um); 5% solution enlarged moldic porosity.

9351-9356.5 Mudstone; light olive gray; dolomitic limestone; burrow mottled, Chondrites; diagenetic mottling at 9354, 9355; tight; (LT-3).

TS9354 Wackestone-mudstone; calcitic dolostone; intraclasts; dolomite (10-20 um); no porosity.
TS9355 Wackestone-mudstone; calcitic dolostone; peloids; dolomite (30-50 um), microspar, celestite, calcspar; no porosity.
TS9356 Mudstone-wackestone; calcitic dolostone; peloids; dolomite (10-50 um), celestite, anhydrite; cementation filled fenestra.

9356.5-9361 Packstone-wackestone; brownish gray; dolomitic limestone; peloids, intraclasts; crystallotopic anhydrite; open vertically fractured, anhydrite closed fractures; (LT-4).

TS9360 Packstone; dolomitic limestone; peloids, intraclasts, trace forams; variably sorted; point packing; dolomite (20-50 um), calcspar, anhydrite, celestite; no porosity.
TS9360.1 Packstone; dolomitic limestone; peloids, rounded intraclasts, forams, gastropods; poorly sorted; point packing; no porosity.

9361-9366 Packstone; light brownish gray; dolomitic limestone; thickly laminated, stromatolitic; peloids, intraclasts; anhydrite nodules at 9363; tight; (LT-5).

TS9363 Grainstone-packstone; dolomitic anhydritic limestone; peloids, intraclasts, forams, molluscs, gastropods; poorly sorted; point packing; dolomite, blocky anhydrite, celestite; 15% cementation reduced interparticle porosity.
TS9364.5 Grainstone-packstone; cherty dolomitic limestone; intraclasts; codiacean algal clasts, gastropods (1.0-2.0 mm), forams (1.0-2.0 mm); well sorted; point packing; dolomite (10-70 um), chert, celestite; no porosity.
TS9366 Grainstone-packstone; dolomitic cherty limestone; rounded intraclasts, peloids, gastropods, codiacean algae; well sorted; point packing; chert, dolomite, celestite, felted anhydrite; 10% cementation reduced interparticle porosity.

9366-9367 Packstone-rudstone; light brownish gray; dolomitic limestone; brachiopods, intraclasts, algal clasts; tight; (LT-4).

TS9367 Packstone; dolomitic limestone; rounded and discoidal intraclasts, peloids, forams, ostracodes; poorly sorted; point and longitudinal packing; dolomite, micrite, celestite, anhydrite; no porosity.

9367-9368.5 Wackestone; grayish black; limestone; crinoids; thinly laminated; microstylolites; tight; (LT-1).

9368.5-9376.3 Wackestone; brownish gray; dolostone; bioturbated, Planolites, cherty packstone nodules at 9372.5, 9374; brachiopods, crinoids, spalled coral at 9375; tight; (LT-3).

TS9372.5 Packstone; dolostone; peloids, bioclasts, forams, crinoids, gastropods, codiacean algae; well sorted; point packing; dolomite (10-30 um), chert, carbonaceous matter; no porosity; silicified allochems.

TS9373 Mudstone; dolostone; bioclasts; dolomite, chert, carbonaceous matter; no porosity.

TS9374 Packstone; cherty dolostone; peloids; well sorted; point packing; chert, dolomite, carbonaceous matter; no porosity.

TS9376 Packstone; cherty dolostone; peloids; well sorted; point packing; dolomite, chert, carbonaceous matter; no porosity.

9376.3-9377.5 Packstone; brownish gray; dolomitic limestone; cross-laminated; intraclasts; tight; (LT-4).

TS9377 Packstone; dolomitic limestone; angular and discoidal intraclasts, bioclasts, molluscs; well sorted; point packing; dolomite, micrite, microspar, trace bitumen, anhydrite; no porosity.

9377.5-9390 Mudstone; brownish gray; dolostone; burrowed, Chondrites at 9380, Teichichnus at 9379; cherty packstone nodule at 9385; bioclasts, corals; cherty nodules, stylolites at 9377, 9379, 9385 and 9387 (1.0-3.0 cm); tight; (LT-3).

TS9382 Mudstone; dolostone; dolomite (30-50 um), bitumen, carbonaceous matter; 10% cementation enlarged intercrystalline porosity.

TS9384.5 Mudstone; dolostone; codiacean algae; dolomite, trace anhydrite, celestite; 2% cementation reduced intercrystalline porosity.

TS9385 Mudstone; dolostone; bioclasts; dolomite (30-120 um), blocky anhydrite, carbonaceous matter; 12% cementation reduced moldic porosity.

TS9385.2 Wackestone; cherty dolostone; bioclasts, pellets; well sorted; no packing; dolomite chert, carbonaceous matter; no porosity.

TS9386.5 Packstone; dolostone; pellets, bioclasts, crinoids; well sorted; point packing; dolomite, trace anhydrite; 15% solution enlarged moldic porosity.

TS9387 Mudstone; dolostone; intraclasts; dolomite (30-100 um), felted anhydrite, celestite; 5% cementation reduced intercrystalline porosity.

9390-9394 Wackestone; brownish gray; dolomitic limestone; rubble and fragments; crinoids; tight, possible fracture debris; (LT-1).

TS9392 Wackestone; dolomitic limestone; crinoids, bioclasts,

peloids; well sorted; dolomite (10-50 um), microspar, micrite; 10% cementation reduced moldic porosity.
TS9392.5 Wackestone; dolomitic limestone; crinoids, bioclasts; well sorted; dolomite, microspar, micrite; 10% solution enlarged interparticle porosity.

9407-9408.5 Mudstone; brownish gray; dolomitic limestone; cross-laminated; tight; (LT-4).
TS9407 Mudstone; dolomitic limestone; dolomite (30-100 um), calcspar, dedolomite; no porosity.

9408.5-9419 Wackestone; brownish gray; dolostone; burrowed, distinct, inclined to horizontal, Teichichnus, Planolites, Chondrites, Corophiodes; crinoids; concretionary halo burrows at 9414; stylolite at 9410 (4.0 cm); poor intercrystalline porosity; (LT-3).
TS9414 Packstone; dolomitic limestone; crinoids, brachiopods, bioclasts; well sorted; point packing; micrite, dolomite, microspar; no porosity.

9419-9425.3 Wackestone; brownish black; limestone; crinoids, corals (Vesiculophyllum, Sychnoelasma), Chrondrites burrows at 9419.5; microstylolites, calcite filled microfractures; tight; (LT-1).
TS9421 Packstone; limestone; bioclasts, crinoids, encrusting bryozoans, molluscs, brachiopods; variably sorted; sutured packing; micrite, dolomite; overpacked, stylolites.

9425.3-9434 Wackestone; brownish gray; calcitic dolostone; burrowed, inclined to vertical, Teichichnus; corals, crinoids; concretionary burrow at 9431; tight; (LT-3).
TS9426.5 Wackestone; calcitic dolostone; crinoids, bioclasts, brachiopods; dolomite, calcspar; 15% cementation reduced intercrystalline and moldic porosity.
TS9427 Wackestone-packstone; calcitic dolostone; crinoids, bioclasts, corals, brachiopods; well sorted; point packing; 5% cementation reduced moldic porosity.
TS9431.5 Wackestone; calcitic dolostone; crinoids, brachiopods; well sorted; no packing; dolomite, calcspar, subfelted nodular anhydrite, interparticle chert; 12% cementation reduced moldic and interparticle porosity; early chert replacement of mud, metasomatic anhydrite.

9434-9445 Wackestone; brownish gray; dolomitic limestone; indistinctly burrowed; crinoids, corals (Vesiculophyllum, Sychnoelasma, Syringopora at 9442, Stelechophyllum banffense at 9444); stylolite (6.0 cm) at 9439.5; tight; (LT-1).
TS9435 Packstone; dolomitic limestone; crinoids, bioclasts, corals, molluscs, encrusting bryozoans, brachiopods; well sorted; point packing; dolomite, micrite, microspar; 10% cementation reduced moldic porosity.
TS9437 Packstone; dolomitic limestone; crinoids, bioclasts,

corals; well sorted; point and longitudinal packing; dolomite, micrite, microspar, pseudospar; 5% cementation reduced moldic porosity.
TS9443 Mudstone; dolostone; calcispheres; dolomite (20-100 um), celestite, trace bitumen; 10% cementation reduced moldic porosity.

9445-9449 Wackestone; brownish gray; calcitic dolostone; burrow mottled; crinoids, brachiopods; anhydrite nodules (1.0-4.0 cm); trace moldic porosity; compacted and replaced burrows as anhydrite nodules and insolubles; (LT-3).
TS9445.5 Wackestone; calcitic dolostone; bioclasts, well sorted; no packing; dolomite, saddle dolomite, anhydrite; 15% solution enlarged moldic porosity.
TS9446 Mudstone; dolostone; bioclasts; dolomite, saddle dolomite, trace carbonaceous matter, bitumen; no porosity.

Belco Petroleum. Roughrider/Federal 1-32 (NDGS-5380)
SE/NW 32-145N-101W McKenzie County, North Dakota
Core Depths: 9234-9260
Log Depths: 9241-9267

9233.9-9234.8 Wackestone-packstone; dusky yellowish brown; dolomitic limestone; intraclasts, crinoids, coral; stylolite at 9234.8; 8% intercrystalline porosity; (LT-1).
TS9234 Packstone; dolomitic limestone; intraclasts, crinoids; well sorted; point packing; dolomite (10-50 um), calcspar, trace anhydrite, saddle dolomite; 10% cementation reduced intercrystalline porosity.

9234.8-9238 Wackestone; light brownish gray; dolomitic limestone; massively bedded, cherty burrow fills at 9235, 9237, 9237.9, Teichichnus at 9236; brachiopods, crinoids; 8% intercrystalline porosity; (LT-3).
TS9235 Packstone; dolomitic cherty limestone; peloids, bioclasts, forams, codiacean algae; well sorted; point packing; chert, dolomite (<20 um), trace carbonaceous matter, blocky anhydrite; no porosity.
TS9235.5 Wackestone; calcitic dolostone; crinoids, brachiopods, molluscs; well sorted; no packing; dolomite (10-30 um), calcspar, anhydrite; 5% cementation reduced intercrystalline porosity.
TS9236 Wackestone; dolostone; crinoids; dolomite (10-70 um), trace calcspar, anhydrite, bitumen; 5% cementation reduced intercrystalline porosity.
TS9237 Packstone; dolomitic cherty limestone; peloids, intraclasts, bioclasts; well sorted; point packing; chert, dolomite, magnesite, anhydrite; no porosity, SEM reveals magnesite envelopes around peloids.

TS9237.1 Wackestone; cherty dolomitic limestone; brachiopods, crinoids; well sorted; no packing; dolomite (10-70 um), chert, magnesite; no porosity.

9238-9242 Wackestone; pale yellowish brown; calcitic dolostone; burrowed, laminated at 9241; brachiopods, algae clasts (Ortonella); laminae bend around burrows; 8% intercrystalline porosity; (LT-4).

TS9238.1 Wackestone-mudstone; calcitic dolostone; bioclasts; dolomite (10-40 um), microspar, calcspar; no porosity.

TS9240 Packstone; dolomitic limestone; crinoids, peloids, brachiopods, coral fragments, ostracodes, gastropods; well sorted; point and concavo-convex packing; micrite, cloudy dolomite (30-100 um), bitumen, microspar, trace pyrite, anhydrite; cementation filled moldic porosity; bitumen filled ostracodes; overgrowths on crinoid ossicles.

9242-9247.4 Wackestone-packstone; dark yellowish brown; calcitic dolostone; burrowed, Chondrites, Zoophycos, halo burrow at 9244.5; thin interbedded mudstones; crinoids, bioclasts; stylolite (3.0 cm) at 9247; 8% intercrystalline and moldic porosity; (LT-3).

TS9242 Wackestone; calcitic dolostone; crinoids, brachiopods, codiacean algae, encrusting bryozoans; poorly sorted; dolomite (20-30 um), calcspar; 5% cementation reduced moldic porosity.

TS9244 Wackestone; limestone; crinoids, forams, brachiopods, encrusting bryozoans, intraclasts; well sorted; longitudinal, concavo-convex packing; microspar, micrite, pseudospar, dolomite, blocky anhydrite; 10% cementation reduced moldic porosity.

TS9245 Wackestone; calcitic dolostone; bioclasts; dolomite (20-50 um), calcspar; 10% cementation reduced moldic porosity; thin section across burrow.

TS9245.2 Mudstone; calcitic dolostone; bioclasts; dolomite (20-50 um), calcspar, bitumen; 15% cementation reduced moldic and intercrystalline porosity; calcspar occluded biomolds.

TS9245.5 Mudstone; calcitic dolostone; crinoids, brachiopods; dolomite (30-70 um), calcspar, bitumen; 10% cementation reduced moldic porosity.

TS9246 Packstone; dolomitic cherty limestone; pellets, molluscs, brachiopods, crinoids; well sorted; point packing; chert, dolomite, calcspar, magnesite, pyrite; no porosity.

TS9246.1 Mudstone; dolostone; dolomite (10-30 um), calcspar, bitumen, pyrite; 5% cementation reduced intercrystalline porosity.

TS9247 Packstone-wackestone; dolomitic limestone; crinoids, brachiopods, molluscs, peloids; well sorted; point packing; 10% cementation reduced-filled moldic porosity.

9247.4-9256 Packstone; pale yellowish brown; dolomitic limestone; indistinctly burrowed, concretionary burrows at 9253.5; bioclasts, brachiopods (Schelwienella), corals (Syringopora, Sychnoelasma); stylolite (3.0 cm) at 9253; tight; (LT-1).

TS9247.5 Packstone; limestone; bioclasts, crinoids, intraclasts, pellets; well sorted; point and concavo-convex packing; micrite, dolomite (10-20 um), microspar, pseudospar, saddle dolomite; 5% cementation reduced intercrystalline porosity.
TS9251 Packstone; limestone; crinoids, brachiopods, peloids, fenestrate bryozoans, forams, gastropods; variably sorted; longitudinal and concavo-convex packing; micrite, saddle dolomite, microspar, pseudospar; 1% cementation reduced moldic porosity.
TS9253 Packstone; dolomitic limestone; crinoids, peloids, brachiopods; well sorted; point and longitudinal packing; microspar, dolomite (30-80 um); no porosity.
TS9254 Packstone; dolomitic limestone; crinoids, brachiopods, ostracodes, bryozoans; poorly sorted; longitudinal and concavo-convex packing; micrite, microspar, dolomite, bitumen; 5% cementation reduced moldic porosity.
TS9255 Packstone; dolomitic limestone; crinoids, brachiopods, bioclasts, corals, ostracodes, calcispheres; poorly sorted; longitudinal packing; micrite, dolomite, bitumen; 8% cementation reduced moldic porosity.
TS9256 Wackestone-packstone; dolomitic limestone; brachiopods, bioclasts, crinoids, codiacean algae tubules; poorly sorted; point packing; dolomite (30-60 um), microspar, micrite, calcspar, dedolomite, bitumen; no porosity.

9256-9259.8 Wackestone; brownish gray and brownish black; limestone; cherty burrow nodule at 9257.8; crinoids, corals (Vesiculophyllum), brachiopods, gastropods; stylolites at 9257, 9258.4, 9259.5; trace intercrystalline porosity; (LT-2).
TS9257 Wackestone; dolomitic limestone; crinoids, brachiopods, trilobites; dolomite (10-50 um), micrite, microspar, bitumen; 5% cementation reduced and filled porosity.
TS9258 Packstone-wackestone; dolomitic limestone; bioclasts, brachiopods, crinoids, pellets, peloids, fenestrate bryozoans; well sorted; point packing; microspar, calcspar, pseudospar, dolomite (15-25 um), celestite; 5% cementation reduced moldic porosity.

Tiger Oil, Roughrider-Federal 3-32 (NDGS-5258)
SW/NE 32-145N-101W McKenzie County, North Dakota
Core Depths: 9274-9289, 9307-9352
Log Depths: 9280-9295, 9306-9351

9274-9284 Wackestone-packstone; dark yellowish brown; calcitic dolostone; massively bedded, burrowed including Zoophycos, Planolites, Chondrites at 9282.5; bioclasts, brachiopods, crinoids, corals; microstylolites; poor vuggy porosity; (LT-2).

TS9274.5 Wackestone; dolomitic limestone; crinoids, brachiopods; well sorted; no packing; microspar, dolomite, pseudospar, trace bitumen; no porosity.
TS9276 Packstone; dolomitic limestone; rounded intraclasts, crinoids, brachiopods, peloids, trilobites, trace molluscs; variably sorted; longitudinal and concavo-convex packing; micrite, dolomite, bitumen; no porosity.
TS9276.2 Wackestone; dolomitic limestone; bioclasts, peloids, crinoids, intraclasts, brachiopods, corals; poorly sorted; micrite, dolomite, microspar, pseudospar, bitumen; 5% cementation reduced moldic and solution enlarged intraparticle porosity; bitumen fills molds and coral septa.
TS9277 Packstone; dolomitic limestone; brachiopods, crinoids, trilobites; well sorted; longitudinal packing; micrite, dolomite (10-50 um), microspar, bitumen; no porosity.
TS9281.8 Wackestone; calcitic dolostone; crinoids, brachiopods; poorly sorted; no packing; dolomite (10-30 um), calcspar, bitumen; 3% cementation filled intercrystalline porosity.
TS9284 Packstone; dolomitic limestone; bioclasts, crinoids, intraclasts, bryozoans, trace ostracodes; poorly sorted; point and longitudinal packing; dolomite, microspar, micrite, saddle dolomite, bitumen; 10% cementation reduced moldic porosity; stylolite (200 um).

9283-9289 Mudstone; pale yellowish brown; dolostone; burrowed. Teichichnus, Zoophycos, Planolites; anhydrite nodules at 9285, 9285.9 and 9286.6; fair intercrystalline porosity; (LT-3).
TS9285 Mudstone-wackestone; dolostone; crinoids, ostracodes; poorly sorted; no packing; dolomite, anhydrite, calcspar, bitumen, celestite; 12% cementation reduced intercrystalline and moldic porosity.

9307-9311 Wackestone-packstone; grayish black; limestone; massively bedded; crinoids, coral fragments, corals (Vesiculophyllum, Sychnoelasma); microstylolites, stylolites (1.0-2.0 cm) at 9309, 9310.5; abundant anhydrite filled vertical fractures; no porosity; (LT-1).
TS9309.5 Packstone; dolomitic limestone; bioclasts, crinoids, corals, molluscs, brachiopods; variably sorted; longitudinal and sutured packing; micrite, dolomite, microcrystalline anhydrite, bitumen, detrital microquartz, celestite; no porosity.
TS9310 Packstone; limestone; brachiopods, crinoids, corals, encrusting bryozoans, molluscs; variably sorted; longitudinal, concavo-convex and sutured packing; micrite, dolomite, bitumen; no porosity.

9311-9316.8 Wackestone-packstone; dark yellowish brown; calcitic dolostone; burrowed, Teichichnus; crinoids, corals; good vuggy porosity; (LT-3).

TS9311.5 Wackestone; calcitic dolostone; crinoids, corals, brachiopods; well sorted; no packing; dolomite (20-120 um), calcspar; no porosity.
TS9314 Wackestone; calcitic dolostone; corals, crinoids, brachiopods, molluscs; poorly sorted; no packing; dolomite (10-30 um), calcspar, bitumen; no porosity; microstylolites.
TS9316.5 Wackestone; calcitic dolostone; crinoids, bioclasts; well sorted; no packing; dolomite (30-50 um), calcspar, bitumen; 6% cementation enlarged intercrystalline porosity.

9316.8-9321 Packstone; dark yellowish brown; calcitic dolostone; massively bedded, concretionary burrows at 9317; crinoids, brachiopods, corals; conjugate microfractures associated with burrow concretion at 9317; poor vuggy porosity; (LT-2).
TS9317 Wackestone-packstone; dolomitic limestone; crinoids, brachiopods, corals, trilobites, trace molluscs; well sorted; longitudinal and concavo-convex packing; micrite, dolomite (10-30 um); no porosity.

9321-9331 Wackestone; brownish gray and grayish black; dolomitic limestone; massively bedded, retrusive Teichichnus burrow at 9323, concretionary burrows at 9330.4; corals (Vesiculophyllum, Sychnoelasma, Syringopora, with Stelechophyllum banfense at 9329.6, crinoids, brachiopods; stylolites (2.0-4.0 cm); no porosity; (LT-1).
TS9323 Wackestone; calcitic dolostone; brachiopods, crinoids, corals, molluscs; poorly sorted; no packing; dolomite, calcspar, micrite, bitumen; no porosity.
TS9325 Packstone; dolomitic limestone; crinoids, brachiopods, corals, intraclasts, molluscs; poorly sorted; concavo-convex and sutured packing; micrite, dolomite, microspar, pyrite; no porosity.
TS9328 Packstone; dolomitic limestone; crinoids, brachiopods, molluscs; well sorted; point and longitudinal packing; micrite, dolomite, microspar, bitumen; 2% solution enlarged interparticle porosity.
TS9331 Packstone-wackestone; limestone; brachiopods, crinoids, corals, bryozoans, codiacean algae, trace molluscs; poorly sorted; point packing; micrite, microspar; no porosity.

9331-9342 Mudstone; dolostone; burrowed, Teichichnus, Planolites, burrows replaced with anhydrite nodules (2.0-5.0 cm), stylolite seam (3.0 cm thick) at 9338.8, insolubles concentrated around nodules at 9338; tight, vertically microfractured; (LT-3).
TS9331.2 Wackestone; dolomitic limestone; crinoids, brachiopods, codiacean algae, ostracodes, coral fragments, encrusting bryozoans; well sorted; no packing; micrite, dolomite (20-70 um), calcspar, bitumen; 8% cementation reduced moldic porosity; microstylolites, compaction laminae around corals, dolomitic chert nodules.

TS9332.5 Wackestone; dolostone; crinoids, brachiopods, ostracodes; poorly sorted; dolomite (10-50 um), framboidal pyrite, bitumen; 15% cementation reduced moldic and reduced intercrystalline porosity; saddle dolomite fills ostracode molds.
TS9336.5 Mudstone; dolostone; crinoids; dolomite (10-30 um), calcspar, pyrite; 5% cementation enlarged moldic porosity.
TS9338 Mudstone; dolostone; crinoids; dolomite (<20 um), anhydrite, saddle dolomite, framboidal pyrite; 11% cementation enlarged intercrystalline porosity.
TS9338.1 Wackestone; calcitic dolostone; bioclasts, crinoids; well sorted; dolomite (10-30 um), calcspar, trace pyrite, carbonaceous matter; 12% calcite cementation reduced and filled moldic porosity.
TS9339 Mudstone; dolomitic limestone; crinoids, intraclasts; poorly sorted; no packing; micrite, dolomite, clay, insolubles, detrital microquartz, pyrite; no porosity; microstylolites; Fryburg gamma-ray marker bed.
TS9340.5 Packstone; dolomitic limestone; crinoids, brachiopods, trilobite spines, coral fragments; poorly sorted; concavo-convex and sutured packing; micrite, dolomite; no porosity.
TS9341 Mudstone; dolostone; crinoids; dolomite (10-30 um), calcspar, bitumen, trace detrital microquartz; no porosity.
TS9342 Mudstone; dolostone; crinoids; dolomite (10-30 um), calcspar, bitumen; no porosity.

9342-9352 Wackestone-mudstone; dusky yellowish brown; calcitic dolostone; burrow mottled (Chondrites, Zoophycos, Planolites), concretionary burrows; corals (Amplexizaphretis, Sychnoelasma), crinoids; cherty burrow fills at 9342.5, 9347.8, anhydrite nodules 9349, 9350; poor intercrystalline and moldic porosity; (LT-3).
TS9346 Wackestone; cherty dolostone; crinoids, brachiopods; well sorted; no packing; dolomite (20-30 um), coarse dolomite (50-120 um), chert, carbonaceous matter, pyrite; no porosity; chert nodule preserves depositional fabric.
TS9347 Packstone; limestone; crinoids, brachiopods, corals, trilobite spines; poorly sorted; longitudinal, concavo-convex and sutured packing; micrite, pyrite, trace saddle dolomite; no porosity; stylolite laminae drape around allochems.
TS9349 Mudstone; dolostone; crinoids; dolomite (10-30 um), felted laths of anhydrite, saddle dolomite, pyrite, celestite; no porosity.
TS9349.1 Mudstone; dolostone; ostracodes, calcispheres, crinoids; well sorted; dolomite, subfelted anhydrite nodules, calcspar, celestite, pyrite; anhydrite filled fractures.
TS9351.5 Mudstone; dolostone; crinoids, brachiopods; dolomite (<20 um), saddle dolomite; no porosity.

Lone Star Producing, Burlington-Northern 1-33 (NDGS-5346)
NE/NW 33-145N-101W McKenzie County, North Dakota
Core Depths: 9180-9205
Log Depths: 9172-9197

9180-9184 Distorted bedded nodular mosaic anhydrite, massively bedded cloudy anhydrite; pale yellowish brown and brownish black; dewatering plumes at 9182, 9184; tight; (LT-6).

TS9180 Wackestone; anhydritic dolostone; pellets, peloids, calcispheres (80-150 um), codiacean algae; well sorted; no packing; subfelted nodular anhydrite, dolomite, trace calcspar, clay; cementation filled fenestral porosity; calcisphere biomold lined with bladed dolospar, late calcspar.

TS9181 Mudstone; dolostone; dolomite (10-15 um), trace calcspar; no porosity.

TS9183 Mudstone; dolostone; crinoids, calcispheres; well sorted; no packing; dolomite (10-30 um), microcrystalline anhydrite; 15% solution enlarged fenestral porosity.

9184-9188 Packstone-wackestone; pale yellowish brown; dolostone; thickly laminated, bedded nodular anhydrite at 9185, 9186.5, mudchips at 9187; peloids, intraclasts; stylolite (4.5 cm) at 9184; fair moldic porosity; spotty brown oil stain; (LT-5).

TS9186 Packstone; anhydritic dolomitic limestone; peloids, intraclasts, calcispheres, ostracodes; well sorted; point packing; microcrystalline anhydrite, isopachous dolomite, celestite; 15% cementation reduced fenestral and moldic porosity.

TS9187 Packstone; limestone; peloids, intraclasts, crinoids, calcispheres, ostracodes, molluscs; poorly sorted; point and sutured packing; micrite, dolomite, microstylolites; no porosity.

9188-9192.5 Wackestone-packstone; brownish black; dolomitic limestone; thinly interbedded; coral fragments; stylolites at 9188, 9189 and 9191, microstylolites; tight; (LT-5).

TS9189 Packstone; dolomitic limestone; peloids, angular intraclasts, calcispheres, pellets, codiacean algae, molluscs, crinoids; well sorted; point packing; micrite, dolomite, microspar, pyrite, trace carbonaceous matter; no porosity.

TS9192.5 Wackestone; cherty dolomitic limestone; peloids, angular and discoidal intraclasts, forams, gastropods; well sorted; no packing; chert, dolomite; no porosity; section is across chert nodule, outside of nodule is overpacking of allochems, overgrowths on crinoids, microspar.

9192.5-9193 Packstone-rudstone; dark yellowish brown; limestone; intraclasts, gastropods, brachiopods; thin bed of Chondrites burrows at base; (LT-4).

TS9192.8 Grainstone; limestone; peloids, intraclasts, gastropods, molluscs, codiacean algae; well sorted; point packing; isopachous bladed calcite, calcspar; no porosity.

9193-9205 Wackestone-packstone; dark yellowish brown and dusky yellowish brown; limestone; indistinctly burrow mottled, burrows Zoophycos, Planolites, Corophiodes at 9198, thin packstone beds; peloids, bioclasts, brachiopods, coral fragments (Vesiculophyllum at 9198.3); chert nodule at 9195.8, microstylolites drape chert nodule, stylolites at 9194, 9196, 9197, 9200.2 and 9204 (1.0-4.0 cm); tight; (LT-3).

TS9193.2 Packstone-wackestone; cherty dolomitic limestone; peloids, intraclasts, forams, brachiopods, calcispheres; poorly sorted; point packing; chert, dolomite; no porosity.

TS9196 Wackestone-packstone; cherty dolomitic limestone; peloids, intraclasts, forams, gastropods, crinoids; poorly sorted; point packing; chert, dolomite, calcspar; no porosity.

TS9197 Packstone; dolomitic limestone; peloids, intraclasts (mud-chips), crinoids, brachiopods; poorly sorted; point packing; micrite, microspar, dolomite, anhydrite, trace bitumen; no porosity; stylolites.

TS9198 Packstone; limestone; crinoids, pellets, angular intraclasts, brachiopods, peloids, ostracodes, codiacean algae, calcispheres; poorly sorted; point and concavo-convex packing; micrite, microspar, pseudospar, dolomite; no porosity; overgrowths on crinoids, intraclasts or algal clasts?

TS9198.3 Packstone; limestone; bioclasts, peloids, crinoids, brachiopods, codiacean algae; poorly sorted; point packing; micrite, microspar, dolomite, trace anhydrite; no porosity.

TS9200 Wackestone; limestone; peloids, brachiopods, bioclasts, crinoids, forams, codiacean algae, calcispheres; poorly sorted; no packing; micrite, microspar, dolomite, trace bitumen; no porosity.

TS9200.1 Wackestone; dolomitic limestone; peloids, rounded intraclasts, bioclasts, crinoids; poorly sorted; no packing; micrite, microspar, dolomite, calcspar, celestite, blocky anhydrite, detrital microquartz; no porosity; microquartz inclusions within intraclasts.

TS9203.5 Packstone-wackestone;limestone; rounded and discoidal intraclasts, bioclasts, crinoids, brachiopods, coral fragments; poorly sorted; point packing; micrite, microspar, dolomite, trace anhydrite; no porosity.

TS9204 Packstone; dolomitic limestone; peloids, angular intraclasts, bioclasts, codiacean algae, crinoids, brachiopods, calcispheres, trace gastropods; poorly sorted; point packing; micrite, dolomite (20-40 um), microspar, bitumen; no porosity.

Texaco, Government-M.Pace 1-14 (NDGS-2667)
SW/NW 14-146N-101W McKenzie County, North Dakota
Core Depths: 9426-9546, 9580-9638
Log Depths: 9428-9548, 9582-9640

9526-9530 Packstone; brownish gray; limestone; fenestral; intraclasts, peloids, algae; abundant crystallotopic anhydrite, pyrite; tight; (LT-4).

TS9529.5 Packstone; anhydritic limestone; angular and discoidal, calcispheres, ostracodes; poorly sorted; longitudinal packing; microcrystalline anhydrite, micrite, microspar, dolomite, celestite; no porosity.

9530-9546 Cloudy nodular mosaic and bedded nodular anhydrite; light olive gray and medium light gray; clayey distorted laminae, thin interbeds of dolomudstone at 9534, 9536 and 9546; tight; (LT-6).

TS9532.5 Mudstone; cherty limestone; micrite, chert, calcspar, dolomite, pyrite; no porosity.

9580-9583 Grainstone; dark yellowish brown; limestone; massively bedded, thin muddy laminae at base; intraclasts, bioclasts, algal clasts (Ortonella); anhydrite; tight; (LT-5).

9583-9586.5 Mudstone-packstone; dark yellowish brown; interlaminated mudstone and peloid packstone; peloids; tight; (LT-5).

9586.5-9592 Mudstone; brownish gray; dolomitic limestone; indistinctly burrow mottled; stylolites (1.0-2.0 cm) at 9586.5, 9588, 9589.7 and 9590.6; tight; (LT-3).

9592-9595 Packstone; dusky yellowish brown; limestone; peloids, bioclasts, corals (Sychnoelasma); tight; (LT-1).

9595-9599 Wackestone; dark yellowish brown; calcitic dolostone; burrowed (Chondrites, Teichichnus); brachiopods, bioclasts, corals; cherty packstones at 9596.4-9596.9; fair intercrystalline porosity; (LT-3).

9599-9603 Wackestone; dark yellowish brown; dolomitic limestone; indistinctly burrowed; cherty packstone at 9601.5-9601.8; brachiopods, corals (Syringopora); stylolite (6.0 cm) at 9601, anhydrite within stylolite teeth, fractured at 9598.7-9599.6; poor intercrystalline porosity; (LT-1).

9605-9612.4 Packstone; dark yellowish brown and dusky yellowish brown; limestone; cross laminated, laminated; peloids; stylolites (0.5-2.0 cm), crystallotopic anhydrite at 9605, 9612; tight; (LT-4).

9612.4-9630 Wackestone-packstone; dusky yellowish brown with dark gray; limestone; massively bedded, burrowed (Planolites at 9615); crinoids, corals, gastropod at 9617, brachiopod packstone zones at 9617.3-9617.5, 9618-9618.3, 9622-9622.3, 9625.7-9625.8, and 9629.8-9629.9; tight, closed vertical fractures; (LT-1, LT-3).

9630-9638 Wackestone-mudstone; brownish gray; dolomitic limestone; burrowed (Teichichnus, Zoophycos, Chondrites); corals (Syringopora, Sychnoelasma); poor intercrystalline porosity; anhydrite replacement of allochems; (LT-3).

REFERENCES

REFERENCES

Adams, J. E., and Rhodes, M. L., 1960, Dolomitization by seepage refluxion: American Association of Petroleum Geologists Bulletin, v. 44, p. 1912-1920.

Altschuld, N., and Kerr, S. D., Jr., 1982, Mission Canyon and Duperow reservoirs of the Billings Nose, Billings County, North Dakota, in Christopher, J. E., and Kaldi, J., eds., Fourth International Williston Basin Symposium: Saskatchewan Geological Society Special Publication No. 6, p. 103-112.

Anderson, S. B., 1958, Mississippian possibilities: North Dakota Geological Survey Report of Investigation No. 31, 9 p.

Barta, C., and Zemlicka, J., 1971, Growth of CaCO3 and CaSO4-2H2O crystals in gels: Journal of Crystal Growth, v. 10, p. 158-162.

Bathurst, R. G. C., 1966, Boring algae, micrite envelopes, and lithification of molluscan biosparites: Journal of Geology, v. 5, p. 15-32.

Bathurst, R. G. C., 1975, Carbonate sediments and their diagenesis (2nd ed.): New York, Elsevier, 658 p.

Bathurst, R. G. C., 1985, Carbonate diagenesis and reservoir development: conservation, destruction and creation of pores: Carbonate depositional environments: modern and ancient, Colorado School of Mines Short Course Notes, 63 p.

Beach, D. K., and Schumacher, A. L., 1982, Stanley Field, North Dakota: economic and quantitative significance of mechanically compacted shallow-water limestone: American Association of Petroleum Geologists Bulletin., v. 66, p. 547.

Bickford, M. E., Van Schmus, W. R. and Zeitz, I., 1986, Proterozoic history of the midcontinent region of North America: Geology, v. 14, p.492-496.

Blatt, H., Middleton,G., and Murray, R., 1980, Origin of sedimentary rocks (2nd ed.): New Jersey, Prentice Hall, 782 p.

Bluemle, J. P., Anderson, S. B., and Carlson, C. G., 1980, North Dakota stratigraphic column: North Dakota Geological Survey, Grand Forks, North Dakota.

Bromley, R. G., and Ekdale, A. A., 1984, Trace fossil preservation in flint in the European chalk: Journal of Paleontology, v. 58, p. 298-311.

Butler, G. P., 1969, Modern evaporite deposition and geochemistry of co-existing brines, the sabkha, Trucial Coast, Arabian Gulf: Journal of Sedimentary Petrology, v. 39, p. 70-89.

Carlson, C. G., and Anderson, S. B., 1965, Sedimentary and tectonic history of the North Dakota part of the Williston Basin: American Association of Petroleum Geologists Bulletin, v. 49, p.1833-1846.

Carlson, C. G., and Anderson, S. B., 1966, A look at the lower and middle Madison of northwestern North Dakota: North Dakota Geological Survey, Report of Investigations No. 43, 14 p.

Carlson, C. G., and LeFever, J. A., 1987, The Madison, a nomenclatural review with a look to the future, in Carlson, C. G. and Christopher, J. E., eds., Fifth International Williston Basin Symposium, Saskatchewan Geological Society Special Publication No. 9, p. 77-92.

Chamberlain, C. K., 1978, Recognition of trace fossils in cores, in, Basan, P. B., ed., Trace fossil concepts: Society of Economic Paleontologists and Mineralogists, Short Course No. 5, p. 133-185.

Choquette, P. W., and Pray, L. C., 1970, Geologic nomenclature and classification of porosity in sedimentary carbonates: American Association of Petroleum Geologists Bulletin, v. 54, p. 207-250.

Collier, A. J., and Cathcart, S. H., 1922, Possibility of finding oil in laccolithic domes south of the Little Rocky Mountains, Montana: United States Geological Survey Bulletin 736-F, p. 171-178.

Davies, G. R., 1976, Radially aragonitic ooids, Lizard Island, Great Barrier Reef, Queensland, Australia: Geology, v. 4, p. 120-122.

Downey, J. S., 1984, Geohydrology of the Madison and associated aquifers in parts of Montana, North Dakota, South Dakota, and Wyoming: United States Geological Survey Professional Paper No. 1273-G, 47 p.

Dunham, R. J., 1962, Classification of carbonate rocks according to depositional texture: in Ham, W. E., ed., Classification of carbonate rocks: American Association of Petroleum Geologists Memoir 1, p. 108-121.

Dunham, R. J., 1969, Vadose pisolite in the Capitan Reef (Permian), New Mexico and Texas: Society of Economic Paleontologists and Mineralogists Special Publication No. 14, p. 182-191.

Durall, R. L., 1987, Diagenesis and porosity development of the Mission Canyon and Charles formations (Mississippian), Tree Top and Whiskey Joe fields, North Dakota: Master's thesis, University of North Dakota, Grand Forks, North Dakota, 208 p.

Edie, R. W., 1958, Mississippian sedimentation and oil fields in southeastern Saskatchewan: American Association of Petroleum Geologists Bulletin, v. 42, p. 94-126.

Ekdale, A. A., Bromley, R. G., and Pemberton, S. G., 1984, Ichnology: the use of trace fossils in sedimentology and stratigraphy: Society of Economic Paleontologists and Mineralogists, Short Course No. 15, 300 p.

Elliott, T. L., 1982, Carbonate facies, depositional cycles and the development of secondary porosity during burial diagenesis, in Christopher, J. E. and Kaldi, J., eds., Fourth International Williston Basin Symposium, Saskatchewan Geological Society Special Publication No. 6, p. 131-151.

Estaban, M., 1976, Vadose pisolite and caliche: American Association of Petroleum Geologists, v. 60, p. 2048-2057.

Fischer, H. J., Luther, M. R., Eylands, K. E., and Quinn, C. F., 1987, Salinity, oxygenation, and topographic controls on Mississippian subtidal sedimentation in a portion of the Mission Canyon Formation, Williston Basin, North Dakota (abstract), in Carlson, C. G. and Christopher, J. E., eds., Fifth International Williston Basin Symposium, Saskatchewan Geological Society Special Publication No. 9, p. 266-267.

Folk, R. L., 1965, Some aspects of recrystallization in ancient limestones, in Pray, L. C., and Murray, R. C., eds., Dolomitization and limestone diagenesis: A symposium: Society of Economic Paleontologists and Mineralogists Special Publication No. 13, p. 14-48.

Folk, R. L., 1974, The natural history of crystalline calcium carbonate: effect of magnesium content and salinity: Journal of Sedimentary Petrology, v. 44, p. 40-53.

Folk, R. L., and Land, L. S., 1975, Mg/Ca ratio and salinity: two controls over crystallization of dolomite: American Association of Petroleum Geologists Bulletin, v. 59, p. 60-68.

Friedman, G. M., 1959, Identification of carbonate minerals by staining methods: Journal of Sedimentary Petrology, v. 29, p. 87-97.

Friedman, G. M., Amiel, A. J., Braun, M., and Miller, D. S., 1973, Generation of carbonate particles and laminates in algal mats - example from sea marginal hypersaline pool, Gulf of Aqaba, Red Sea: American Association of Petroleum Geologists Bulletin, v. 57, p. 541-557.

Fuller, J. G. C. M., 1956, Mississippian rocks and oil fields in southeastern Saskatchewan: Department of Mineral Resources Report. 19, p. 72.

Gerhard, L. C., Anderson, S. B., and Berg, J., 1978, Mission Canyon porosity development, Glenburn Field, North Dakota Williston Basin, in, The economic geology of the Williston basin: Williston Basin Symposium, Montana Geological Society, Billings, Montana, p. 177-189.

Gerhard, L. C., Anderson, S. B., LeFever, J. A., and Carlson, C. G., 1982, Geological development, origin, and energy mineral resources of the Williston Basin, North Dakota: American Association of Petroleum Geologists Bulletin, v. 66, p. 989-1020.

Goddard, E. N., 1963, Rock color chart: Geological Society of America.

Habicht, J. K. A., 1979, Paleoclimate, paleomagnetism and continental drift: American Association of Petroleum Geologists Studies in Geology, no. 9, 31 p.

Halley, R. B., 1977, Ooid fabric and fracture in the Great Salt Lake and the geologic record: Journal of Sedimentary Petrology, v. 47, p. 1099-1120.

Halvorson, D. L., ed., 1984, Oil in North Dakota 1983: North Dakota Industrial Commission, p. 465-507.

Harris, S. H., Land, C. B. Jr., and McKeever, J. H., 1966, Relation of Mission Canyon stratigraphy to oil production in north-central North Dakota: American Association of Petroleum Geologists Bulletin, v. 50, p. 2269-2276.

Harrison, R. L. and Flood, A. L., 1956, Mississippian correlations in the international boundary areas: First International Williston Basin Symposium, North Dakota Geological Society, p. 36-51.

Heckel, P. H., 1972, Recognition of ancient shallow marine environments, in Rigby, J. K. and Hamblin, W. K., eds., Recognition of ancient sedimentary environments: Society of Economic Paleontologists and Mineralogists Special Publication No. 16, p. 226-286.

Hedgepeth, J. W., ed., 1957, Treatise on Marine Ecology and Paleoecology: Geological Society of America Memoir 67, Vol. 1, 1296 p.

Himebaugh, J. P., 1979, Petroleum potential of the Tilston interval (Mississippian) of central North Dakota: Master's thesis, University of North Dakota, Grand Forks, North Dakota, 156 p.

Holland, F. D. Jr., 1952, Stratigraphic details of lower Mississippian rocks of northeastern Utah and southwestern Montana: American Association of Petroleum Geologists Bulletin, v. 36, p. 1697-1734.

Horner, T. C., 1986, Depositional environments, diagenesis and porosity relationships in the Mission Canyon formation, Elkhorn Ranch field, Billings County, North Dakota: Master's thesis, Texas Tech University, Lubbock, Texas, 114 p.

Irwin, M. L., 1965, General theory of epeiric clear water sedimentation: American Association of Petroleum Geologists Bull., v. 49, p.455-459.

Kahle, C. F., 1966, Some observations on compaction and consolidation in ancient oolites: Compass, v. 44, p. 19-29.

Kahle, C. F., 1974, Ooids from Great Salt Lake, Utah, as an analogue for the genesis and diagenesis of ooids in marine limestones: Journal of Sedimentary Petrology, v. 44, p. 30-39.

Kendall, A. C., 1984, Evaporites: in, Walker, R. G., ed., Facies models: Geoscience Canada, p. 259-296.

Kendall, C. G. St. C., and Skipwith, P. A. d'E., 1969, Holocene shallow water carbonate and evaporite sediments of Khor al Bazam, Abu Dhabi, southwest Persian Gulf: American Association of Petroleum Geologists Bulletin, v. 53, p. 841-869.

Land, L. S., Behrens, E. W., and Frishman, S. A., 1979, The ooids of Baffin Bay, Texas: Journal of Sedimentary Petrology, v. 49, p. 1269-1278.

LeFever, J. A., LeFever, R. D., and Anderson, S. B., 1984, Mississippian Frobisher-Alida-Kisbey Sandstone, north-central North Dakota (abstract): American Association of Petroleum Geologists Bulletin, v. 68, p. 940.

LeFever, R. D., Thompson, S. C. and Anderson, D. B., 1987, Earliest Paleozoic history of the Williston Basin in North Dakota, in Carlson, C. G. and Christopher, J. E., eds., Fifth International Williston Basin Symposium, Saskatchewan Geological Society Special Publication No. 9, p. 22-36.

Lindsay, R. F., and Roth, M. S., 1982, Carbonate and evaporite facies, dolomitization and reservoir distribution of the Mission Canyon Formation, Little Knife Field, North Dakota: in Christopher, J. E. and Kaldi, J., eds., Fourth International Williston Basin Symposium, Saskatchewan Geological Society Special Publication No. 6, p. 203-210.

Lippman, F., 1973, Sedimentary carbonate minerals: New York, Springer Verlag, 228 p.

Longman, M. W., 1980, Carbonate diagenetic textures from near-surface diagenetic environments: American Association of Petroleum Geologists Bulletin, v.64., p. 461-487.

Loreau, J. P., and Purser, B. H., 1973, Distribution and ultrastructure of Holocene ooids in the Persian Gulf, in Purser, B. H., ed., The Persian Gulf: Holocene carbonate sedimentation and diagenesis in a shallow epicontinental sea: New York, Springer-Verlag, p. 279-328.

Luther, M. R., 1987, Deposition and diagenesis of a portion of the Frobisher-Alida interval (Mississippian Madison Group), Wiley Field, North Dakota: Master's thesis, University of North Dakota, Grand Forks, North Dakota, 212 p.

Maiklem, W. R., Bebout, D. G., and Glaister, R. P., 1969, Classification of anhydrite - a practical approach: Bulletin of Canadian Petroleum Geology, v. 17, p. 194-233.

Mander, M. L. M., 1980, Petrography and environments of deposition of the Mission Canyon formation, Rough Rider field, North Dakota: Master's thesis, University of Colorado, Boulder, Colorado, 91 p.

McKee, E. D., and Weir, G. W., 1953, Terminology for stratification and cross-stratification in sedimentary rocks: Geological Society of America Bulletin, v. 64, p. 381-390.

Nordquist, J. W., 1953, Mississippian stratigraphy of northern Montana, in Guidebook Fourth Annual Field Conference: Billings Geological Society, p.68-82.

Obelenus, T. J., 1985, Depositional environments and diagenesis of carbonates and associated evaporites, Frobisher-Alida interval, Madison Group (Mississippian), Williston Basin, northeastern North Dakota: Master's Thesis, University of North Dakota, Grand Forks, North Dakota, 313 p.

Peale, A. C., 1893, The Paleozoic section in the vicinity of Three Forks, Montana: United States Geological Survey Bulletin 110, 56 p.

Peterman, Z. E., and Hedge, C. E., 1964, Age of basement rocks from the Williston Basin of North Dakota and adjacent areas: United States Geological Survey Professional Paper No. 475-d, Article 141, p.100-104.

Peterson, J. A., 1981, Stratigraphy and sedimentary facies of the Madison Limestone and associated rocks in parts of Montana, North Dakota, South Dakota, Wyoming and Nebraska: United States Geological Survey Open File Report No. 81-642, 85 p.

Petty, D. M., 1989, Depositional facies, textural characterisitics, and reservoir properties of dolomites in Frobisher-Alida Interval in southwest North Dakota: American Association of Petroleum Geologists Bulletin, v. 72, p. 1229-1253.

Quinn, C. F., 1986, Depositional history and diagenesis of the Sherwood and Bluell beds (Mississippian) southwestern Renville County, North Dakota: Master's Thesis, University of North Dakota, Grand Forks, North Dakota, 254 p.

Radke, B. M., and Mathis, R. L., 1980, On the formation and occurrence of saddle dolomite: Journal of Sedimentary Petrology, v. 50, p. 1149-1168.

Sando, W. J., and Dutro, J. T., Jr., 1974, Type sections of the Madison Group (Mississippian) and its subdivisions in Montana: United States Geological Survey Professional Paper No. 842, 22 p.

Saskatchewan Geological Society, 1956, Report of the Mississippian names and correlations committee: Regina, Saskatchewan, 4 p.

Schreiber, B. C., 1981, Marine evaporites: facies development and relation to hydrocarbons and mineral genesis: American Association of Petroleum Geologists Fall Education Conference, Calgary, 62 p.

Schreiber, B. C., and Hsu, K. J., 1980, Evaporite, in, Hobson, G. D., ed., Developments in Petroleum Geology - 2: England, Applied Science p. 87-138.

Schreiber, B. C., Roth, M. S., and Helman, M. L., 1982, Recognition of primary facies characteristics of evaporites and the differentiation of these from diagenetic overprints: in, Handford, C. R., Loucks, R. G., and Davies, G. R., eds., Depositional and diagenetic spectra of evaporites: Society of Economic Paleontologists and Mineralogists Core Workshop no. 3, Calgary, p. 1-32.

Schwartz, D. A., 1987, The deposition and diagenesis of the Bluell zone, Upper Mission Canyon Formation (Mississippian), Flaxton Field, Burke County, North Dakota: Master's Thesis, University of North Dakota, Grand Forks, North Dakota, 246 p.

Scotese, C. R., Bambach, R., Barton, C., Van der Voo, R., and Ziegler, A. M., 1979, Paleozoic base maps: Journal of Geology, v. 87, p. 217-277.

Seager, O. A., 1942, A test on the Cedar Creek Anticline, southeastern Montana: American Association of Petroleum Geologists Bulletin, v. 26, p. 861-864.

Shanley, K. W., 1983, Stratigraphy and depositional model, upper Mission Canyon Formation (Mississippian), northeast Williston Basin, North Dakota: Master's thesis, Colorado School of Mines, Golden, Colorado, 172 p.

Shaw, A. B., 1964, Time and stratigraphy: New York, McGraw-Hill, 365 p.

Shearman, D. J., 1978, Evaporites of coastal sabkhas, in, Dean, W. E., and Schreiber, B. C., eds., Marine Evaporites: Society of Economic Paleontologists and Mineralogists Short Course Notes no. 4, p. 6-42.

Sheldon, R. P., and Carter, M. D., 1979, Paleotectonic investigation of the Mississippian system of the United States, Part 1, Introduction and regional analysis of the Mississippian system-Williston Basin Region: United States Geological Survey Professional Paper No. 1010, Chapter 0, p. 245-271.

Shinn, E. A., and Robbin, D. M., 1983, Mechanical and chemical compaction in fine-grained shallow-water limestones: Journal of Sedimentary Petrology, v. 53, p. 595-618.

Shourd, M. L., and Levin, H. L., 1976, Chondrites in the Upper Plattin Subgroup (Middle Ordovician) of eastern Missouri: Journal of Paleontology, v. 50, p. 260-268.

Sloss, L. L., and Hamblin, R.H., 1942, Stratigraphy and insoluble residues of Madison Group (Mississippian) of Montana: American Association of Petroleum Geologists Bulletin, v. 26, p. 305-335.

Sloss, L. L., and Moritz, C. A., 1951, Paleozoic stratigraphy of south-western Montana: American Association of Petroleum Geologists Bulletin, v. 35, p. 2135-2169.

Smith, M. H., 1960, Revised nomenclature for the Williston Basin: American Association of Petroleum Geologists Bulletin (abstract), v. 44, p. 959-960.

Stephens, R. A., 1986, Depositional history and diagenesis of the upper Mission Canyon and lower Charles Formations (Mississippian), Billings County, North Dakota: Master's Thesis, University of North Dakota, Grand Forks, North Dakota, 236 p.

Stockman, K. W., Ginsburg, R. N., and Shinn, E. A., 1967, The production of lime mud by algae in south Florida: Journal of Sedimentary Petrology, v. 37, p. 633-648.

Swirydczuk, K., 1988, Mineralogy control on porosity type in Upper Jurassic Smackover ooid grainstones, southern Arkansas and northern Louisiana: Journal of Sedimentary Petrology, v.58, p. 339-347.

Taylor, J. M., 1950, Pore space reduction in sandstones: American Association of Petroleum Geologists Bulletin, v. 34, p. 701-716.

Thomas, G. E., 1954, The Mississippian of the northeastern Williston Basin: Canadian Mining and Metallurgical Bulletin, v. 503, p. 136-142.

Valvik, J. R., 1988, Bioturbation patterns and near-anoxic events in Frobisher-Alida beds of western North Dakota (abstract): American Association of Petroleum Geologists Bulletin, v. 72, p.883.

Wanless, H. R., 1979, Limestone response to stress: pressure solution and dolomitization: Journal of Sedimentary Petrology, v. 49, p. 437-462.

Waters, D. L., 1984, Depositional cycles and coral distribution, Mission Canyon and Charles formations, Madison Group (Mississippian), Williston basin, North Dakota: Master's thesis, University of North Dakota, Grand Forks, North Dakota, 173 p.

Weed, W., 1896, Sedimentary rocks- description of the Yellowstone National Park sheets: United States Geological Survey Atlas, Yellowstone National Park Folio No. 30.

Wood, G. V., and Wolfe, M. J., 1969, Sabkha cycles in the Arab/Darb Formation off the Trucial Coast of Arabia: Sedimentology, v. 12, p. 165-191.